Port of Abbot Point Ambient Marine Water Quality Monitoring Program (November 2017 – July 2018)

Nathan Waltham, Christina Buelow, James Whinney, Rachael Macdonald and Alex Olsen

Report No. 18/19

November 2018



Port of Abbot Point Ambient Marine Water Quality Monitoring Program (November 2017 – July 2018)

A Report for North Queensland Bulk Ports Corporation

Report No. 18/19

November 2018

Prepared by
Nathan Waltham, Christina Buelow, James Whinney,
Rachael Macdonald and Alex Olsen

Centre for Tropical Water & Aquatic Ecosystem Research
(TropWATER)
James Cook University
Townsville
Phone : (07) 4781 4262
Email: TropWATER@jcu.edu.au
Web: www.jcu.edu.au/tropwater/

Information should be cited as:
Waltham N, Buelow C, Whinney J, Macdonald R & Olsen A, 2018, 'Port of Abbot Point Ambient Marine Water Quality Monitoring Program (November 2017 – July 2018)', Centre for Tropical Water & Aquatic Ecosystem Research (TropWATER) Publication 18/19, James Cook University, Townsville, 89 pp.

For further information contact:
Dr Nathan Waltham
Centre for Tropical Water & Aquatic Ecosystem Research (TropWATER)
James Cook University
Nathan.waltham@jcu.edu.au

This publication has been compiled by the Centre for Tropical Water & Aquatic Ecosystem Research (TropWATER), James Cook University.

SUMMARY POINTS

Background

1. In November 2017, North Queensland Bulk Ports implemented an ambient marine water quality monitoring program surrounding the Port of Abbot Point. The objective of the program is to collect a long term water quality dataset to characterise marine water quality conditions within the Abbot Point region, and to support future planned Port activities. This document reports on data collected from November 2017 to July 2018, however a similar program was undertaken from October 2015 by a separate contractor (monitoring locations remained consistent, Vision 2017)
2. This program has incorporated a combination of spot field measurements and high frequency continuous data loggers, and laboratory analysis for a range of nutrients, herbicides and heavy metals.
3. There are five sites for monitoring that align with key sensitive receptor habitats (e.g. corals or seagrass), along with key features in the study region (e.g. river flow points).

Climatic conditions

1. To date, the total wet season rainfall within the study area during 2017/2018 was low in comparison to wet season totals since 1961. Data also shows that there has been high inter-annual variability in rainfall; in particular rainfall in the previous year (2016/2017), and therefore catchment flow, was significantly higher.
2. This highlights the necessity for long term commitment to ambient marine monitoring programs, as continued monitoring will allow changes in environmental conditions with rainfall to be better understood.
3. The daily average wind speed and direction recorded at Abbot Point for the reporting period was predominantly from the south east, with 30% of days having wind speeds greater than 24km/hr. There were also strong north-easterly winds (>24km/hr), but these did not occur as regularly as the south-easterly winds (<15% of days).

Water chemistry

1. Field water quality conditions were measured at all sites for water temperature, electrical conductivity, pH, dissolved oxygen, and secchi disk depth on a 6wkly basis, for three depth horizons (surface (0.2m), mid water and bottom).
2. Seasonal differences in water quality were minor, except for temperature which was highest during the summer months.
3. The water column was well mixed during each survey, with little differences among the three horizons examined.
4. Particulate nutrient concentrations exceeded relevant guidelines for the region, but not at every site, and primarily during wet season months (November to April). Chlorophyll-*a* concentrations were also elevated above the relevant guideline during November 2017, February and April 2018.
5. Ultra-trace heavy metals and pesticides/herbicides levels were undetectable at most sites in April 2018. At sites where these parameters were detectable, they did not exceed relevant guidelines.
6. An assessment of the plankton community (both phytoplankton and zooplankton) was completed during this reporting period. There was a clear separation in the plankton community species composition between surveys, suggesting seasonal variation. As the

dataset grows, relationships between the plankton community and other physiochemical/nutrient parameters will be evaluated.

Sediment deposition and turbidity

1. RMS water height values were mostly driven by weather events and this is clearly evident in the data as peaks in RMS water heights were observed at the same times at all sites over the survey year. Variation in the magnitude of RMS water height values during peak events and during non-event periods differs among sites due to differences in water depth and site exposure to wave energy.
2. The NTUe/SSC time series data at each site followed a typical pattern of low background values with recurring peak events. These peak events occurred at the same times at each site and coincided with peaks in RMS water height. This is a typical pattern which is similar to data collected in coastal locations in north Queensland
3. Time series deposition data shows that deposition tends to peak following high RMS water height events but with a lag so that peak deposition occurs at a time when RMS water height has decreased to near background levels. An explanation for this lag is that as waves resuspend sediment, little deposition is expected because the energy in the system will keep the sediment in suspension. It is only when waves decrease and there is no longer enough energy in the system to keep the same quantity of sediment in suspension that deposition begins to occur.
4. Current meter data indicates the prominent current direction and velocity at each site and shows that coastal current, tidal current or a combination of both influence current direction and magnitude.

Light attenuation (Photosynthetically active radiation; PAR)

Benthic PAR was highly variable within sites throughout the year, with peaks and troughs occurring both regularly and intermittently over time. Semi-regular oscillations between low and high PAR levels were overridden by larger episodic events caused by storm or rainfall events. It is important to note that a full year of PAR data has not yet been collected. As the data set increases, this will enable a greater insight into any trends that occur, whether these be tidally influenced or dependant on seasonality and cloud cover. Benthic PAR is also important to assess and validate NTUe sensor data.

Recommendations

The program thus far includes five monitoring sites, and it is recommended that these same five sites remain for the 2018/19 period in order to continue to capture local water quality conditions.

TABLE OF CONTENTS

Summary Points i

1 INTRODUCTION 5

1.1 Port operations 5
1.2 Program outline 5
1.3 Rainfall and river flows 6
1.4 Wind for Abbot Point 8
1.5 Project objectives 8

2 METHODOLOGY 9

2.1 Ambient water quality 9
2.2 Plankton community 11
2.3 Multiparameter water quality logger 12
2.3.1 Turbidity 12
2.3.2 Sediment deposition 12
2.3.3 Pressure 13
2.3.4 Water temperature 14
2.3.5 Photosynthetically Active Radiation (PAR) 14

3 RESULTS AND DISCUSSION 17

3.1 Ambient water quality 17
3.1.1 Spot water quality physio-chemical 17
3.1.2 Nutrients and chlorophyll-*a* 22
3.1.3 Ultra-trace water heavy metals 26
3.1.4 Water pesticides and herbicides 26
3.1.5 Ordination of data 26
3.2 Plankton communities 28
3.2.1 Plankton ordinations 30
3.3 Multiparameter water quality logger 31
3.3.1 RMS water height 31
3.3.2 NTUe/SSC 33
3.3.3 Deposition 34
3.3.4 Water temperature 35
3.4 Photosynthetically Active Radiation (PAR) 36
3.4.1 Similarities in patterns of PAR among sites 40
3.4.2 Relationship between light attenuation and suspended solid concentrations 41
3.4.3 Current meter 41
3.5 River Plumes 48
3.5.1 Site specific outputs 48

4 CONCLUSIONS AND RECOMMENDATIONS 55

4.1 Conclusions 55
4.1.1 Climatic conditions 55
4.1.2 Ambient water quality 55
4.1.3 Sediment deposition and turbidity 55
4.1.4 Photosynthetically active radiation (PAR) 56
4.2 Recommendations 56
4.2.1 Consolidation of the water quality loggers 56
4.2.2 Data base repository 56

5 LITERATURE SOURCED 57

6. APPENDIX 63

A.1 Calibration procedures 63

A.2 Time series data 64

AMB 1: Euri Creek 64

AMB 2: Spoil Grounds 65

AMB 3: Elliot River 66

AMB 4: Camp Island 67

AMB 5: Holbourne 68

A.3 Summary of monthly statistics 69

AMB 1: Euri Creek 69

AMB 2: Spoil Grounds 73

AMB 3: Elliot River 77

AMB 4: Camp Island 81

AMB 5: Holbourne 85

1 INTRODUCTION

1.1 Port operations

The Port of Abbot Point is situated in naturally deep waters off the central Queensland Coast (Figure 1.1). The Port of Abbot Point is located approximately 25 kilometres north of Bowen, and North Queensland Bulk Ports Corporation (NQBP) is the Port Authority. The Port has one operating terminal and provides important services for the surrounding region.

1.2 Program outline

Routine maintenance dredging is periodically required at the Port of Abbot Point to maintain vessel navigational depths, and has only been triggered once in the last 25 years. In order to better define the potential impacts associated with port operations and to characterise the natural variability in key water quality parameters within the adjacent sensitive habitats, NQBP committed to an ambient marine water quality monitoring program in and around the coastal waters of the Port of Abbot Point (Figure 1.1; Table 1.1). As part of this program, water quality parameters are being investigated at a range of sites. This monitoring program contains a range of ambient water quality components that collectively continue to characterise the natural variability in key water quality parameters, including those experienced at the nearest sensitive receiving habitats.

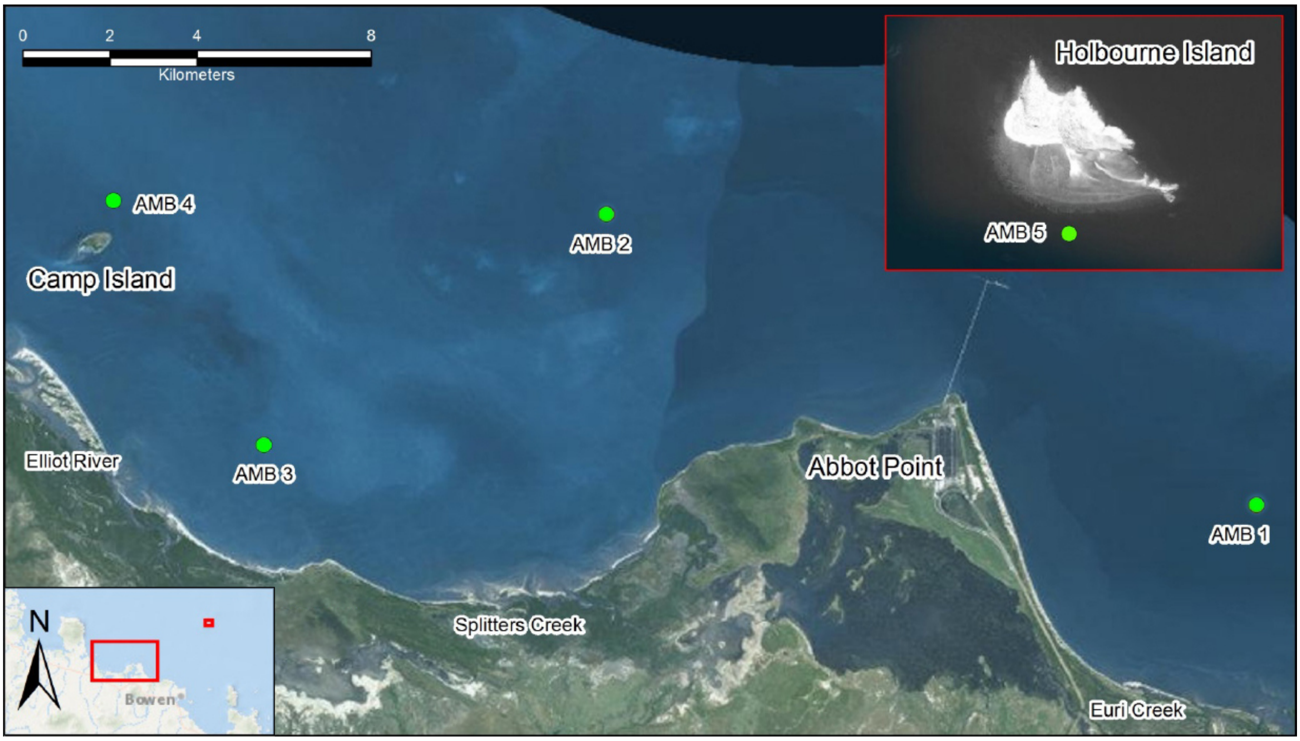

Figure 1.1 Geographical positions for the locations of the ambient marine water quality monitoring program sites at the Port of Abbot Point

Table 1.1 Descriptions for the locations of the ambient marine water quality monitoring program sites

Location	AMB site no.	Lat.	Long.	Water quality	Deposition/PAR logger
Euri Creek	1	-19.9047	148.1418	Yes	Yes
Spoil Grounds	2	-19.8444	148.0077	Yes	Yes
Elliot River	3	-19.8922	147.9368	Yes	Yes
Camp Island	4	-19.8417	147.9058	Yes	Yes
Holbourne	5	-19.7358	148.3593	Yes	Yes

1.3 Rainfall and river flows

To date, the total wet season rainfall within the study area during 2017/2018 was low in comparison to wet season totals since 1961 and significantly lower than the higher than average wet season of 2016/2017 (Figure 1.2). Rainfall in recent years has also been highlighted (Figure 1.2), indicating that the influence of rainfall, and therefore catchment flow, can have high inter-annual variability. This highlights the necessity for long term commitment to ambient marine monitoring programs.

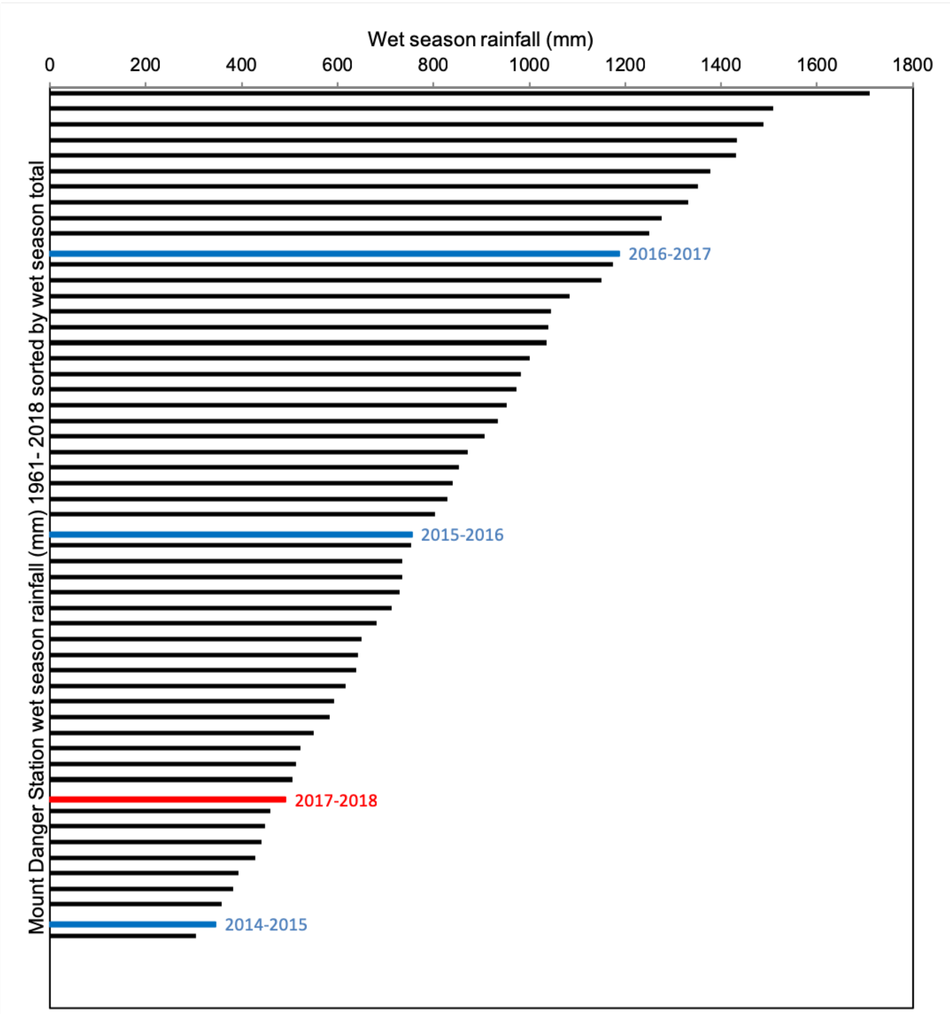

Figure 1.2 BOM wet season (Nov – March) rainfall data for Mount Danger Station ranked in order of decreasing total rainfall (mm). Blue bars show total rainfall over the past few years, and the red bar represents the 2017/18 ambient marine water quality monitoring period

A hydrograph for Euri River near Abbot Point (Figure 1.3) shows a large increase in river discharge at the end of February 2018 due to high rainfall from a low pressure system (Figure 1.4). River discharge associated with this rainfall event was higher than the maximum flow rate (22,640 ML/day) recorded during TC Debbie in 2016/2017.

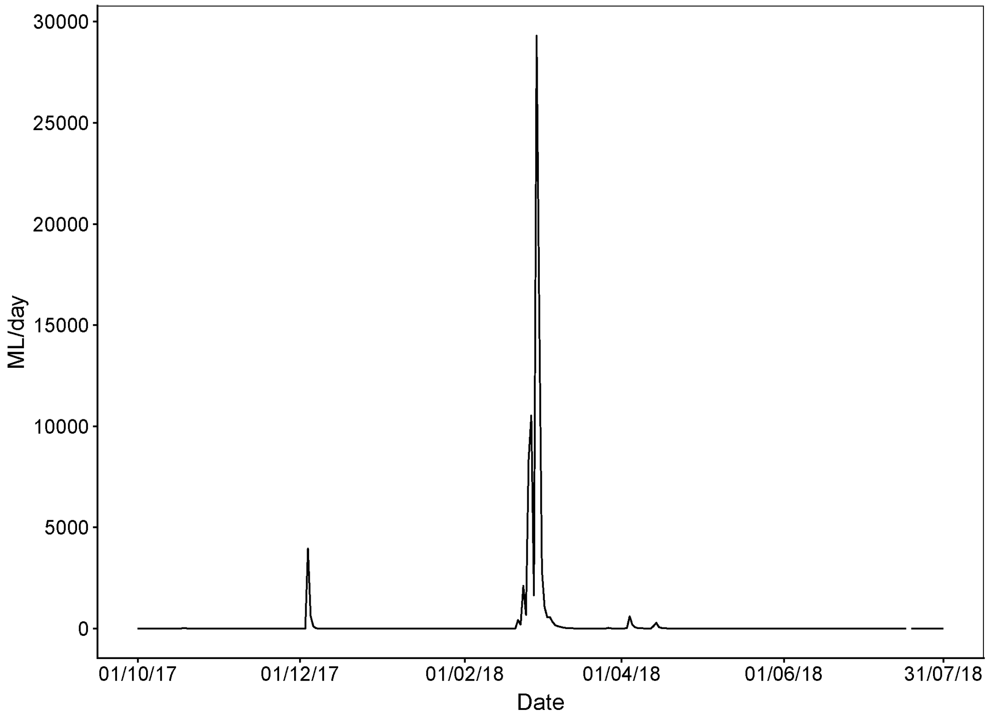

Figure 1.3 Flow (Megalitres/day) recorded for Euri River during October 2017 – July 2018.

Figure 1.4 Low pressure system delivering high rainfall to Abbot Point on 27 February 2018

1.4 Wind for Abbot Point

The daily average wind speed and direction recorded at Abbot Point airport for the reporting period was predominantly from the south east, and ~30% of days had wind speeds greater than 24km/hr (Figure 1.5). Wind rarely came from the north west direction during this reporting period (< 5% of the days) (Figure 1.5).

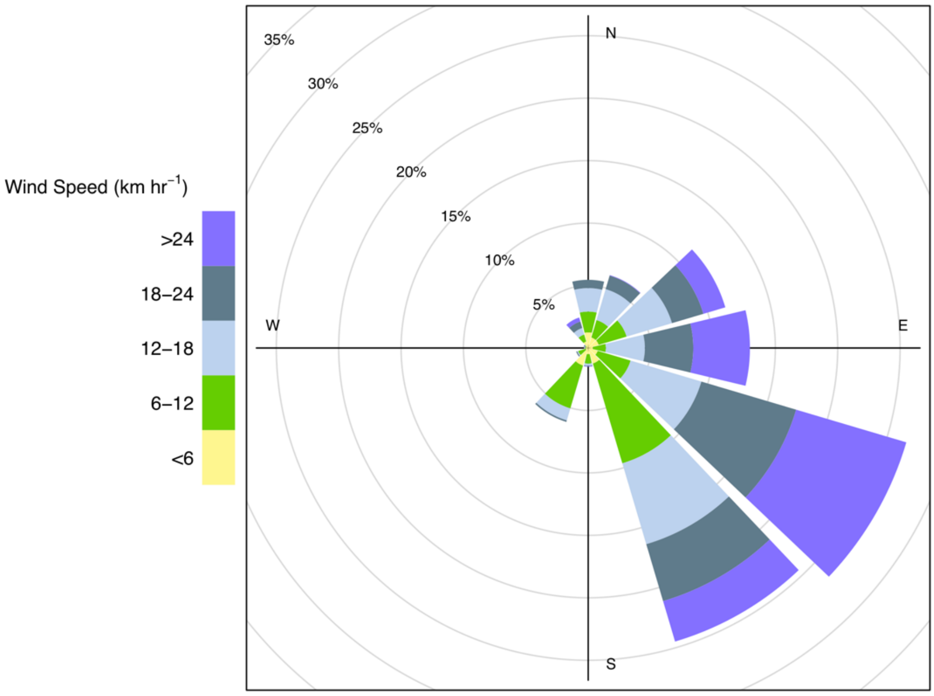

Figure 1.5 Daily average wind direction and strength recorded at Abbot Point throughout November 2017 to July 2018

1.5 Project objectives

The goal of the program is to characterise the ambient marine water quality monitoring within the region and adjacent to the Port of Abbot Point. This report provides a review and analysis of data collected between November 2017 and July 2018. These data are part of a longer-term commitment to monitor and characterise receiving water quality conditions, in particular to support future planned asset management and protection for both these ports.

2 METHODOLOGY

2.1 Ambient water quality

Spot water quality samples were collected at sites approximately on a 6wk basis (Table 2.1) from a research vessel. At each site, a calibrated multiprobe is used to measure water temperature, salinity, dissolved oxygen (%), pH, and turbidity (Figure 2.1). In addition to spot measurements, secchi disk depth is recorded, as a measure of the optical clarity of the water column, along with light attenuation using a LiCor meter. These field *in-situ* measurements are recorded at three depth horizons: a) surface (0.25m); b) mid-depth; and c) bottom horizon. The measurements assist in characterising water quality conditions in the water column.

In considering key priority outcomes outlined in recently published Coastal Strategic Assessment and Marine Strategic Assessments for the Great Barrier Reef World Heritage area (DEHP, 2013; GBRMPA, 2013), the water quality program design below was completed. The list of parameters examined consisted of:

- Ultra-trace dissolved metals : arsenic (As), cadmium (Cd), copper (Cu), mercury (Hg), nickel (Ni), lead (Pb), and zinc (Zn);
- Nutrients (particulate nitrogen and phosphorus);
- Chlorophyll-*a*; and
- Pesticides/herbicides (Low LOR suite (EP234(A-I)) including: diuron, ametryn, atrazine, terbutryn. Note that pesticides are suspected to be in low concentrations during periods of low rainfall runoff, and only detectable following rainfall. As a consequence sampling of only two events at all sites for pesticides, one during the dry and a wet season – though note that the timing of each are dependent on prevailing weather conditions, so the timing of each survey could differ from year to year.


Figure 2.1 TropWATER staff conducting field water quality sampling

Table 2.1 Summary of instrument maintenance and water quality surveys completed during the 2017/18 reporting period

Date	Nutrients, Chloro	Metals, herbicides	Plankton	Logger maintenance
November 2017	Yes	-	Yes	Yes
December 2017	Yes	-	Yes	Yes
February 2018	Yes	-	Yes	Yes
April 2018	Yes	Yes	-	Yes
June 2018	Yes	-	-	Yes

Sampling methodology, sample bottles, preservation techniques and analytical methodology (NATA accredited) were in accordance with standard methods (i.e., DERM 2009b; APHA 2005; Standards Australia 1998). Field collected water samples were stored on ice in eskies immediately during field trips aboard the vessel, and transported back to refrigeration, before delivery to the TropWATER laboratory. For chlorophyll analysis, water was placed into a 1L dark plastic bottle and placed on ice for transportation back to refrigeration. For dissolved metals and nutrients, water was passed through a 0.45 µm disposable membrane filter (Sartorius), fitted to a sterile 60 mL syringe (Livingstone), and placed into 60 mL bottles (metals) and 10 mL bottles (nutrients) for posterior analysis in the laboratory. (The use of these field sampling equipment and procedures have been previously shown to reduce the risk of contamination of samples, contributing to false positive results for reporting; TropWATER, 2015). Unfiltered sample for total nitrogen and total phosphorus analysis were frozen in a 60 mL tube. All samples are kept in the dark and cold until processing in the laboratory, except nutrients which are stored frozen until processing.

Water for chlorophyll determination was filtered through a Whatman 0.45 µm GF/F glass-fibre filter with the addition of approximately 0.2 mL of magnesium carbonate within (less than) 12 hours after collection. Filters are then wrapped in aluminium foil and frozen. Pigment determinations from acetone extracts of the filters were completed using spectrophotometry, method described in 'Standard Methods for the Examination of Water and Wastewater, 10200 H. Chlorophyll'.

Water samples are analysed using the defined analysis methods and detection limits outlined in Table 2.2. In summary, all nutrients were analysed using colorimetric method on OI Analytical Flow IV Segmented Flow Analysers. Total nitrogen and phosphorus and total filterable nitrogen and phosphorus are analysed simultaneously using nitrogen and phosphorous methods after alkaline persulphate digestion, following methods as presented in 'Standard Methods for the Examination of Water and Wastewater, 4500-NO3- F. Automated Cadmium Reduction Method' and in 'Standard Methods for the Examination of Water and Wastewater, 4500-P F. Automated Ascorbic Acid Reduction Method'. Nitrate, Nitrite and Ammonia were analysed using the methods 'Standard Methods for the Examination of Water and Wastewater, 4500-NO3- F. Automated Cadmium Reduction Method', 'Standard Methods for the Examination of Water and Wastewater, 4500-NO2- B. Colorimetric Method', and 'Standard Methods for the Examination of Water and Wastewater, 4500-NH3 G. Automated Phenate Method', respectively. Filterable Reactive Phosphorous is analysed following the method presented in 'Standard Methods for the Examination of Water and Wastewater, 4500-P F. Automated Ascorbic Acid Reduction Method'. Filterable heavy metals, and herbicides are analysed by Australian Laboratory Service (ALS).

For all water quality plots, boxes are 20th and 80th quantile, centre line is median, and whiskers represent the 5th and 95th percentile.

Table 2.2 Water analyses performed during the program

Parameter	APHA method number	Reporting limit
Routine water quality analyses		
pH	4500-H^+ B	-
Conductivity (EC)	2510 B	5 µS/cm
Total Suspended Solids (TSS)	2540 D @ 103 - 105°C	0.2 mg/L
Turbidity	2130 B	0.1 NTU
Salinity		
Dissolved Oxygen		
Light Attenuation		
Pesticides/herbicides		
Organophosphate pesticides	In house LC/MS method: EP234A	0.0002-0.001 µg/L
Thiocarbamates and Carbamates Thiobencarb	In house LC/MS method: EP234B	0.0002 µg/L
Dinitroanilines Pendimethalin	In house LC/MS method: EP234C	0.001 µg/L
Triazinone Herbicides Hexazinone	In house LC/MS method: EP234D	0.0002 µg/L
Conazole and Aminopyrimidine Fungicides Propiconazole, Hexaconazole, Difenoconazole, Flusilazole, Penconazole	In house LC/MS method: EP234E	0.0002 µg/L
Phenylurea Thizdiazolurea Uracil and Sulfonylurea Herbicides Diuron, Ametryn, Atrazine, Cyanazine, Prometryn, Propazine, Simazine, Terbuthylazine, Terbutryn	In house LC/MS method: EP234F	0.0002 µg/L
Nutrients		
Total Nitrogen and Phosphorus (TN/TP)	Simultaneous 4500-NO_3^- F and 4500-P F analyses after alkaline persulphate digestion	25 µg N/L 5 µg P/L
Filterable nutrients (nitrate, nitrite, ammonia, Nox)	4500-NO_3^- F	1 µg N/L
Ammonia	4500- NH_3 G	1 mg N/L
Filterable Reactive Phosphorus (FRP)	4500-P F	1 µg P/L
Chlorophyll	10200-H	0.1 µg/L
Trace Metals		
Arsenic, Cadmium, Copper, Lead, Nickel, Silver, Zinc, Mercury	3125B ORC/ICP/MS	0.05 to 100 µg/L

2.2 Plankton community

At all sites, a 60µm plankton net (for phytoplankton) and a 500µm plankton net (for zooplankton) was towed behind the survey vessel for approximately 100m. The boat speed is reduced to approximately 6kts, with a GPS point taken at the start and end of each plankton tow. At the end of each plankton tow, the nets are retrieved, and the contents retained in the plastic jar attached to the net was immediately transferred to preservation containers. Samples were identified to the lowest possible taxon.

a) b)

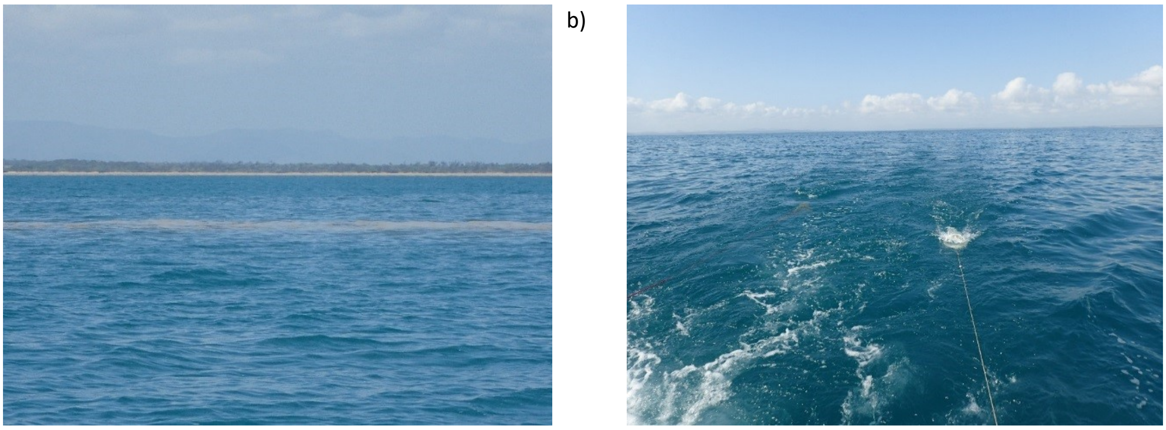

Figure 2.2 Example plankton sample. a) Trichodesmium bloom on sea surface; b) phytoplankton (60µm) tow behind the survey vessel

2.3 Multiparameter water quality logger

Sediment deposition, turbidity, Photosynthetically Available Radiation (PAR), water depth, Root Mean Squared (RMS) water depth and water temperature were measured at seven sites using multiparameter water quality instruments manufactured at the Marine Geophysics Laboratory, School of Engineering and Physical Sciences, James Cook University (Figure 2.3). These instruments are based on a Campbell's Scientific 1000 data logger that has been programmed to measure and store these marine physical parameters using specifically designed sensors.

2.3.1 Turbidity

The turbidity sensor provides data in Nephelometric Turbidity Unit's equivalent (NTUe) and can be calibrated to Suspended Sediment Concentration (SSC) in mg/L (Larcombe et al., 1995). The sensor is located on the side of the logger, pointing parallel light-emitting diodes (LED) and transmitted through a fibre optic bundle. The backscatter probe takes 250 samples in an eight second period to attain an accurate turbidity value. The logger is programmed to take these measurements at 10 minute intervals. The sensor interface is cleaned by a mechanical wiper at a two hour interval allowing for long deployment periods where bio-fouling would otherwise seriously affect readings.

It must be noted the international turbidity standard ISO7027 defines NTU only for 90 degree scatter, however, the Marine Geophysics Laboratory instruments obtain an NTUe value using 180 degree backscatter as it allows for much more effective cleaning. Because particle size influences the angular scattering functions of incident light (Ludwig and Hanes 1990; Conner and De Visser 1992; Wolanski et al., 1994; Bunt et al., 1999), instruments using different scattering angles can provide different measurements of turbidity (in NTU). This has to be acknowledged if later comparison between instruments collecting NTUe and NTU are to be made. To enhance the data, all sites were calibrated to provide a measure of SSC (mg/L) and enable for the accurate comparison between 90 degree backscatter and 180 degree backscatter measurements.

2.3.2 Sediment deposition

Deposition is recorded in Accumulated Suspended Sediment Deposition (ASSD) (mg/cm^2). The sensor is wiped clean of deposited sediment at a 2 hour interval to reduce bio-fouling and enable sensor sensitivity to remain high. The deposition sensor is positioned inside a small cup shape (16mm diameter *x* 18mm deep) located on the flat plate surface of the instrument facing towards the water surface. Deposited sediment produces a backscatter of light that is detected by the sensor. Deposited sediment is calculated by subtracting, from the measured data point, the value taken after the sensor was last wiped clean. This removes influence of turbidity from the value and re-zeros the deposition sensor every 2 hours.

If a major deposition event is in progress, the sensor reading will increase rapidly and will be considerably above the turbidity sensor response. Gross deposition will appear as irregular spikes in the data where the sediment is not removed by the wiper but by re-suspension due to wave or current stress. When a major net deposition event is in progress the deposited sediment will be removed by the wiper and the deposition sensor reading should fall back to a value similar to the turbidity sensor. The data will have a characteristic zigzag response as it rises, perhaps quite gently, and falls dramatically after the wipe (see Ridd et al., 2001).

Deposition data is provided as a measurement of deposited sediment in mg/cm^2 and as a deposition rate in mg/cm^2/day. The deposition rate is calculated over the 2 hour interval between sensor wipes and averaged over the day for a daily deposition rate. The deposition rate is useful in deposition analysis as it describes more accurately the net deposition of sediment by smoothing spikes resulting from gross deposition events.

2.3.3 Pressure

A pressure sensor is located on the horizontal surface of the water quality logging instrument. The pressure sensor is used to determine changes in water depth due to tide and to produce a proxy for wave action. Each time a pressure measurement is made the pressure sensor takes 10 measurements over a period of 10 seconds. From these 10 measurements, average water depth (m) and Root Mean Square (RMS) water height are calculated. RMS water height, D_{rms}, is calculated as follows:

$$D_{rms} = \sqrt{\sum_{n=1}^{10} (D_n - \overline{D})^2 / n}$$

Equation 1 : where Dn is the *n*th of the 10 readings and $\overline{D}$ is the mean water depth of the *n* readings.

The average water depth and RMS water depth can be used to analyse the influence that tide and water depth may have on turbidity, deposition and light levels at an instrument location. The RMS water height is a measure of short term variation in pressure at the sensor. Changes in pressure over a 10 second time period at the sensor are caused by wave energy. RMS water height can be used to analyse the link between wave re-suspension and SSC. It is important to clearly establish that RMS water height is not a measurement of wave height at the sea surface. What it does provide is a relative indication of wave shear stress at the sea floor that is directly comparable between sites of different depths. For example, two sites both have the same surface wave height, site one is 10m deep and has a measurement of 0.01 RMS water height and site two is 1m deep and has a measurement of 0.08 RMS water height. Even though the surface wave height is the same at both sites, the RMS water height is greater at the shallower site and we would expect more re-suspension due to wave shear stress at this site.

2.3.4 Water temperature

Water temperature values are obtained with a thermistor that records every 10 minutes. The sensor is installed in a bolt that protrudes from the instrument and gives sensitive temperature measurements.

a)

b)

Figure 2.3 Example coastal multiparameter water quality instrument: a) site navigation beacon for safety and instrument retrieval; b) instrument showing sensors and wiping mechanisms

2.3.5 Photosynthetically Active Radiation (PAR)

A PAR sensor, positioned on the horizontal surface of the water quality logging instrument, takes a PAR measurement at ten (10) minute intervals for a one second period. To determine total daily PAR (mol photons m^2/day) the values recorded are multiplied by 600 to provide of PAR for a 10 minute period and then summed for each day.

2.4 Marotte current meter

The Marotte HS (High Sampling Rate) is a drag-tilt current meter invented at the Marine Geophysics Laboratory (Figure 2.4). The instrument records current speed and direction with an inbuilt accelerometer and magnetometer. The current speed and direction data are smoothed over a 10-minute period. The instruments are deployed attached the nephelometer frames and data is download when the instruments are retrieved. Inclusion of this current meter has been added to the program as a way to trial new technology, gather new data and to value add to project outcomes and deliverables.

a)

b)

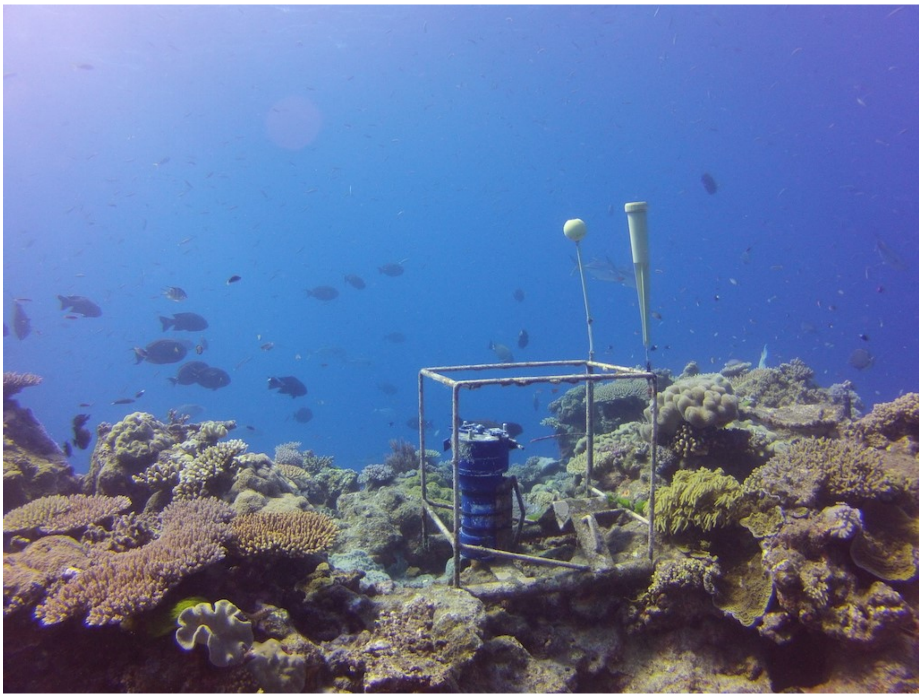

Figure 2.4 a) Basic schematic of Marotte HS current meter; and b) Marotte HS alongside Marotte at Moore Reef. Image courtesy of Eric Fisher

2.4.1 Measuring environmental controls on SSC

Stepwise regression analysis was used to investigate the environmental controls on SSC at the ambient sites, with data selected including:

(a) Ambient sites:
[1] "AMB1"[2] "AMB2"
[3] "AMB3"[4] "AMB4"
[5] "AMB5"

(b) River Gauge Station:
[1] "Euri"[2] "Don"

(c) Wind Station:
[1] "Station 33327 – Bowen"

(d) Tide Gauge Station:
[1] "Bowen"

In this assessment, the environmental parameters with control on SSC were analysed by stepwise regression analysis followed by relative importance analysis (Grömping, 2006) using R language (R Core Team, 2015). The stepwise analysis allowed the selection of the environmental variables that explain the SSC variability in the water column. The relative importance analysis allowed these selected variables to be ranked based on their overall explanation of the SSC variability. In order to visualize the effect of each environmental parameter selected in the stepwise analysis, a partial plot analysis (Crawley, 2007) was carried out. These partial plots indicate the dependence between

SSC and each selected variable when all the other variables in the model are kept constant (Crawley, 2007). The data set used in the stepwise analysis was log-transformed, if needed, in order to satisfy requirements for regression analysis. For each site, all the following variables were tested in an initial model against SSC: RMS of water depth, mean daily wind, maximum tide amplitude and the Don and Euri River discharges. These rivers were selected due to their proximity to the sampling sites. Mean daily wind was calculated from 8 daily readings decomposed into NE-SW and NW-SE components. Maximum tide amplitude was calculated as the maximum absolute difference between two consecutive maximum or minimum tide readings. Wind components were calculated as the mean value of 8 daily measurements decomposed to in two diagonals, NE-SW and NW-SE. Variables presenting autocorrelation were excluded based on a variance inflation test (Fox and Monett, 1992) > 4 and outliers were removed based on Bonferroni Outlier Test (Cook and Weisberg 1982).

3 RESULTS AND DISCUSSION

3.1 Ambient water quality

3.1.1 Spot water quality physio-chemical

For the reporting period between November 2017 and July 2018 water temperature ranged between 21.2 and 30.4°C (Figure 3.1). There is a strong seasonal effect on water temperatures in the region, with the highest water temperatures observed during surveys in the summer months, and cool water temperatures observed during the winter months (Figure 3.1). These patterns are consistent throughout the water column, indicating that the water column profile is vertically well mixed. There are no guidelines for water temperature in coastal areas, however, temperature is an essential interpretative aid for ecological assessment in environments. For example, species such as fish and other animals have thermal stress point which causes discomfort and could be misconstrued as being a toxicological impact (example are the coral trout; Johansen et al. 2015). There were no observed or known impacts on aquatic species in the region during this monitoring period.

A)

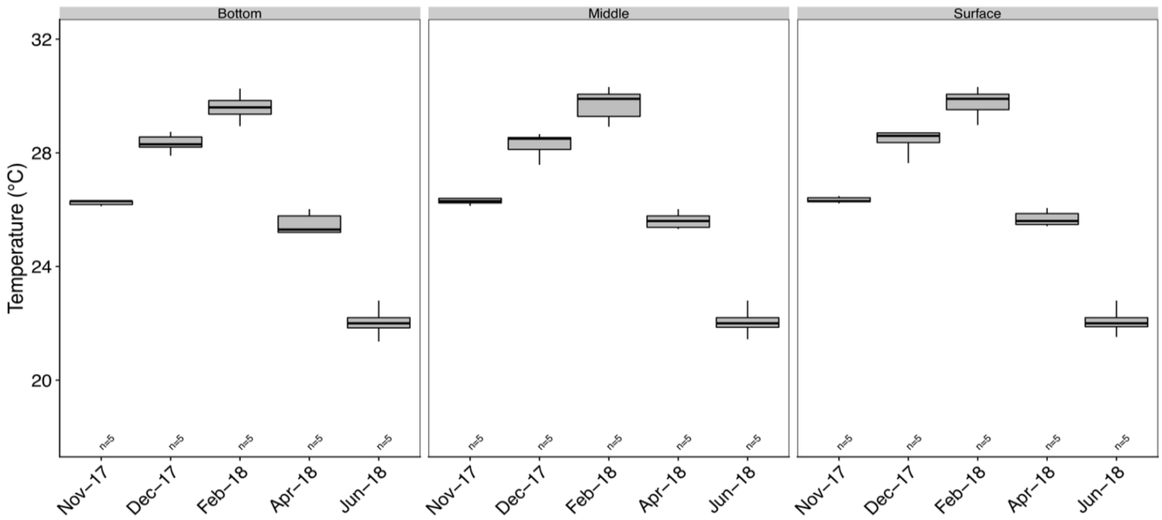

B)

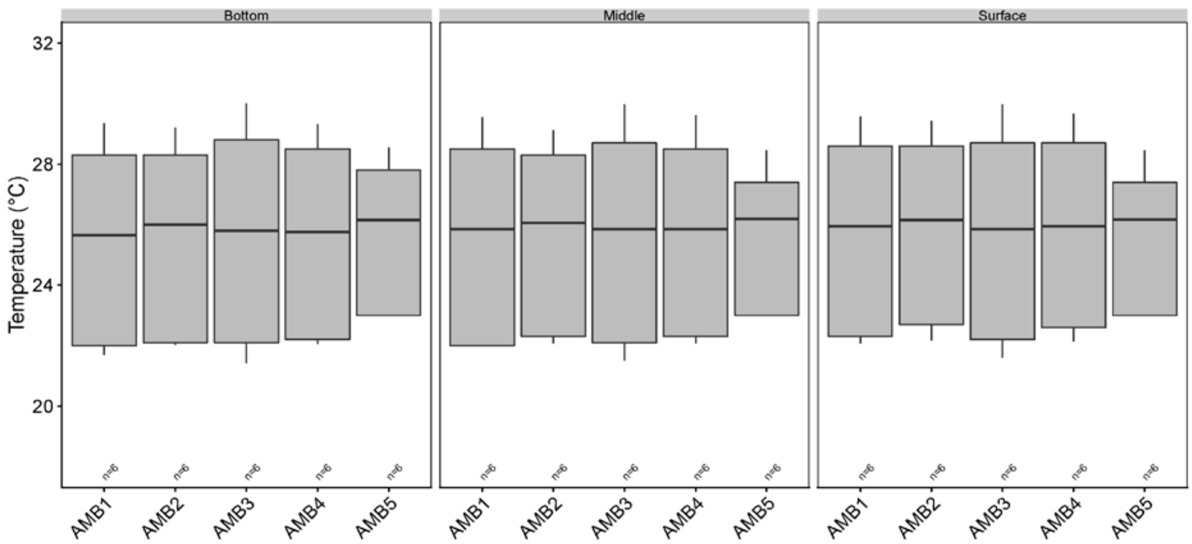

Figure 3.1 Water temperature box plots recorded: (a) the three depth horizons during each survey (sites pooled) from November 2017 to July 2018 and (b) the three depth horizons for each site (pooled across all months)

Salinity (ppt) was recorded in the field and then converted to Electrical conductivity (EC) using the relationship between EC measured in surface water samples, and the field salinity records. While the relationship between laboratory EC and salinity was good, use of these data will require caution. The corrected EC field data appears stable among sites and surveys, with little evidence of changing conditions throughout the water column (Figure 3.2). Overall EC has remained between 51.7 mS/cm and 52.8 mS/cm, generally indicating oceanic conditions (Figure 3.2).

A)

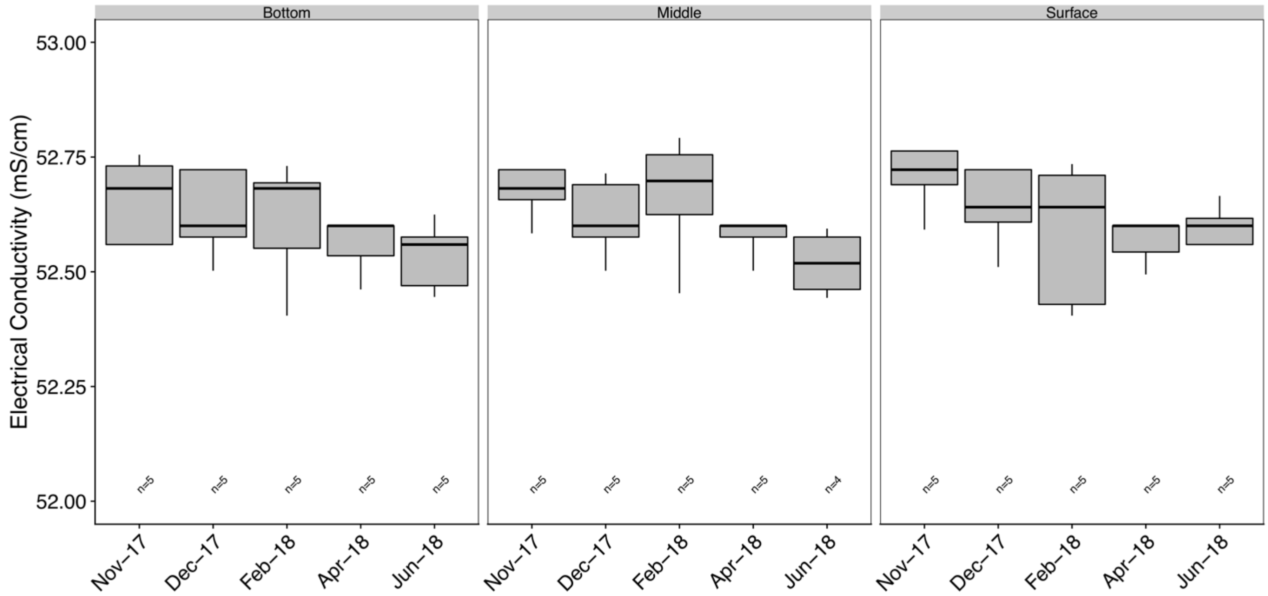

B)

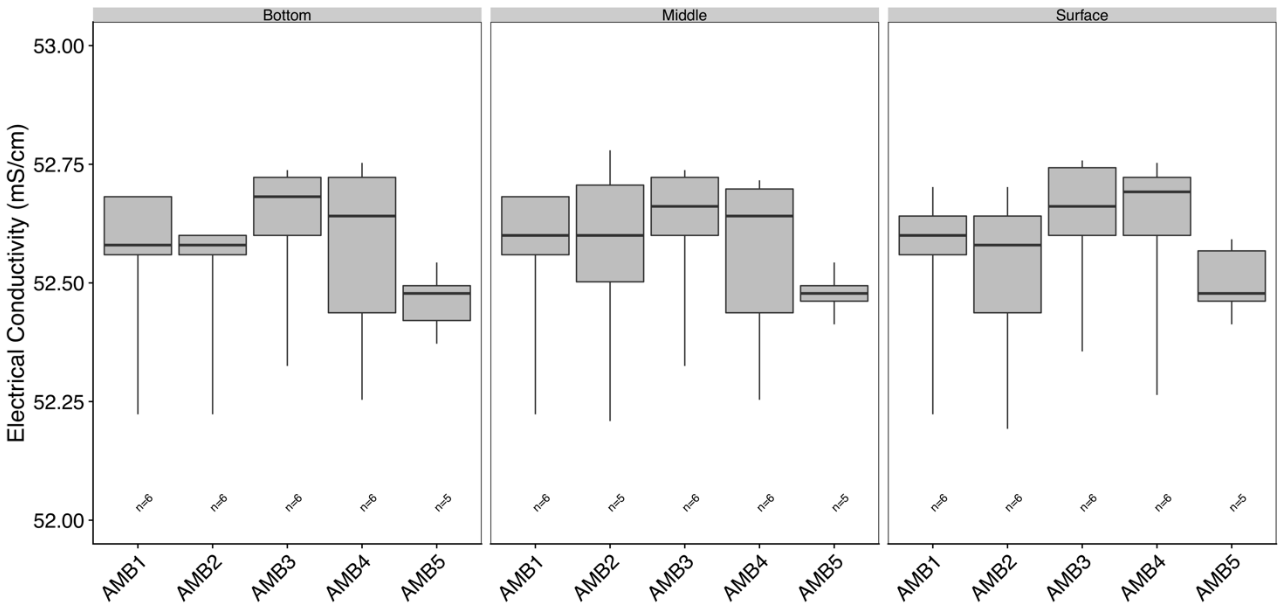

Figure 3.2 Salinity box plots recorded: (a) the three depth horizons during each survey (sites pooled) from November 2017 to July 2018 and (b) the three depth horizons for each site (pooled across all months)

Dissolved oxygen saturation levels ranged between 88 to 105% (Figure 3.3) and were relatively stable across sites (Figure 3.3b). There was some variability among sampling months, with the lowest levels recorded in November 2017 (Figure 3.3a). The water column continues to be well mixed with dissolved oxygen levels similar along the depth profile (Figure 3.3). Field pH measurements were also stable across sites and depths, primarily ranging between 7.2 and 8.2 (Figure 3.4).

A)

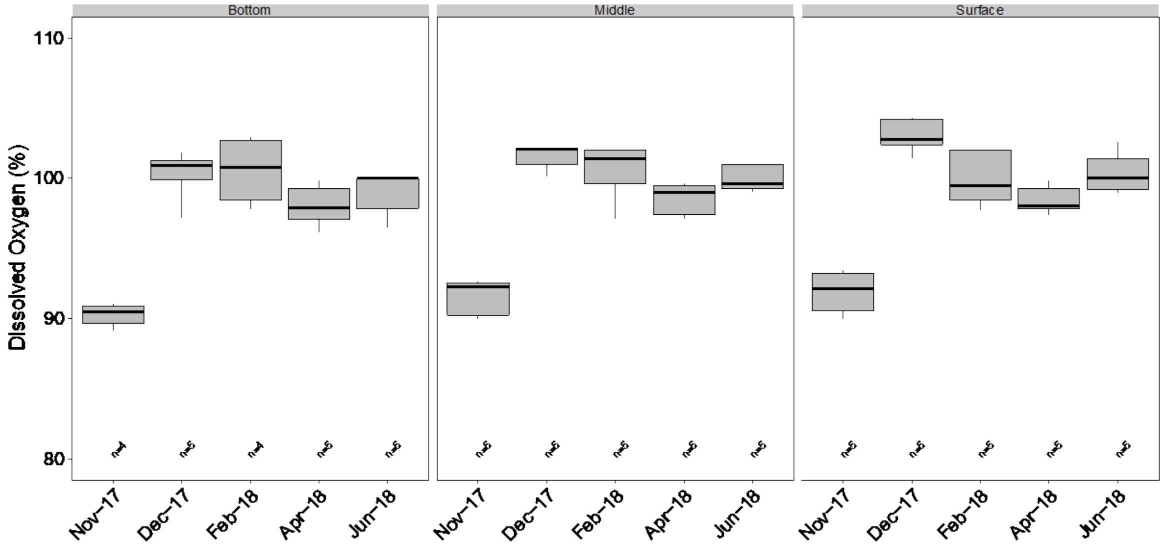

B)

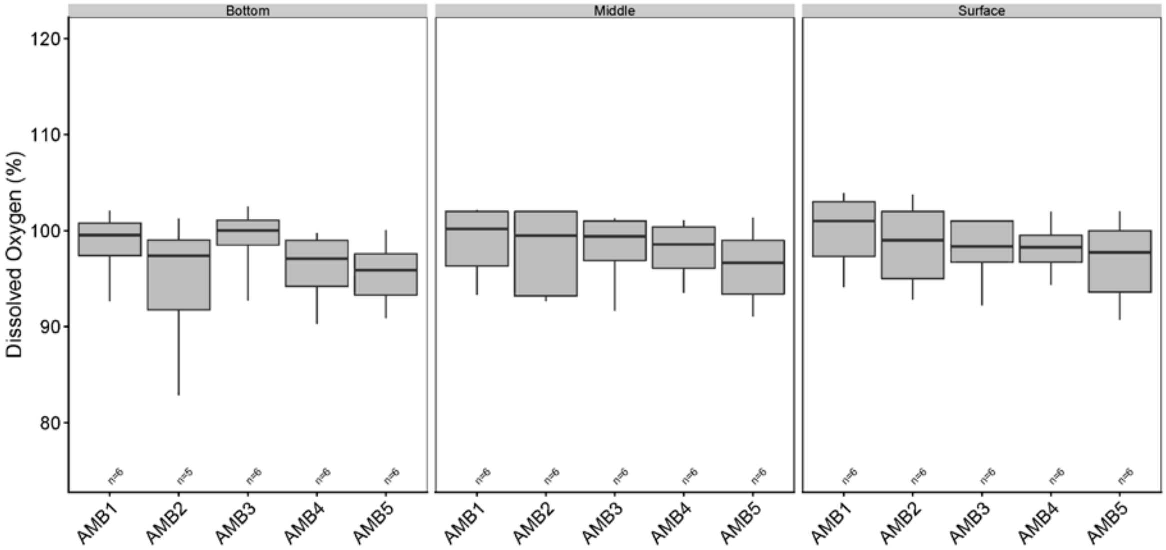

Figure 3.3 Dissolved oxygen box plots recorded: (a) the three depth horizons during each survey (sites pooled) from November 2017 to July 2018 and (b) the three depth horizons for each site (pooled across all months)

A)

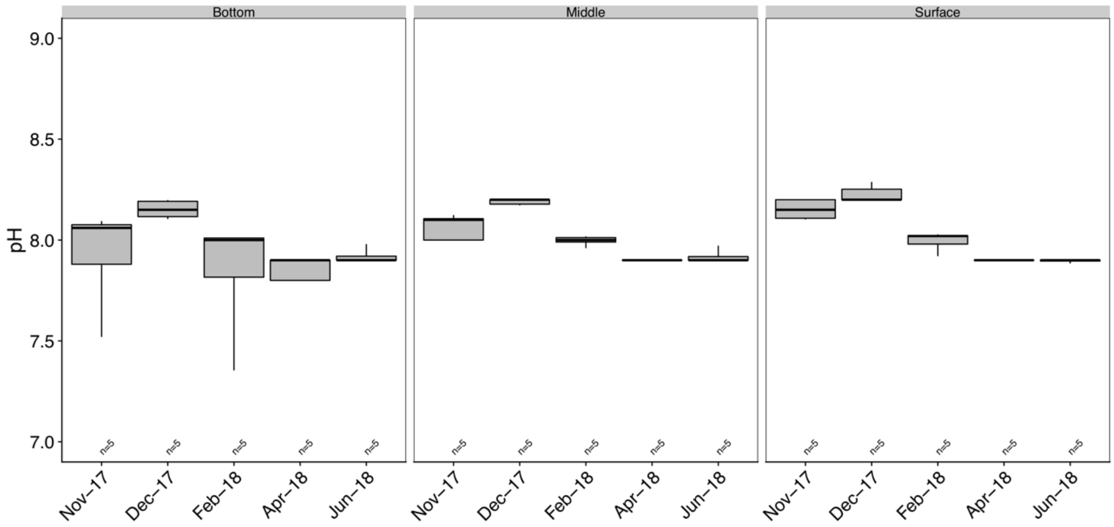

B)

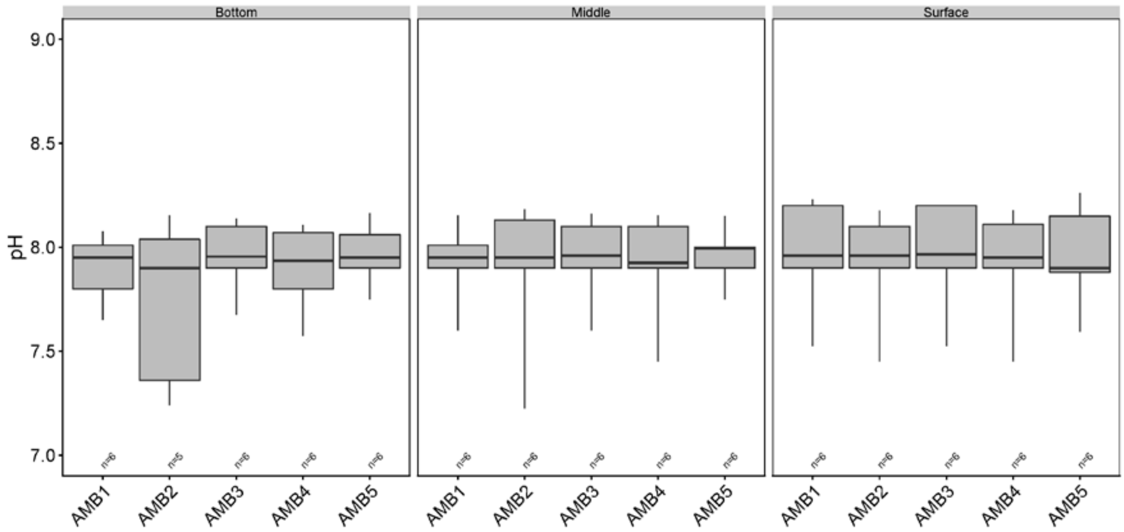

Figure 3.4 pH box plots recorded: (a) the three depth horizons during each survey (sites pooled) from November 2017 to July 2018 and (b) the three depth horizons for each site (pooled across all months)

Field turbidity measurements typically ranged between <1 to 60 NTU, with notable exceptions in June 2018 where turbidity was higher at the bottom of the water column (Figure 3.5a). Turbidity was similar among sites and relatively consistent throughout the water column (Figure 3.5b). Secchi disk depth (m) is a vertical measure of the optical clarity of water column and ranged between 1 and 10m (Figure 3.6a). The range measured is a response to localised variation in water quality, most likely a difference in tidal stage among sites during a survey, short term localised changes in turbidity that is associated with tide (see section 3.2) or algal blooms that reduce vertical clarity. The secchi disk depth to depth ratio (Zeu:Z, Figure 3.6b) was calculated for each site and survey. This ratio corrects the secchi disk depth for water depth, and ranged between 20 and 100% of the water column.

A)

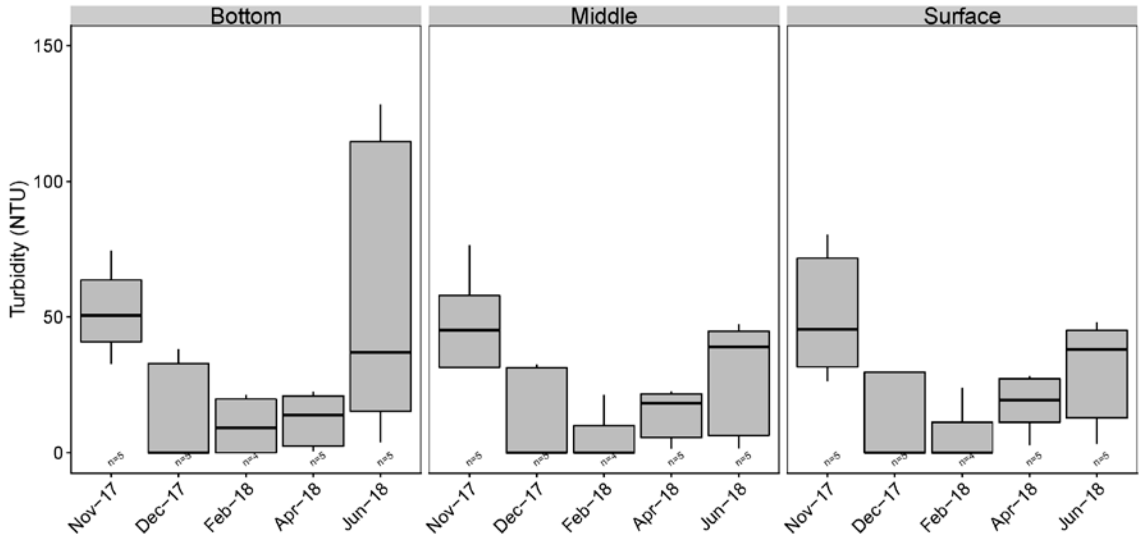

B)

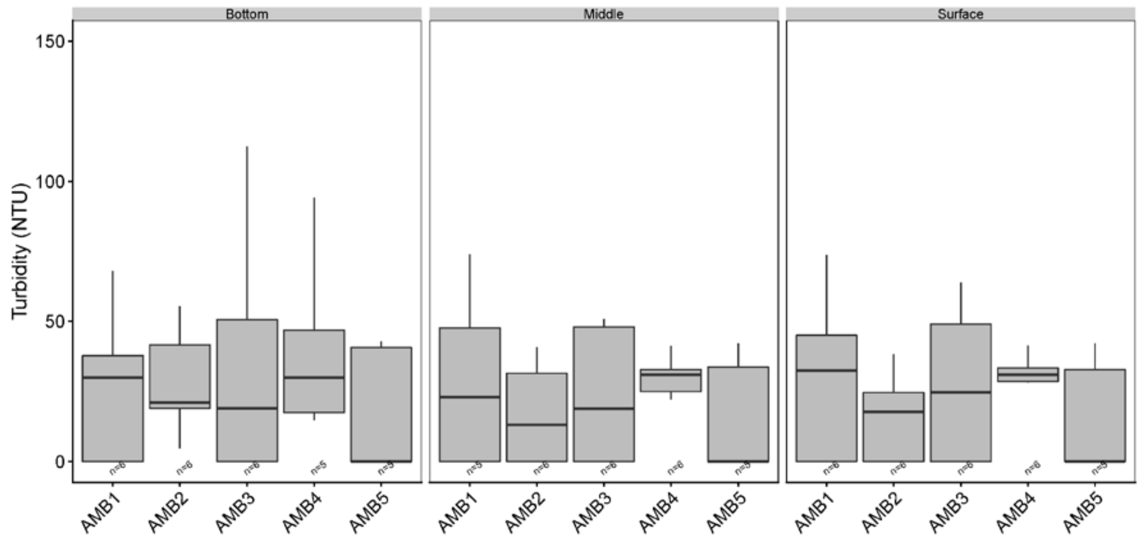

Figure 3.5 Turbidity box plots recorded: (a) the three depth horizons during each survey (sites pooled) from November 2017 to July 2018 and (b) the three depth horizons for each site (pooled across all months)

A)

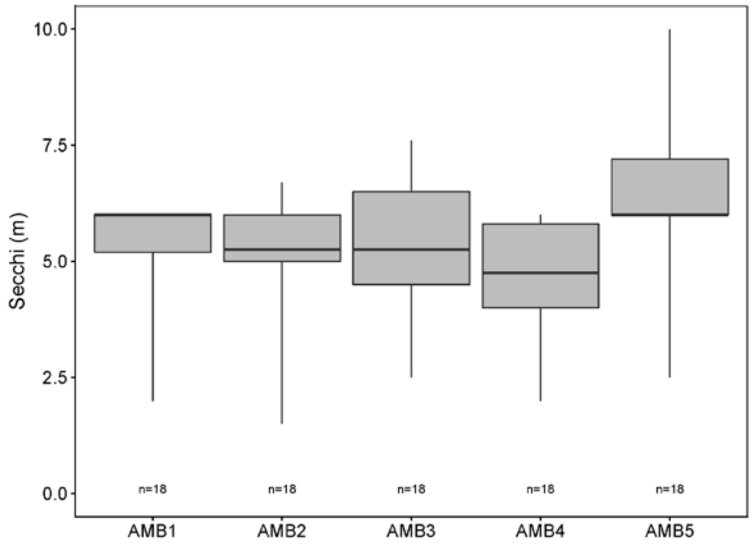

B)

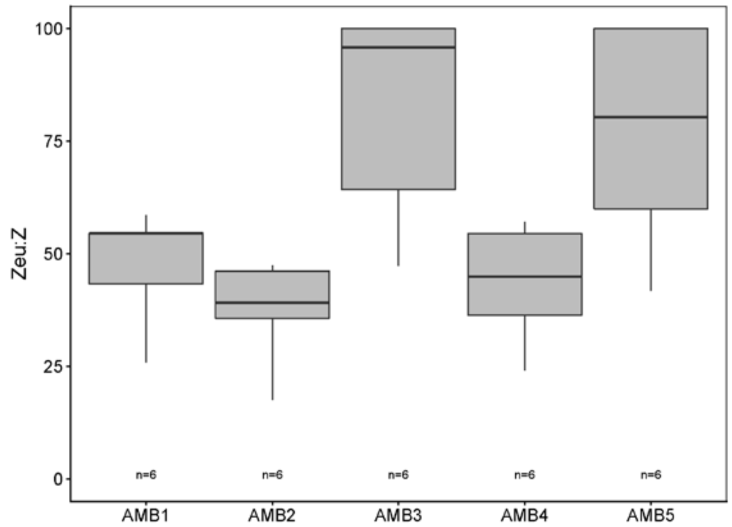

Figure 3.6 (a) Water secchi disk depth for all sites (surveys pooled); and (b) light attention depth to depth ratio (Zeu:Z) for sites (surveys pooled)

3.1.2 Nutrients and chlorophyll-*a*

Particulate nitrogen (PN) and phosphorus (PP) concentrations were compared to the Water Quality Guidelines for the Great Barrier Marine Park Authority (GBRMPA, 2010). Particulate nitrogen concentrations exceeded the guideline in November 2017, December 2017, and June 2018 (Figure 3.7a). Also, when pooled across all surveys, concentrations exceeded guidelines at AMB2 and AMB5. High concentrations of PN might be associated with the contribution from local land use activities, as base flow from rivers and local rainfall is known to contribute to nutrient loadings to coastal regions (Brodie et al. 2012; Kroon et al. 2012; Schaffelke et al. 2012; Logan et al. 2014). In addition, other sources of the nutrients might be via remobilisation of coastal sediments, and release of available nutrients adsorbed to coastal sediments (Devlin et al. 2012). Elevated nutrients may also be related to reprocessing of nutrients with algal blooms, where there has been an obvious trichodesmium (a marine cyanobacteria; Capone et al. 1997) bloom across the region during most surveys, but most notably during late spring and early summer.

A)

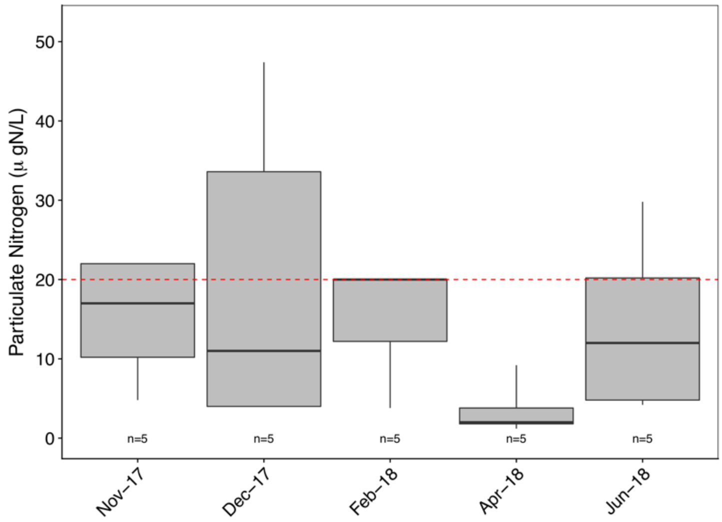

B)

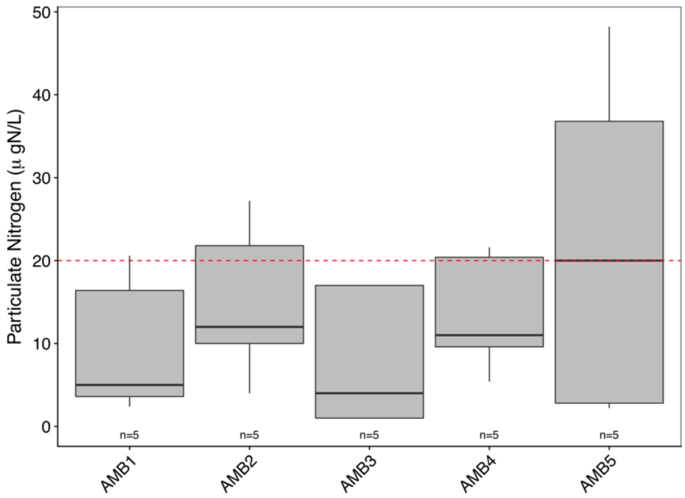

Figure 3.7 Particulate nitrogen box plots: (a) during each survey (sites pooled) from November 2017 to July 2018 and (b) at each site over this same survey period (surveys pooled)

Particulate phosphorus concentrations were relatively similar across seasons and sites and exceeded the GBRMPA (2010) Water Quality Guideline in November 2017, and February and June 2018 (Figure 3.8). The only sites to exceed the guideline were AMB2 and AMB3 (Figure 3.8b). Chlorophyll-*a* concentrations exceeded the GBRMPA (2010) Water Quality Guideline in all months and sites surveyed, except for December 2017, June 2018, and at AMB2 (pooled across months; Figure 3.9). Relationships between nutrient levels (i.e. PN, PP, Chlor-a, and Phaeophytin-a) across all sites and sampling periods were weak (correlation coefficients (r) ranged between -0.01 – 0.25; Figure 3.10).

A)

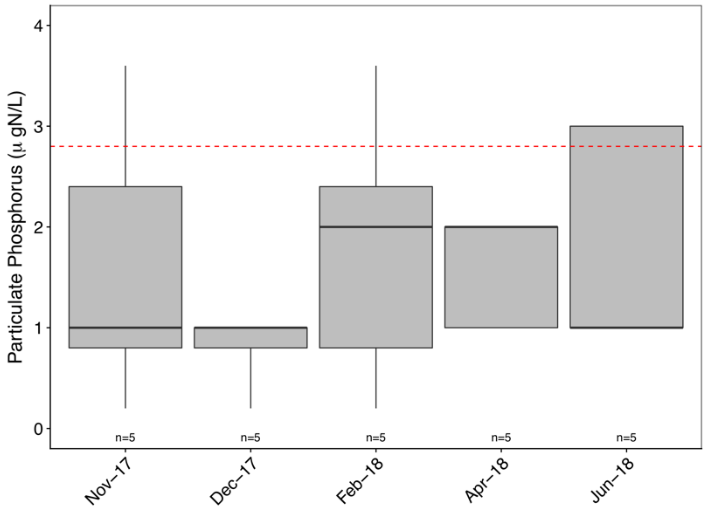

B)

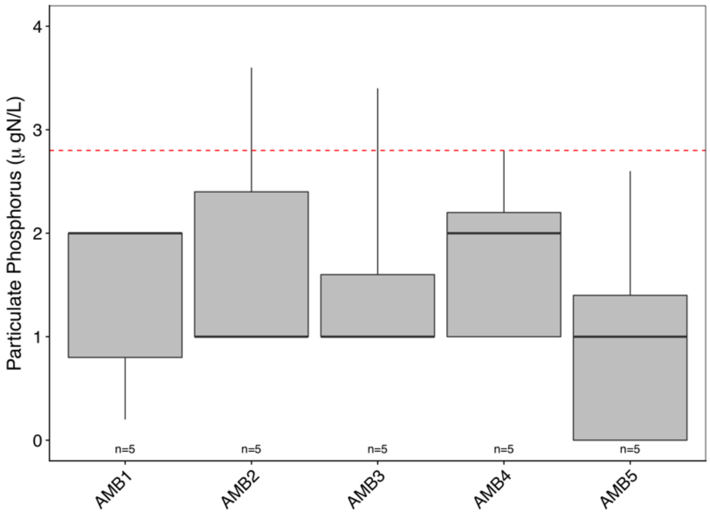

Figure 3.8 Particulate phosphorus box plots: (a) during each survey (sites pooled) from November 2017 to July 2018 and (b) at each site over this same survey period (surveys pooled)

A)

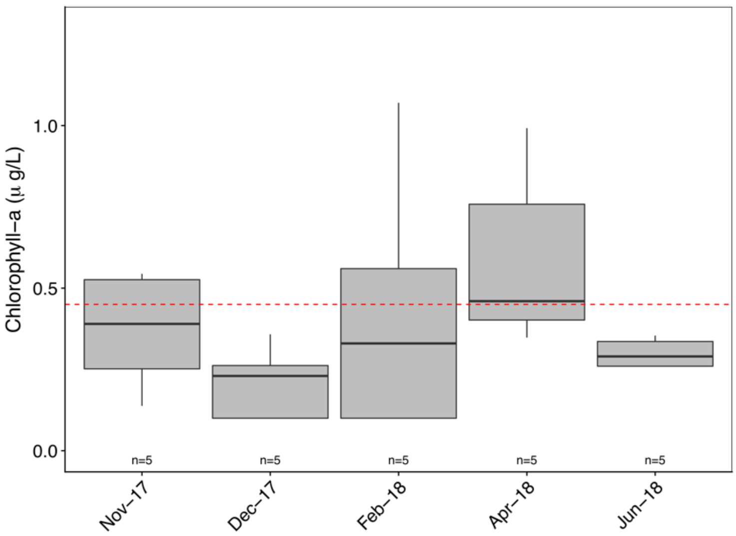

B)

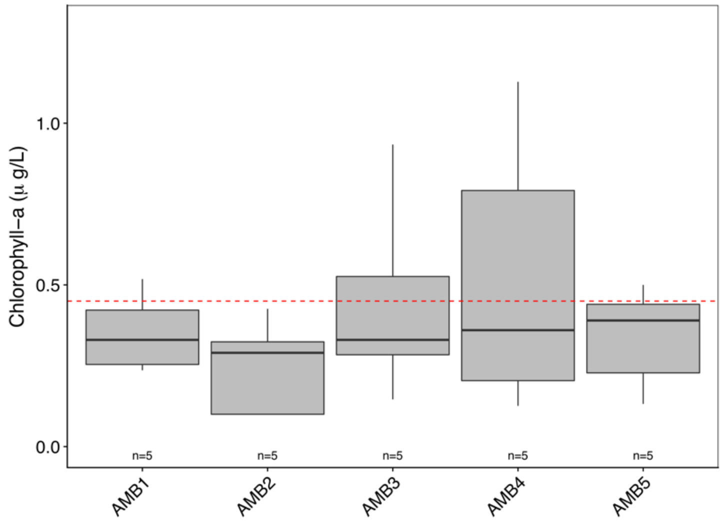

Figure 3.9 Chlorophyll-*a* box plots: (a) during each survey (sites pooled) from November 2017 to July 2018 and (b) at each site over this same survey period (surveys pooled)

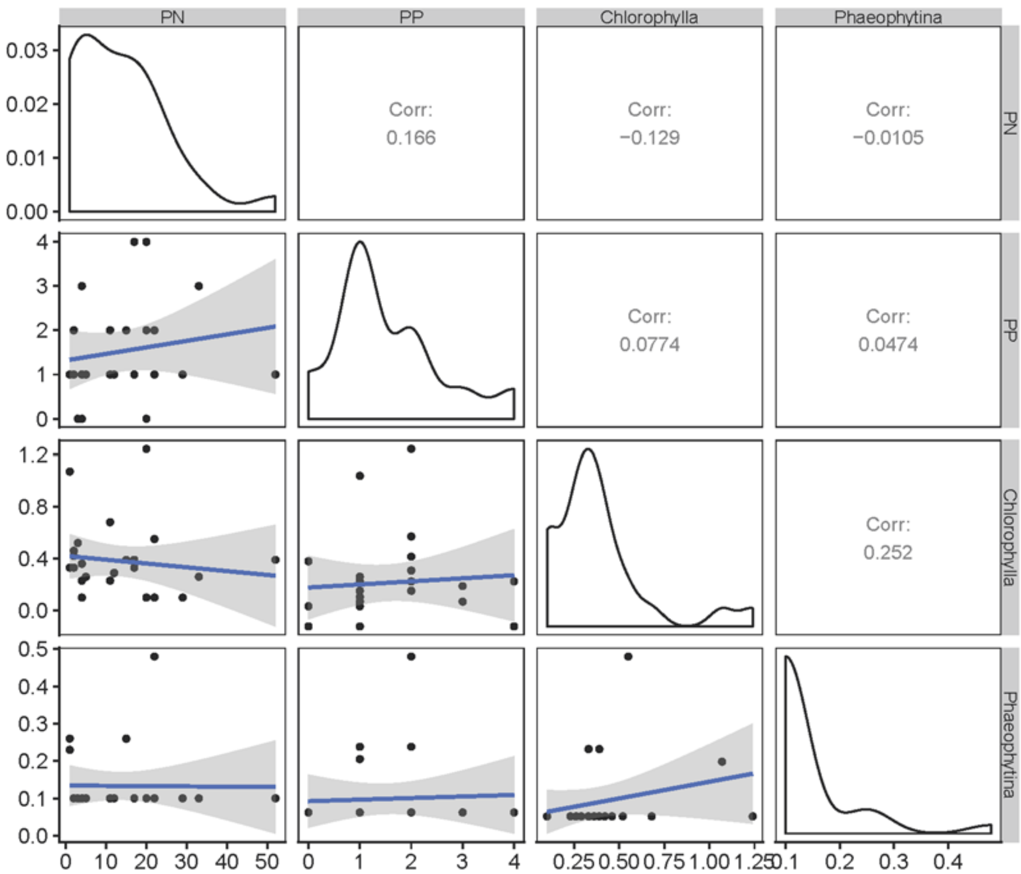

Figure 3.10 Scatterplot of nutrient relationships at pooled across all sites and surveys. Lines of best fit with 95% confidence intervals are displayed in blue, and correlation coefficients are shown in corresponding plots. Density plots show the distribution of the data.

3.1.3 Ultra-trace water heavy metals

Ultra-trace heavy metal concentrations were compared to the ANZECC and ARMCANZ 2000 water quality guidelines (ANZECC, 2000). The filterable metals were not detected above the Limit of Reporting (LOR) (Table 3.1). However, note that ANZECC guidelines have not been established for arsenic. Arsenic is released into the environment naturally by weathering of arsenic-containing rocks and volcanic activity. It can be in the form of As (III) or As (V), which can be toxic to marine aquatic life. A low reliability marine guideline trigger value of 4.5 µg/L for As (V) and 2.3 µg/L for As (III) has been derived (ANZECC, 2000), however, these trigger guidelines are only an indicative interim working level. Although Arsenic was detected, the measured concentrations were below low reliability guidelines, and similar values have recorded consistently at these sites since mid 2016. Therefore, Arsenic is likely to be a present naturally in this region. Zinc was undetectable at all sites except for AMB5 (6 ug/L), and future monitoring will determine whether this is an outlier.

Table 3.1 Summary statistics for metals data recorded at all sites during the program. Values are pooled across sites. Values are compared to the ANZECC 95% protection guideline values (2000).

		Arsenic	Cadmium	Copper	Lead	Nickel	Silver	Zinc	Mercury	Tributyltin
	Unit	ug/L	ug/L	ug/L	ug/L	ug/L	ug/L	ug/L	mg/L	ngSn/L
	LOR	-	0.2	1	0.2	0.5	0.1	5	0.001	2
	ANZECC	-	5.5	1.3	4.4	70	1.4	15	0.4	0.006
Apr-18	Mean	1.64	<0.2	<1	<0.2	<0.5	<0.1	3.2	<0.001	-
	Min	1.5	<0.2	<1	<0.2	<0.5	<0.1	<5	<0.001	-
	Max	1.7	<0.2	0.5	<0.2	<0.5	<0.1	6	<0.001	-

3.1.4 Water pesticides and herbicides

The major pesticide and herbicide concentrations were not detected above water quality improvement guidelines for the Great Barrier Reef Marine Park (GBRMPA, 2010) and all detected concentrations were well below the 95% protection values (Table 3.2).

Table 3.2 Summary (average) statistics for pesticides/herbicides recorded at all sites during the program (all values are µg/L). Values are pooled across sites for each survey and compared to the Water Quality Guidelines for the Great Barrier Reef Marine Park (GBRMPA, 2010) 95% protection level

Survey	Guideline	Atrazine ug/L	Ametyn ug/L	Diuron ug/L	Hexazinone ug/L	Tebutryn ug/L
	GBRMPA (2010)	1.4	1.0	1.6	1.2	-
April 2018		0.0005	<0.0002	0.007	0.0015	0.0001

3.1.5 Ordination of data

Spot water quality measurements have been collected at all sites for: water temperature, electrical conductivity, dissolved oxygen (%), pH, nutrients (particulate nitrogen and phosphorus), and chlorophyll-a. In addition to these spot measurements, secchi depth has also been recorded, as a measure of the optical clarity of the water column. These measurements continue to assist in characterising water quality conditions within the water column, among sites and surveys.

Principal components analysis (PCA) was used to explore relationships between physiochemical and nutrient data collected at the water surface at each site during each month of sampling. Results show that 46.6% of the variability among sites and sampling months is explained by physiochemical and nutrient variables (Figure 3.11). Dissolved oxygen levels (DO) and Electrical Conductivity (EC) are negatively correlated, and are not associated with monthly (Figure 3.11a) or seasonal (Figure 3.11b) differences between sites. However, increasing particulate nitrogen levels (PN), Secchi disc depth (m), temperature (°C), and pH are associated with environmental conditions in November 2017 and wet season months (December 2017 and February 2018; Figure 3.11a). Alternatively, increasing levels of particulate phosphorus (PP) and chlorophyll-*a* are associated with environmental conditions in the dry season months of April and June 2018 (Figure 3.11b).

A)

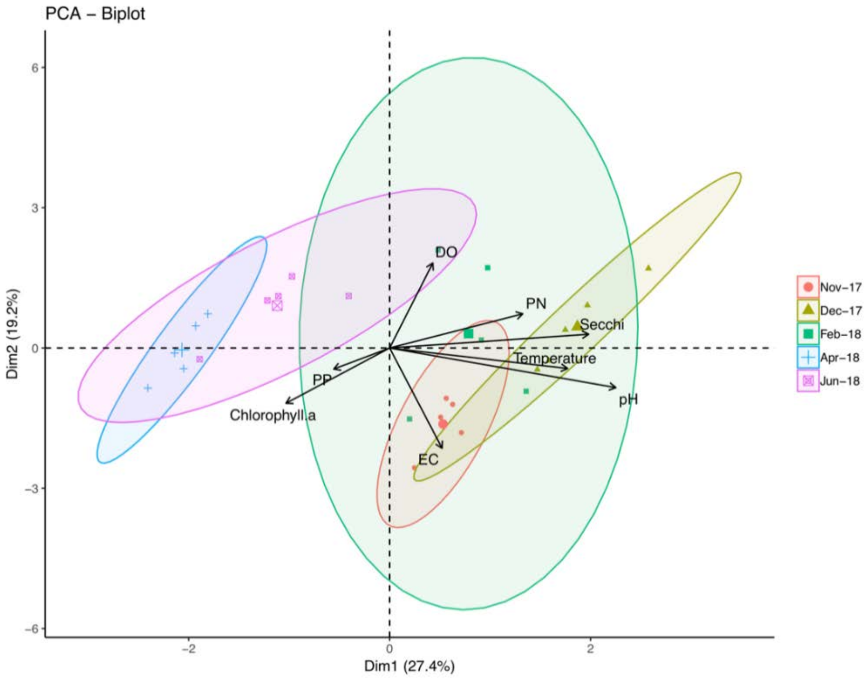

B)

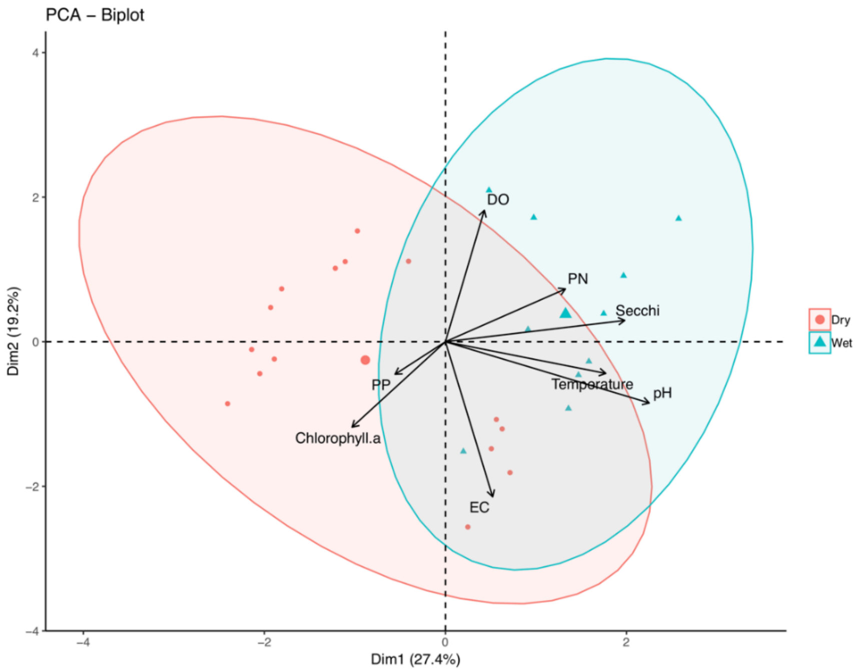

Figure 3.10 Principal components analysis (PCA) exploring relationships between nutrients and physiochemical parameters (black vectors) and monitoring sites. The 95% confidence interval ellipses show overall differences between: A) sites grouped by month and B) sites grouped by season. Vector labels are abbreviated as follows: PP = Particulate Phosphorus, PN = Particulate Nitrogen, EC = Electrical

Conductivity, and DO = Dissolved Oxygen. Total variance explained by Dimension 1 and Dimension 2 = 46.6%

3.2 Plankton communities

3.2.1 Diversity and abundance

A total of 49 phytoplankton species have been identified, comprising cyanobacteria, diatoms, flagellates and green algae taxa. Several species were recorded at all sites, including *Ceratium gibberum, Ceratium trichoceros, Chaectoceros spp, Chlamydomonas spp, Guinardia spp, Hillea spp, Odontella sinesis spp, Phormidium spp, Thalalssionema nitzchioides, and Trichodesmium spp. Trichodesmium spp*. were generally the most abundant phytoplankton species recorded across all sites. AMB2 had the highest phytoplankton species richness in November 2017 (28 species), while the lowest diversity was recorded in February 2018 at AMB3 and AMB5 (8 species) (Figure 3.12a). There were large increases in phytoplankton abundance at AMB1 and AMB4 in November 2018 and February 2018, respectively (Figure 3.12b). These peaks can be attributed primarily to increases in *Trichodesmium spp* (Figure 3.12b).

A)

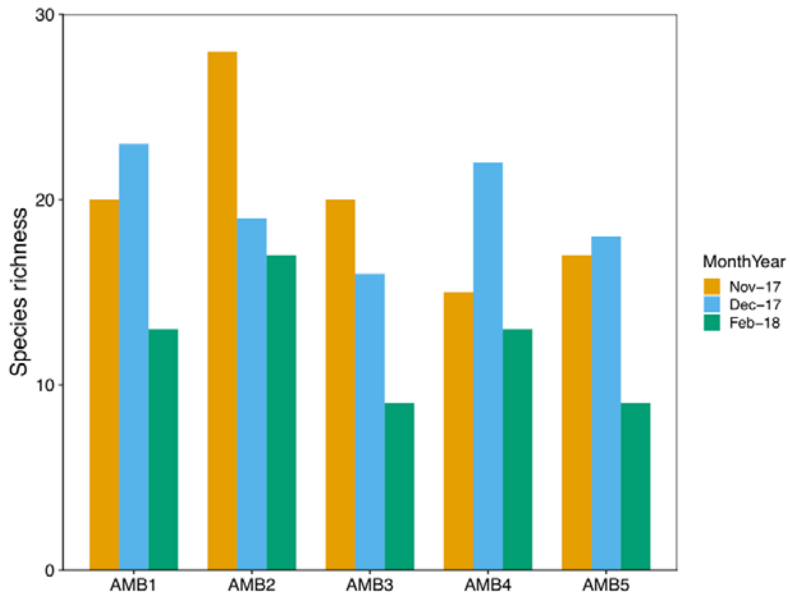

B)

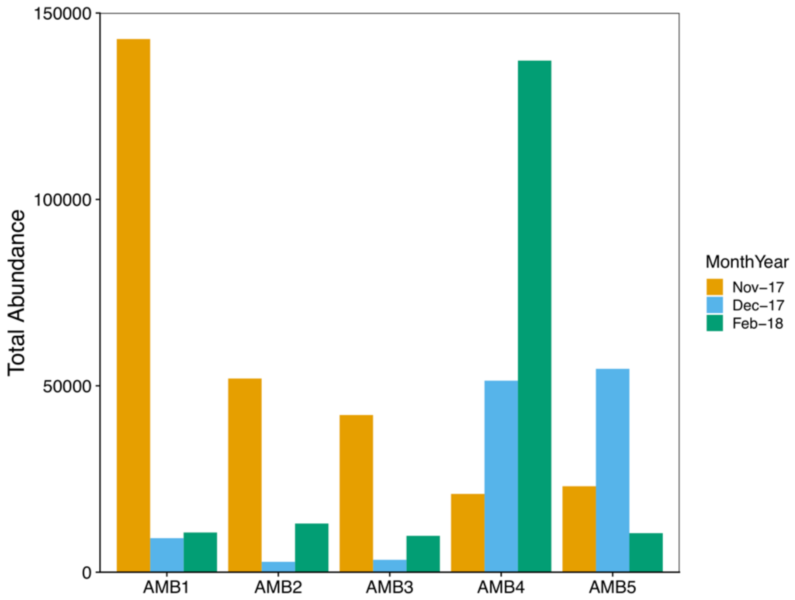

Figure 3.12 a) Species richness of phytoplankton; and b) total abundance of phytoplankton at each site during the following survey periods: November 2017, December 2017, and February 2018

A total of 27 different species of zooplankton were recorded during all surveys. Several species were recorded at all sites, including *Acartia pacifica, Calanopia elliptica, Dictocysta spp, Echinoidea spp, Gastropoda, Penaeus spp, Portunidae, Flaccisagitta enflata*, *Favella serrata*, and Siphonophorae. AMB1 had the highest diversity of zooplankton species in December 2017 (16 species) (Figure 3.13a). Alternatively, AMB3 had the lowest diversity of zooplankton species, also in December 2017 (5 species) (Figure 3.13b). The highest abundance of zooplankton was recorded in November 2017 at AMB4, mainly due to high numbers of *Acanthometra spp, Calanopia elliptica, and Echiniodea* (Figure 3.13b). Zooplankton abundance was relatively low at all sites during February 2018 and at AMB3 (Figure 3.13b).

A)

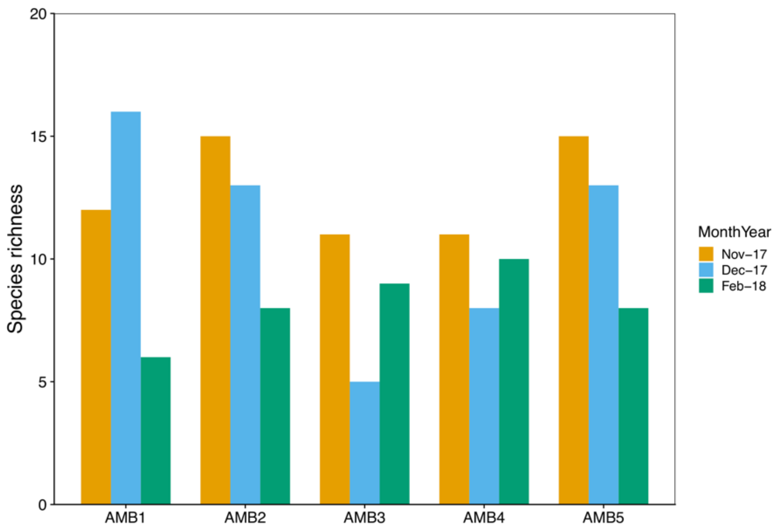

B)

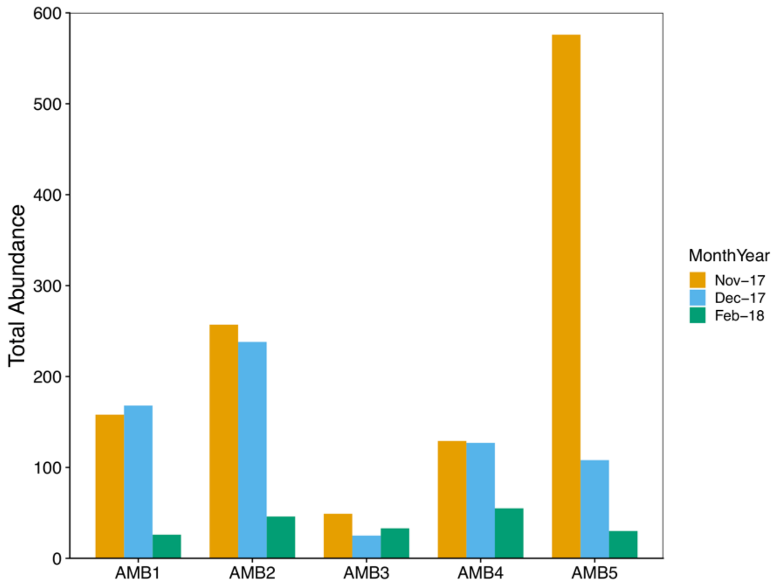

Figure 3.13 a) Species richness of zooplankton and b) total abundance of zooplankton at each site during the following survey periods: November 2017, December 2017, and February 2018

3.2.1 Plankton ordinations

Exploratory statistical analysis of the plankton using non-dimensional scaling (nMDS) revealed differences in species composition of phytoplankton (Figure 3.14) and zooplankton (Figure 3.15) between survey periods. Overlap of 95% confidence interval ellipses suggests that phytoplankton and zooplankton communities were most similar in their species composition during November and December 2017, and relatively distinct in February 2018 (Figure 3.14, 3.15). It is possible that the unique plankton communities are associated with the large river discharge event in February 2018.

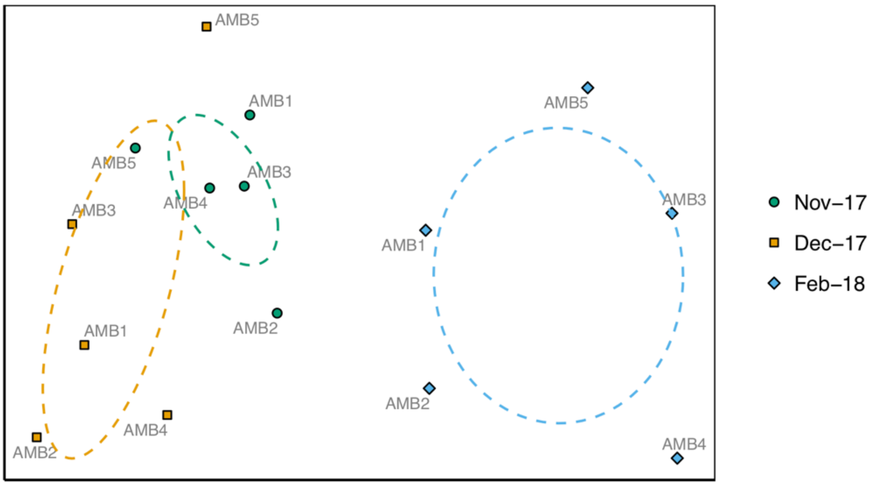

Figure 3.14 Non-dimensional ordination plot for phytoplankton collected during three surveys throughout 2017-2018. Dashed lines represent 95% confidence interval ellipses for each survey period. Data has been squared root transformed on the Bray Curtis distance matrix (stress = 0.15, Clarke and Gorley 2006)

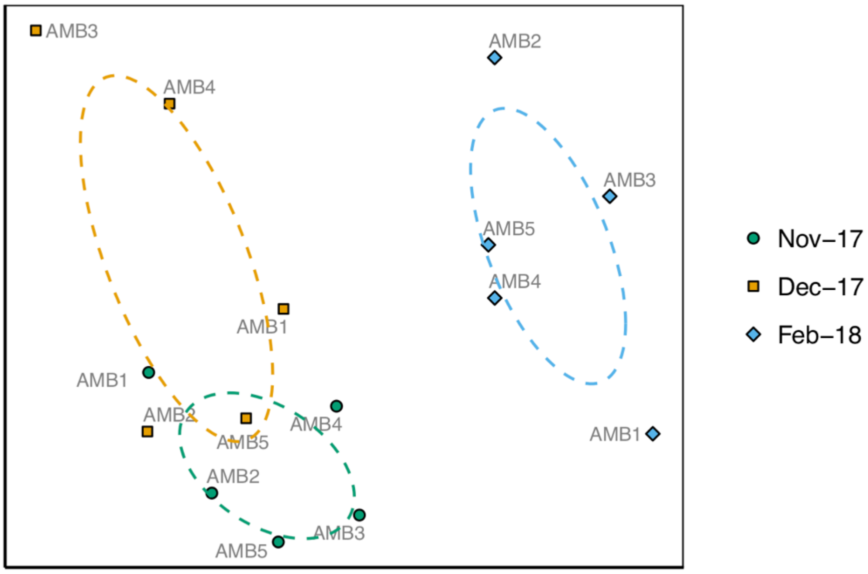

Figure 3.15 Non-dimensional ordination plot for zooplankton collected during three surveys throughout 2017-2018. Dashed lines represent 95% confidence interval ellipses for each survey period. Data has been squared root transformed on the Bray Curtis distance matrix (stress = 0.13, Clarke and Gorley 2006)

3.3 Multiparameter water quality logger

Instruments were deployed at five sites, AMB 1 to 5, from November 2017 to July 2018 (see Table 1.1). Using standard statistics, we describe observed trends and differences between sites and discuss the driving forces in these environments.

Data is presented throughout the text (and in attached appendices) in a time series format, monthly and yearly statistical summaries. The box plots provide a visual representation of the descriptive statistics for Suspended Sediment Concentration (SSC), deposition rate (mg cm^{-2} day^{-1}), water temperature (°C), RMS water height (m) and PAR (mol m^{-2} day^{-1}). In the box plots, the central diamonds represent the mean value, the central line represents the median value and the central box represents the range of the middle two quartiles. The vertical bars represent the range of the 90th percentile and 10th percentile data points.

3.3.1 RMS water height

RMS water height values are mostly driven by weather events and this is clearly evident in the data as peaks in RMS water heights are observed at the same times at all sites over the survey year. Variation in the magnitude of RMS water height values during peak events and during non-event periods differs among sites due to differences in water depth and site exposure to wave energy. Figure 3.16 provides a box plot of the yearly statistics of RMS at sites. All sites had similar RMS values, ranging from medians of 0.014 m to 0.025 m. AMB2 had the lowest values with a median RMS of 0.014.

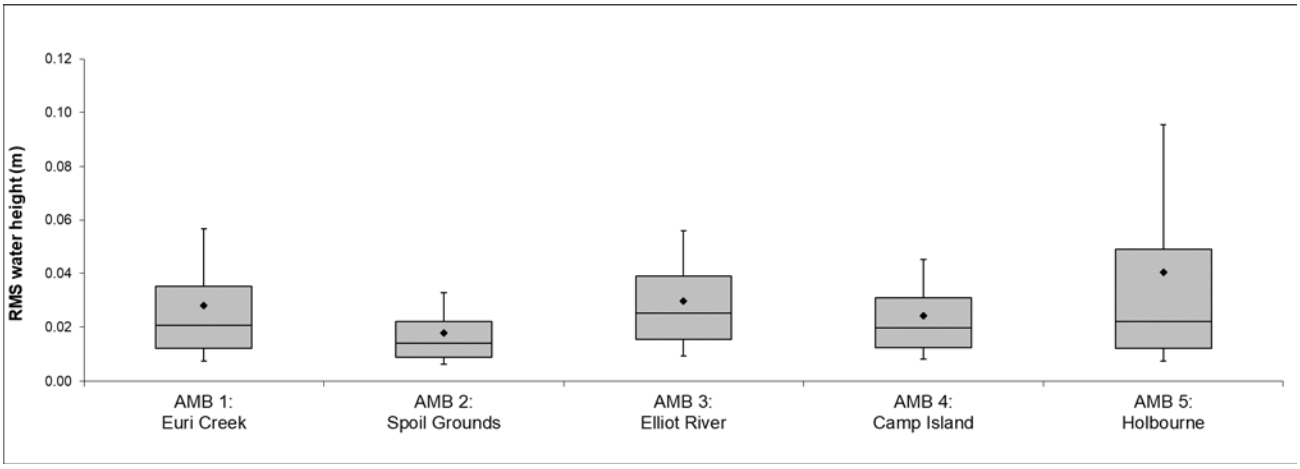

Figure 3.16 Box plot of RMS water height (m) at the five sites for the monitoring period from November 2017 to July 2018

Table 3.2 Summary of RMS water height (m) statistics at the five sites for the monitoring period from November 2017 to July 2018

Site	AMB 1: Euri Creek	AMB 2: Spoil Grounds	AMB 3: Elliot River	AMB 4: Camp Island	AMB 5: Holbourne
Mean	0.028	0.018	0.030	0.024	0.040
Median	0.021	0.014	0.025	0.020	0.022
Minimum	0.000	0.000	0.000	0.000	0.000
Lower quartile	0.012	0.009	0.015	0.012	0.012
Upper quartile	0.035	0.022	0.039	0.031	0.049
Maximum	0.345	1.832	0.223	0.317	0.875
90th percentile	0.057	0.033	0.056	0.045	0.096
10th percentile	0.007	0.006	0.009	0.008	0.008
n	34201	16780	34347	19194	25347
St. Dev	0.025	0.019	0.020	0.018	0.049
St. Error	0.000	0.000	0.000	0.000	0.000

Figure 3.17 provides an example of when weather driven wave energy in combination with tide are evident in the RMS data for AMB3 during the reporting period. Figure 3.17 shows several large spikes in RMS water height throughout the displayed period. These spikes are the result of weather driven wave events and are followed by periods where RMS water height falls to its background value as the weather events pass. Comparing the 12-point averaged trend line with the water depth data shows a similar periodicity in the RMS water height and water depth data. It is interesting to note that a reduction in water depth does align with the periodic peaks in RMS water height and it is thought that other factors such as current and changes in the sites exposure at different tides alters the wave dynamics of the site. This will be explored further in future year's reports by comparing more sheltered sites with those that are more exposed to wind and wave energy.

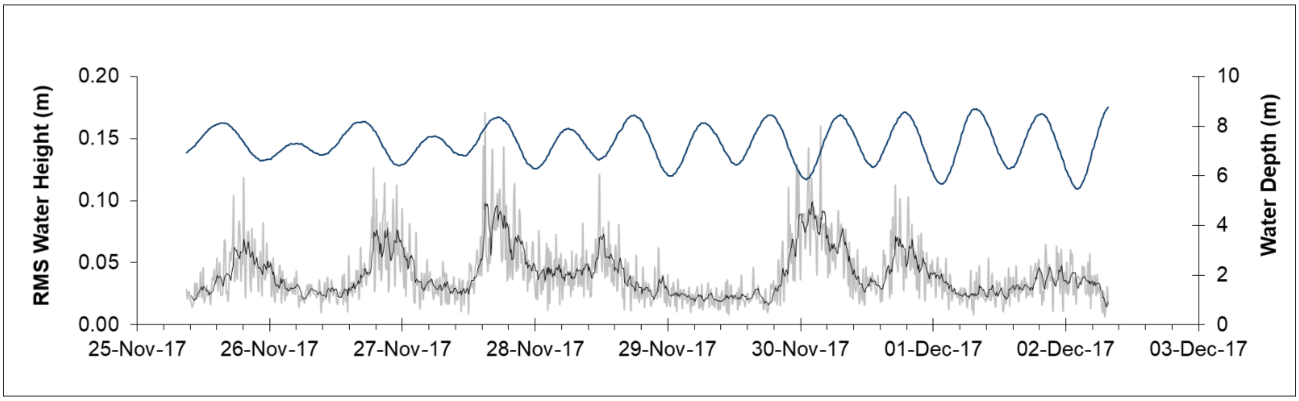

Figure 3.17 Elliot River (AMB 3) RMS water height (gray), 12 point moving average RMS trend line (black) and water depth (blue). Data shows periodic wave events followed by calmer periods

3.3.2 NTUe/SSC

The NTUe/SSC time series data at each site (seen in the appendix) follows a typical pattern of low background values with recurring peak events. These peak events occurred at the same times at each site and coincide with peaks in RMS water height. This is a typical pattern which is similar to data collected in coastal locations in north Queensland by the James Cook University Marine Geophysics group (Ridd et al., 2001). Yearly statistical values and individual peak values differ between sites. These differences are the result of variation in influencing factors such as RMS water height, site depth, benthic geology, hydrodynamics and proximity to river mouths. Figure 3.18 provides a box plot of the yearly statistics of SSC values at sites, while Table 3.3 summaries the same yearly statistics.

Both AMB3 and 5 show high variance with standard deviations of 33 and 28 respectively. These sites also have high mean SSC values (13.4 and 11.0 mg/l), however their medians are similar to the other sites. All median SSC levels are below 2.3 mg/l. This indicates that while AMB 3 and 5 have high SSC events, overall SSC levels are very similar to the other sites.

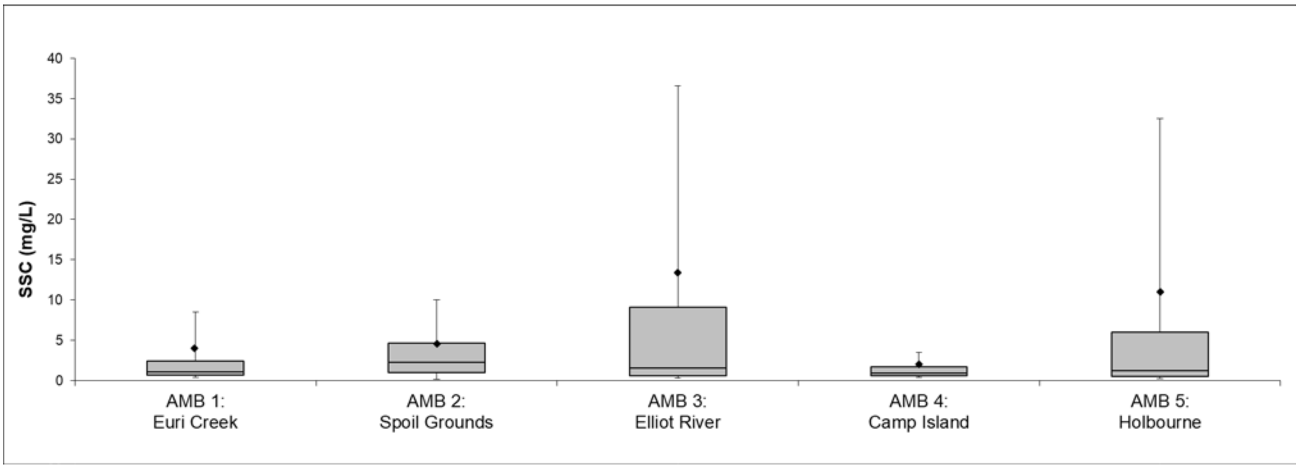

Figure 3.18 Box plot of SSC (mg/L) at the five sites for the monitoring period from November 2017 to July 2018

Table 3.3 Summary of SSC (mg/L) statistics at the seven sites for the monitoring period from November 2017 to July 2018

Site	AMB 1: Euri Creek	AMB 2: Spoil Grounds	AMB 3: Elliot River	AMB 4: Camp Island	AMB 5: Holbourne

Mean	4.03	4.56	13.40	2.00	11.03
Median	1.05	2.24	1.56	0.91	1.25
Minimum	0.00	0.00	0.00	0.00	0.00
Lower quartile	0.63	1.01	0.58	0.57	0.54
Upper quartile	2.39	4.64	9.06	1.73	5.99
Maximum	137.59	272.12	372.29	90.36	344.04
90th percentile	8.48	10.01	36.58	3.45	32.56
10th percentile	0.37	0.11	0.30	0.39	0.22
n	21971	18066	29199	18540	15123
St. Dev	10.64	8.53	32.71	4.40	27.85
St. Error	0.07	0.06	0.19	0.03	0.23

3.3.3 Deposition

Deposition of sediment is a natural process occurring in all coastal marine waters. Suspended sediment naturally deposits in environments where the systems energy is not sufficient to keep it suspended. Deposition of sediment in a marine environment is of interest to environmental monitoring studies when it changes from its natural state. The Water Quality Guidelines for the Great Barrier Reef Marine Park (2010) references De'ath and Fabricius (2008) in noting that 10 mg cm^{-2} day^{-1} sedimentation is valid in areas of coarse sediment, but that where sediments are smaller and of high organic content the trigger limits need to be lower. The guidelines set the sedimentation trigger value at a mean annual value of 3 mg cm^{-2} day^{-1} and a daily maximum of 15 mg cm^{-2} day^{-1}. The statistical summary of the daily average deposition rates for each site are presented in Figure 3.10 as box plots and summarised in Table 3.4.

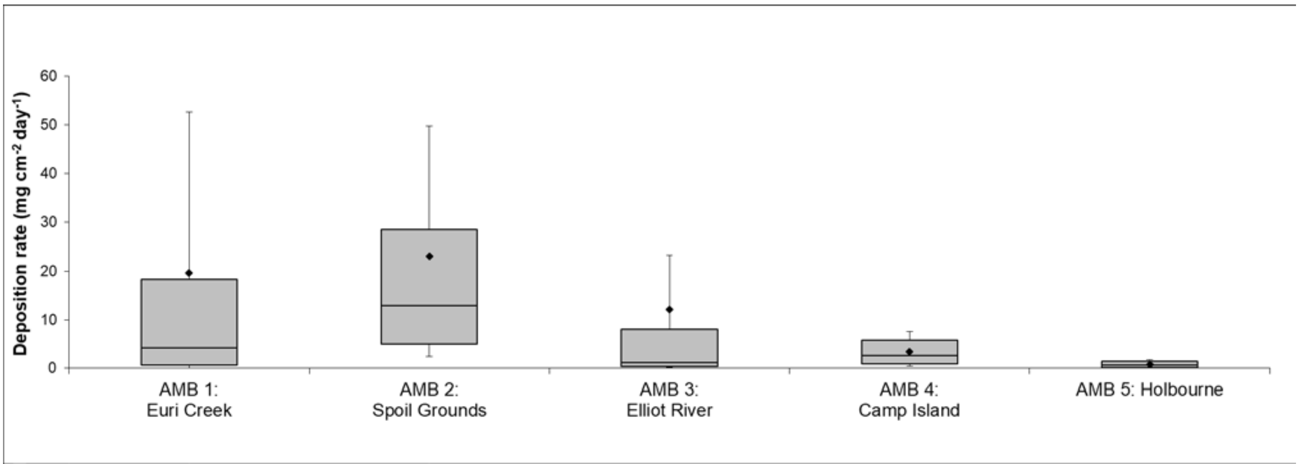

Figure 3.19 Box plot of two-hourly deposition rate (mg/cm^2/day) at the five sites for the monitoring period from November 2017 to July 2018

Table 3.4 Summary of two-hourly deposition rate (mg/cm^2/day) statistics at the five sites for the monitoring period from November 2017 to July 2018

Site	AMB 1: Euri Creek	AMB 2: Spoil Grounds	AMB 3: Elliot River	AMB 4: Camp Island	AMB 5: Holbourne
Mean	19.66	23.13	12.06	3.38	0.82
Median	4.26	12.96	1.13	2.56	0.63
Minimum	0.00	0.17	0.04	0.21	0.00
Lower quartile	0.60	5.00	0.36	0.89	0.06
Upper quartile	18.31	28.51	8.04	5.74	1.38
Maximum	650.91	201.63	370.43	10.50	4.63
90th percentile	52.74	49.75	23.32	7.60	1.75
10th percentile	0.04	2.49	0.12	0.44	0.01

n	745	123	98	74	91
St. Dev	46.38	32.44	42.38	2.90	0.84
St. Error	1.70	2.93	4.28	0.34	0.09

The data indicates that AMB1 and 2 had the greatest deposition with means of 19.66 and 23.13 mg cm^{-2} day^{-1} respectively. Median daily average deposition rates of 4.26 and 12.96 mg cm^{-2} $day^{-1}$are also in the highest values across all sites. Again, it is suggested that the median rather than the mean values be used in analysis to provide an un-skewed value of the data. The median daily average deposition rate ranged from 0.63-12.96 mg cm^{-2} day^{-1} across all five sites. These values may be more easily visualised by calculating them into the thickness of the sediment deposited. For example, using the relationship between density, mass and volume: a deposition value of 5 mg cm^{-2} day^{-1} is equivalent to a layer of sediment of thickness less than 35 µm, assuming a sediment density of 1.5 g/cm3.

It can be seen in the time series deposition data (see appendix) that deposition tends to peak following high RMS water height events but with a lag so that peak deposition occurs at a time when RMS water height has decreased to near background levels. An explanation for this lag is that as waves resuspend sediment, little deposition is expected because the energy in the system will keep the sediment in suspension. It is only when waves decrease and there is no longer enough energy in the system to keep the same quantity of sediment in suspension that deposition begins to occur.

3.3.4 Water temperature

The statistical summary of the water temperature for each site are presented in Figure 3.20 as box plots and summarised in Table 3.5. Water temperature data matched closely among all sites. Seasonal changes in water temperature were apparent, with the mean monthly temperature peaking between December and February at approximately 28.92-28.27 °C (Figure 3.20); a factor that was also observed in the field in-situ water temperature surveys. The lowest mean monthly temperatures were observed between June and July, where values dropped to 23.23-20.85 °C. Decreases in temperature over short time periods match with increases in RMS water depth. Water temperature is generally not considered to be a compliance condition for approval operations, however the temperature data presented here holds importance in future interpretation of ecological processes in the region, and across the GBR (e.g. Johanson et al., 2015).

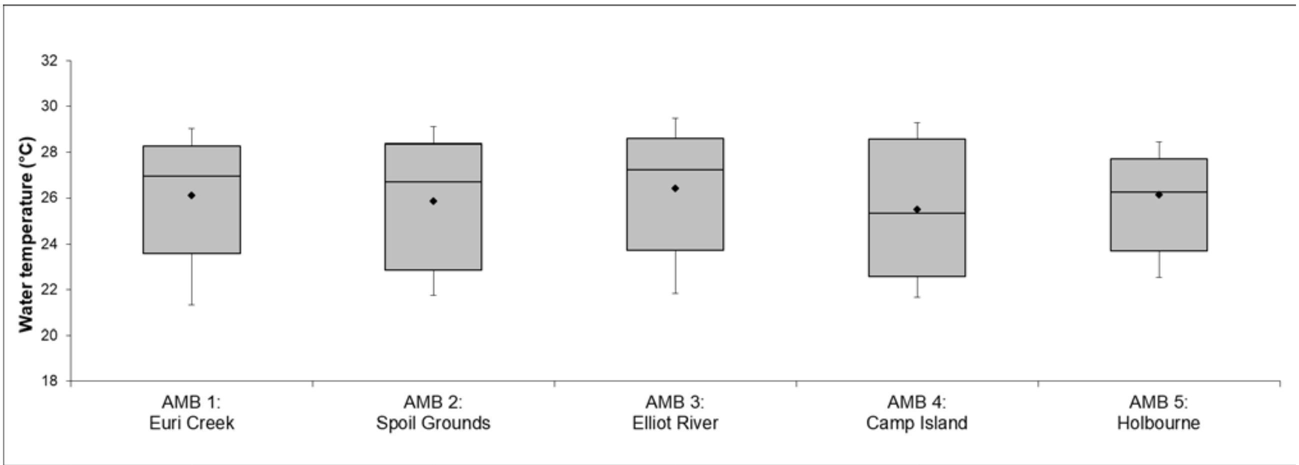

Figure 3.20 Box plot of the water temperature (°C) at the five sites for the monitoring period from November 2017 to July 2018

Table 3.5 Summary of water temperature (°C) statistics at the five sites for the monitoring period from November 2017 to July 2018

Site	AMB 1: Euri Creek	AMB 2: Spoil Grounds	AMB 3: Elliot River	AMB 4: Camp Island	AMB 5: Holbourne
Mean	26.10	25.86	26.41	25.50	26.15
Median	26.95	26.69	27.25	25.34	26.25
Minimum	20.04	19.05	20.54	19.52	20.97
Lower quartile	23.58	22.86	23.72	22.58	23.70
Upper quartile	28.29	28.36	28.59	28.57	27.72
Maximum	30.60	31.37	30.85	32.52	783.00
90th percentile	29.01	29.11	29.46	29.28	28.42
10th percentile	21.33	21.75	21.83	21.65	22.52
n	34201	23961	34347	19360	22195
St. Dev	2.72	2.89	2.76	3.09	13.29
St. Error	0.01	0.02	0.01	0.02	0.09

3.4 Photosynthetically Active Radiation (PAR)

Benthic photosynthetically active radiation (PAR) was monitored at the five sites from November 2017 to July 2018 (Figure 3.21). The statistical summary of the PAR for each site are presented in Figure 3.21 as box plots and summarised in Table 3.7. Mean levels of benthic PAR varied from 1.69 to 4.70 mol m^{-2} day^{-1}. AMB3 and 5 had the greatest variance and highest medians (3.82 and 2.85 mol m^{-2} day^{-1} respectively), which is due to the site locations. These two sites are likely to exhibit similar PAR as they are both located in areas with similar depths of 7-8m and are also likely to hold similar sediment profiles.

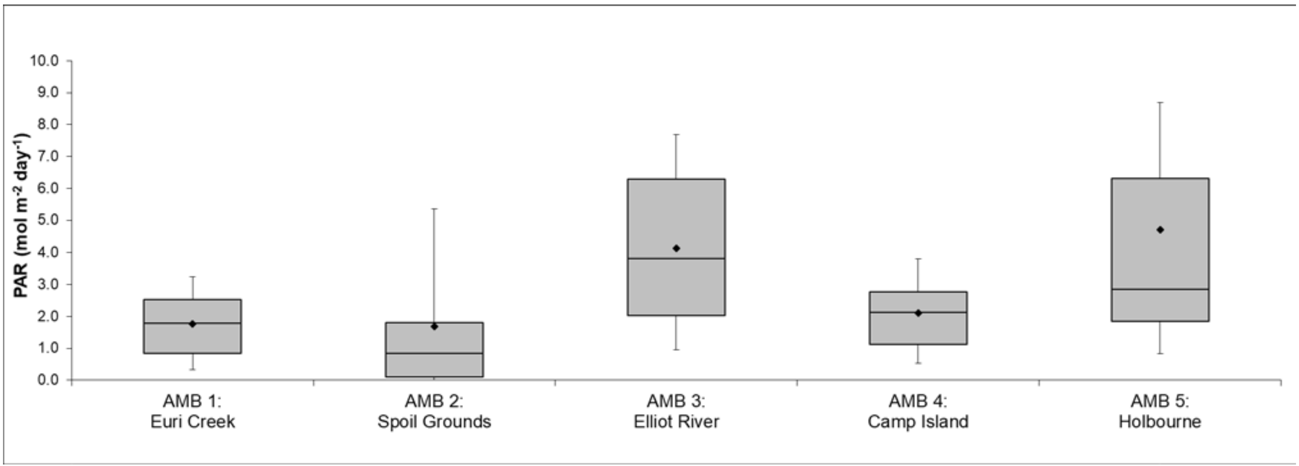

Figure 3.21 Box plot of the daily PAR (mol m^{-2} day^{-1}) at the five sites for the monitoring period from November 2017 to July 2018

Table 3.7 Summary of daily PAR (mol m^{-2} day^{-1}) statistics at the five sites for the monitoring period from November 2017 to July 2018

Site	AMB 1: Euri Creek	AMB 2: Spoil Grounds	AMB 3: Elliot River	AMB 4: Camp Island	AMB 5: Holbourne
Mean	1.76	1.69	4.13	2.11	4.70
Median	1.78	0.84	3.82	2.13	2.85

Minimum	0.00	0.00	0.06	0.01	0.10
Lower quartile	0.84	0.09	2.03	1.13	1.84
Upper quartile	2.52	1.80	6.29	2.77	6.30
Maximum	4.94	10.91	10.68	6.08	24.98
90th percentile	3.25	5.36	7.68	3.81	8.68
10th percentile	0.33	0.01	0.94	0.52	0.83
n	238	163	238	134	176
St. Dev	1.10	2.36	2.59	1.26	4.97
St. Error	0.07	0.18	0.17	0.11	0.37

Using these above summary statistics and graphical representations of the full time series data (Figure 3.22) and monthly variational data (Figure 3.23) per site, we describe trends and temporal differences among sites and investigate possible drivers of significant decreases in PAR.

Benthic PAR was highly variable within sites throughout the year, with peaks and troughs occurring both regularly and intermittently over time. Semi-regular oscillations between low and high PAR levels were overridden by larger episodic events caused by storm or rainfall events.

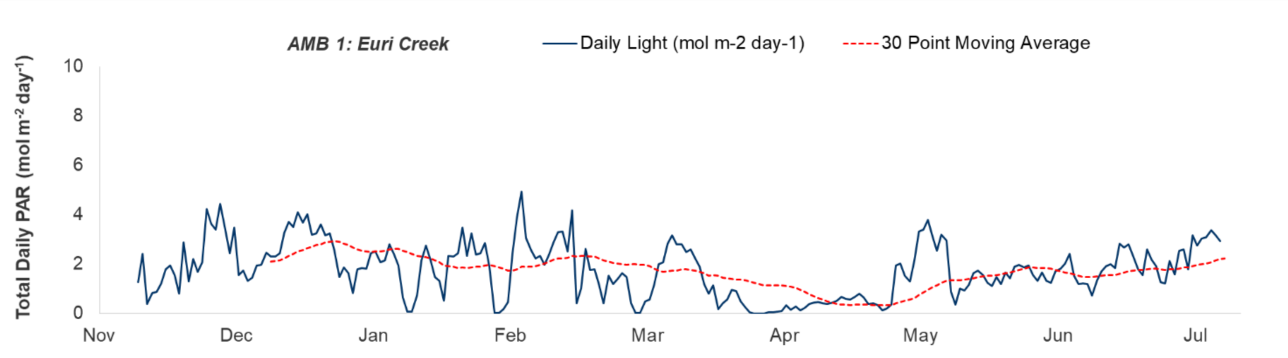
AMB 1: Euri Creek
Daily Light (mol m-2 day-1)
30 Point Moving Average
Total Daily PAR (mol m⁻² day⁻¹)
0
2
4
6
8
10
Nov
Dec
Jan
Feb
Mar
Apr
May
Jun
Jul

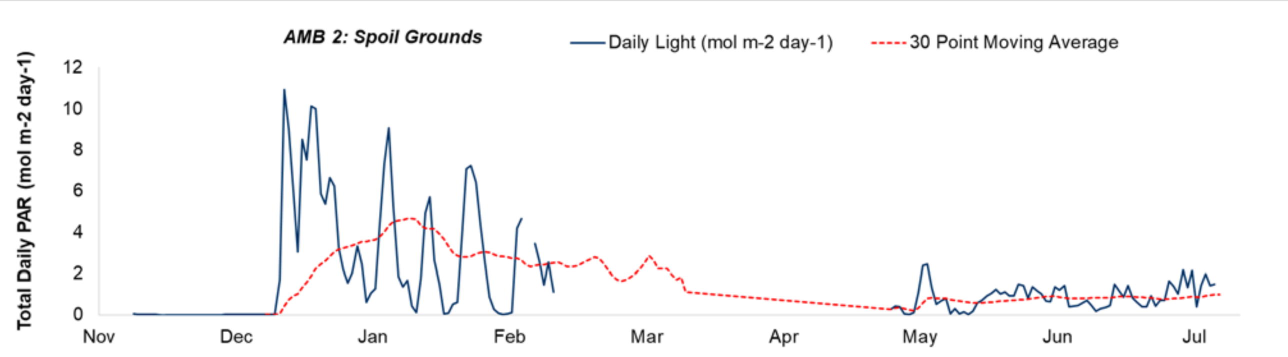
AMB 2: Spoil Grounds
Daily Light (mol m-2 day-1)
30 Point Moving Average
Total Daily PAR (mol m-2 day-1)
0
2
4
6
8
10
12
Nov
Dec
Jan
Feb
Mar
Apr
May
Jun
Jul

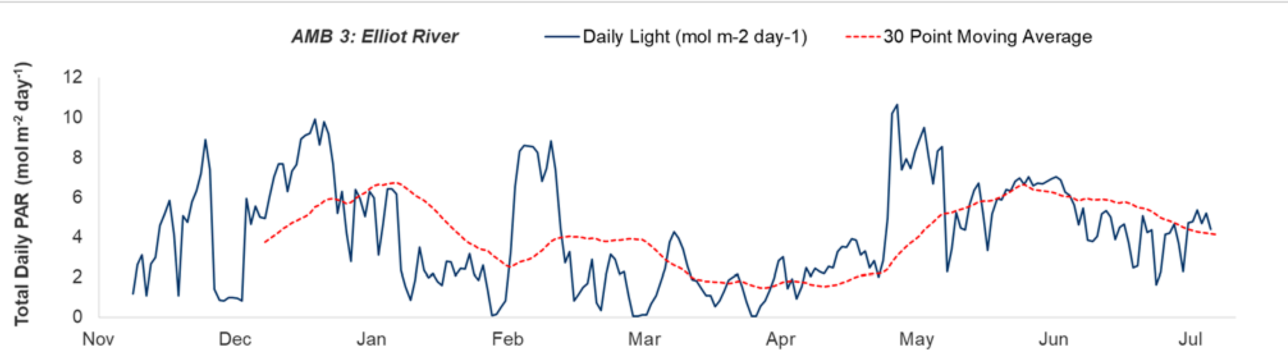
AMB 3: Elliot River
Daily Light (mol m-2 day-1)
30 Point Moving Average
Total Daily PAR (mol m⁻² day⁻¹)
0
2
4
6
8
10
12
Nov
Dec
Jan
Feb
Mar
Apr
May
Jun
Jul

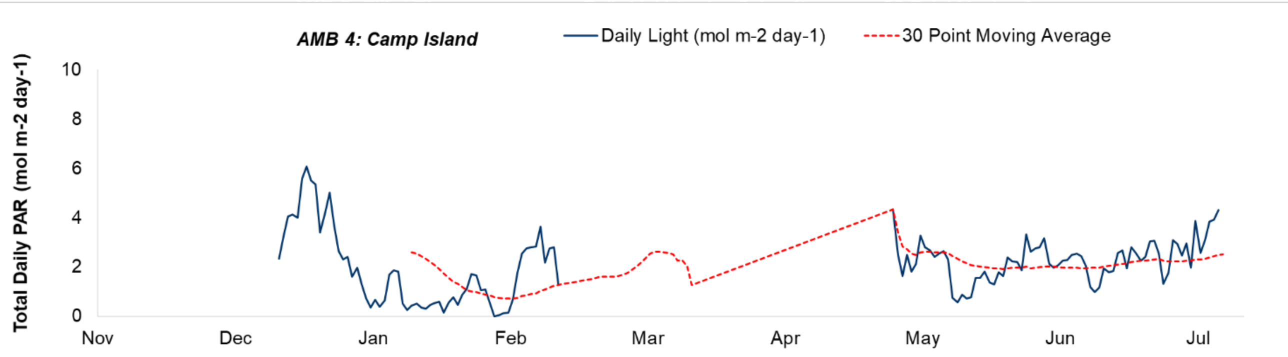
AMB 4: Camp Island
Daily Light (mol m-2 day-1)
30 Point Moving Average
Total Daily PAR (mol m-2 day-1)
0
2
4
6
8
10
Nov
Dec
Jan
Feb
Mar
Apr
May
Jun
Jul

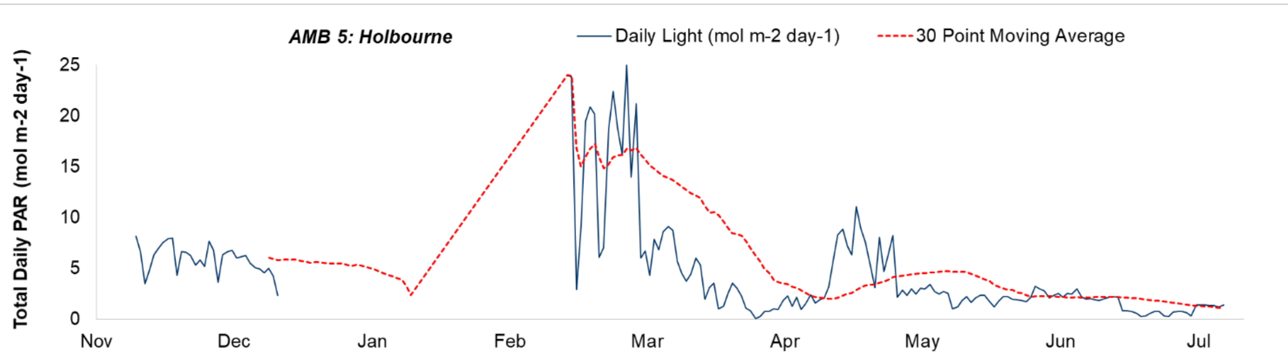
AMB 5: Holbourne
Daily Light (mol m-2 day-1)
30 Point Moving Average
Total Daily PAR (mol m-2 day-1)
0
5
10
15
20
25
Nov
Dec
Jan
Feb
Mar
Apr
May
Jun
Jul

Figure 3.22 Time series of mean total daily PAR (mol m-2 day-1) recorded at all sites for the monitoring period from November 2017 to July 2018. Note that there were significant data losses mainly due to instrument losses and mechanical failures.

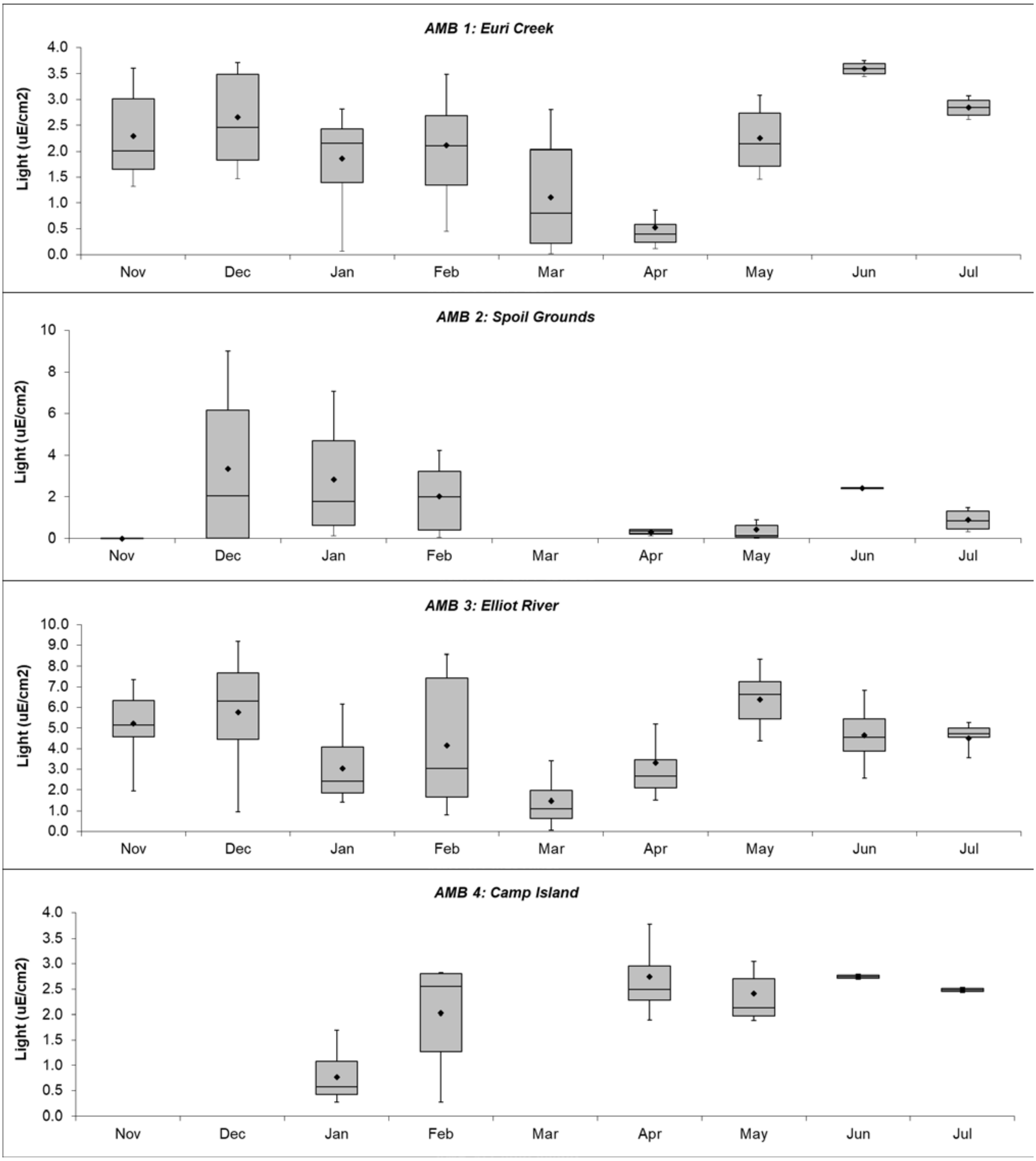

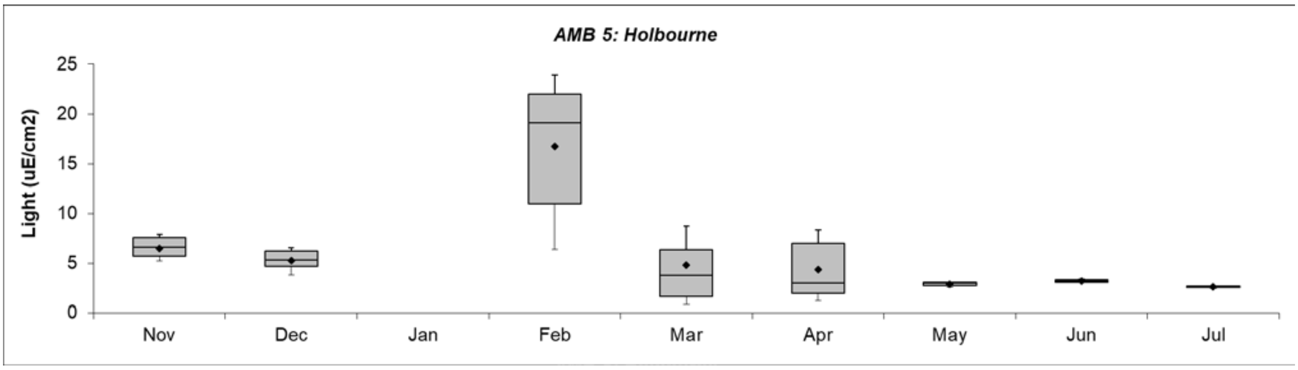

Figure 3.23 Monthly boxplots illustrating the variation in total daily PAR (mol photons m2 day -1) at the five representative sites

3.4.1 Similarities in patterns of PAR among sites

As sites were located at various depths below the lowest astronomical tide datum (LAT), direct comparisons of PAR among sites are not statistically valid. Therefore, the similarity in patterns of PAR over time among different sites was compared by plotting total daily PAR to examine the strength of the relationship using pairwise comparisons (Figure 3.24). The strength of the linear relationship between sites was measured using an R^2 value shown on each pairwise scatterplot.

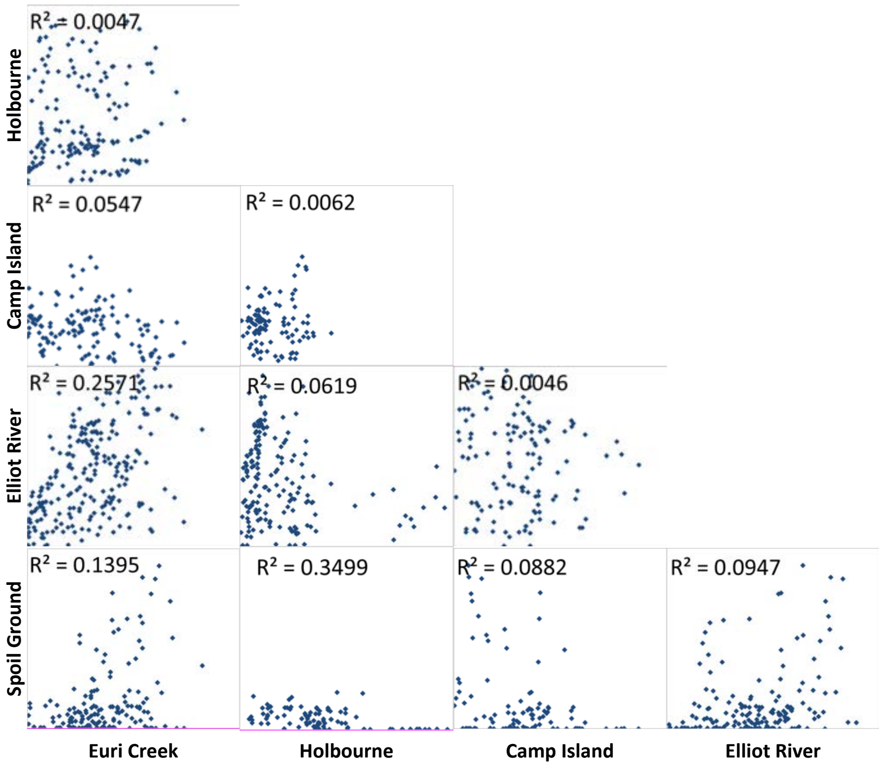

Figure 3.24 Scatterplots of the pairwise comparisons among sites indicating the strength of the relationships between patterns of daily PAR. R^2 values are presented for each comparison

Relationships in patterns of benthic PAR are found among distant coastal sites that were located in similar environments. None of the correlations were very high. Holbourne and Spoil Ground have the highest correlation, $R^2 = 0.35$. Elliot River and Euri Creek have the second highest correlation, $R^2 = 0.26$, which is expected due to similar site characteristics. Camp Island exhibited the least similarities among other coastal sites with very weak relationships in pairwise comparisons. This analysis assists in understanding site redundancy opportunities, without missing important detail in characterising water quality in the region.

3.4.2 Relationship between light attenuation and suspended solid concentrations

In sediment-rich coastal waters, the dominant physical process that reduces PAR light intensity is scattering, which if turbidity levels are high enough, can cause underwater light to become isotropic. Investigations into the light attenuation coefficient provides an insight into the dynamic relationship between suspended solid concentrations and PAR light intensities.

Absorption and scattering describe the attenuation of light through water by interacting in a nonlinear and complex fashion within the radiative transport equations (Mobley 1994). These equations cannot be solved analytically; however the diffuse attenuation coefficient (k_d) (averaged across the PAR waveband 400-700 nm) may be approximated in ocean waters by using Beer-Lambert's law (Gordon 1989; Dennison et al. 1993; Kirk 1994),

$$\boldsymbol{I_z = I_{z0} e^{-k_d(z-z_0)}}$$

where I_{z0} and I_z are the downward directed irradiances at an upper depth (z_0) and a lower depth (z) respectively, and k_d is the diffuse attenuation coefficient (averaged across the PAR waveband 400-700 nm) (Jerlov 1976; Kirk 1977). k_d is comprised of a component due to clear water and a component due to SSC.

Light attenuation and suspended sediment concentration (*SSC*) are examined for all five sites. A general relationship is found, whereby as SSC increases, light levels decrease exponentially, as is well described by Beer-lambert's Law. An example of this relationship can be seen in Figure 3.25 where during periods of high SSC, light is attenuated and when SSC exceeds approximately 10 mg/L, light extinction occurs.

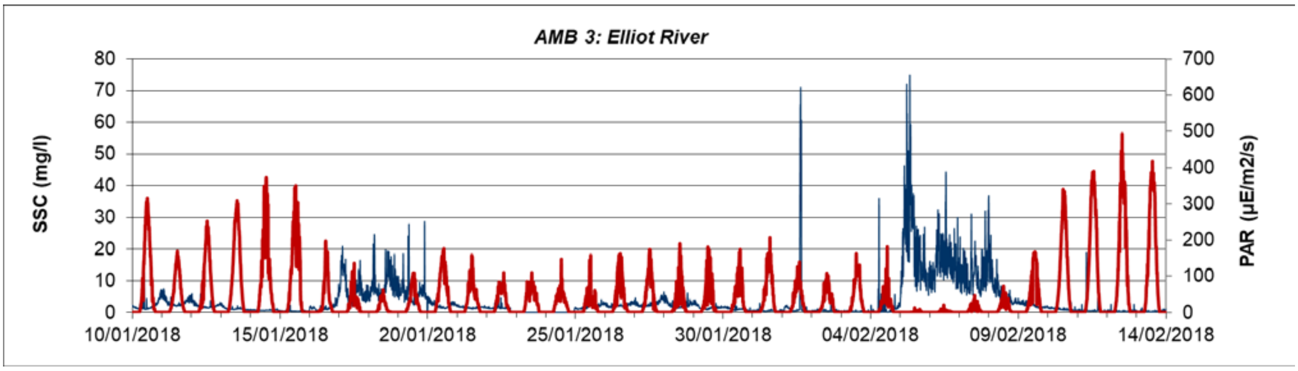

Figure 3.25 A typical example of the relationship between SSC and PAR light, showing light levels decreasing as SSC increases during March-April 2018 at Elliot River

3.4.3 Current meter

Current meter data was collected at all five sites. Marotte HS current meter instruments were deployed for the full monitoring period from November 2017 to July 2018 for sites AMB 2, 3, 4 and 5; however, only a month long deployment from November 2017 to December 2018 was made for AMB 1 (Euri Creek).

The current meter data indicates the prominent current direction and velocity at each site. Data shows that coastal current, tidal current or a combination of both influence current direction and magnitude. The figures below display the current meter data in current rose and average current speed rose diagrams. The current rose diagrams provide a visual representation of relative prominence of current velocity and direction. The average current speed rose diagrams displays the average current speed in every direction. Presented together these diagrams highlight the prominent direction of current and the average velocity of the current in this direction.

A video illustrating how the current speed and direction changes over time at each site is shared privately on YouTube: https://www.youtube.com/watch?v=fmyrrZHkAbM

AMB 1: Euri Creek

The current at Euri Creek ranges from SSE to WNW with peaks at SSE and SW and average velocities are between 0.1 m/s and 0.3 m/s (as shown in Figures 3.26 and 3.27). This shows that the current is flowing along the coast. Changes in current velocity are likely the result of tidal current influence.

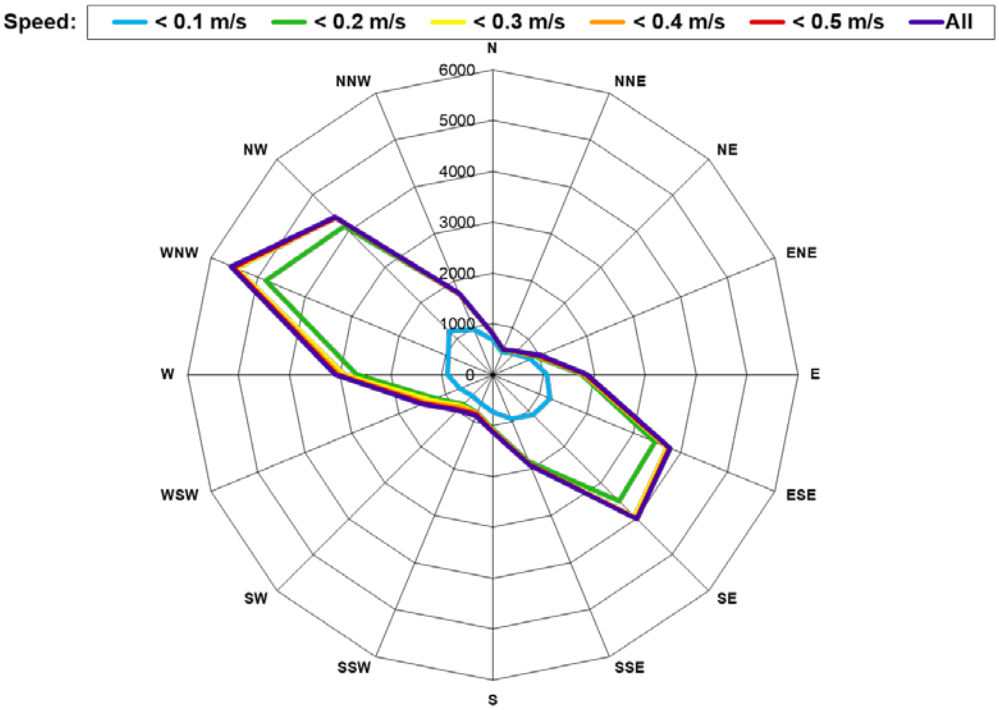

Figure 3.26 Current rose at Euri Creek (AMB 1) for the monitoring period from November 2017 to July 2018. The current rose plots the number of currents recorded in each direction within the ranges of different current speeds (*cs*) indicated in the legend

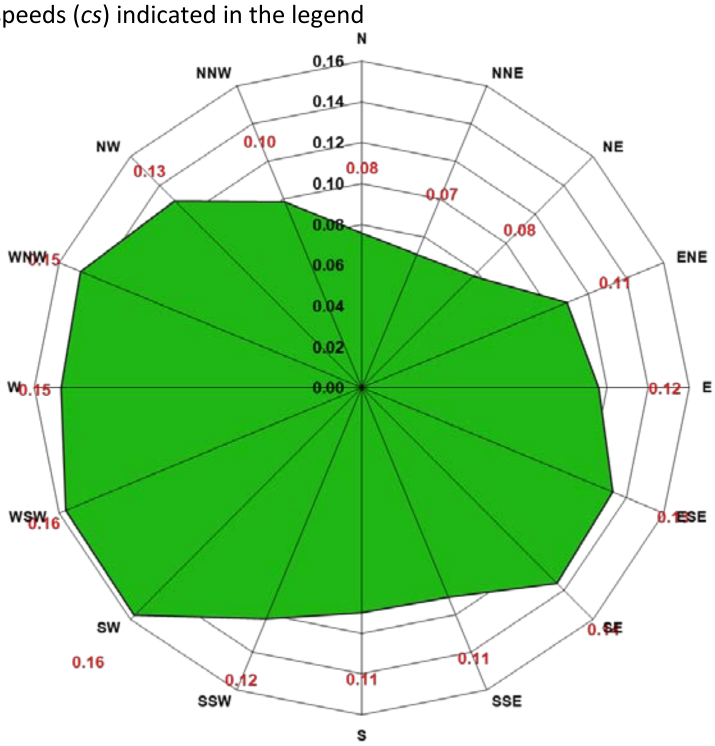

Figure 3.27 Average current speed rose at Euri Creek (AMB 1) for the monitoring period from November 2017 to July 2018. The average current speed is rose is coloured in green, while the red values indicate the average current value at each specific direction

AMB 2: Spoil Grounds

The current at the spoil grounds ranges from SSE to WNW with peaks at SSE and SW and average velocities are between 0.1 m/s and 0.3 m/s (as shown in Figures 3.28 and 3.29). This corresponds to the sites position away from the coast where the tidal currents would be expected to rotate with the changing tides.

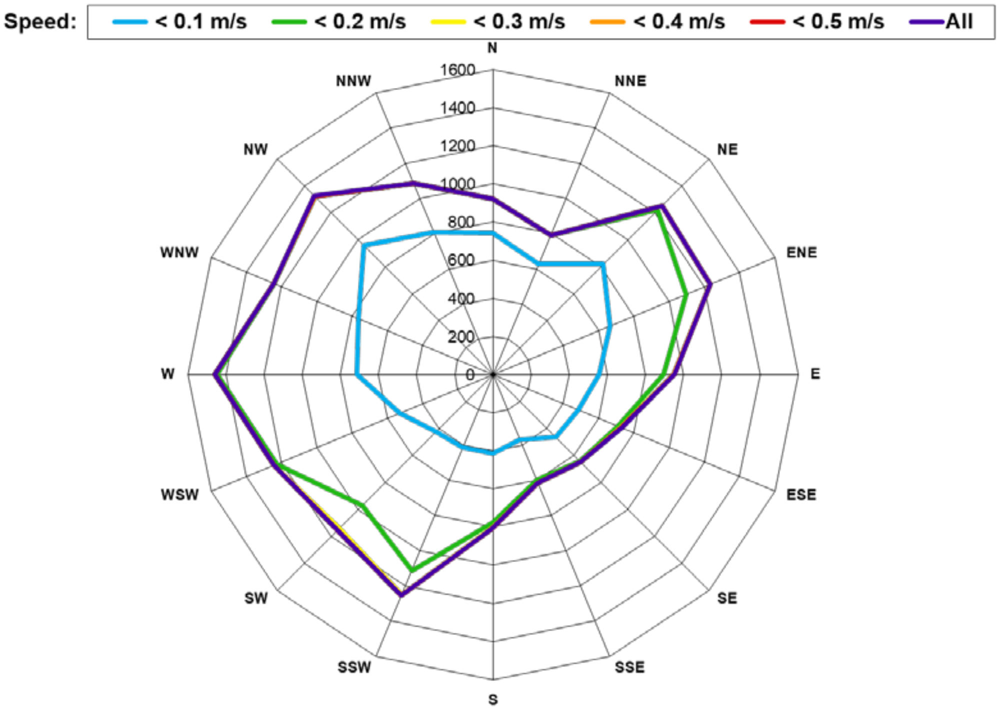

Figure 3.28 Current rose at Camp Island (AMB 4) for the monitoring period from November 2017 to July 2018. The current rose plots the number of currents recorded in each direction within the ranges of different current speeds (*cs*) indicated in the legend

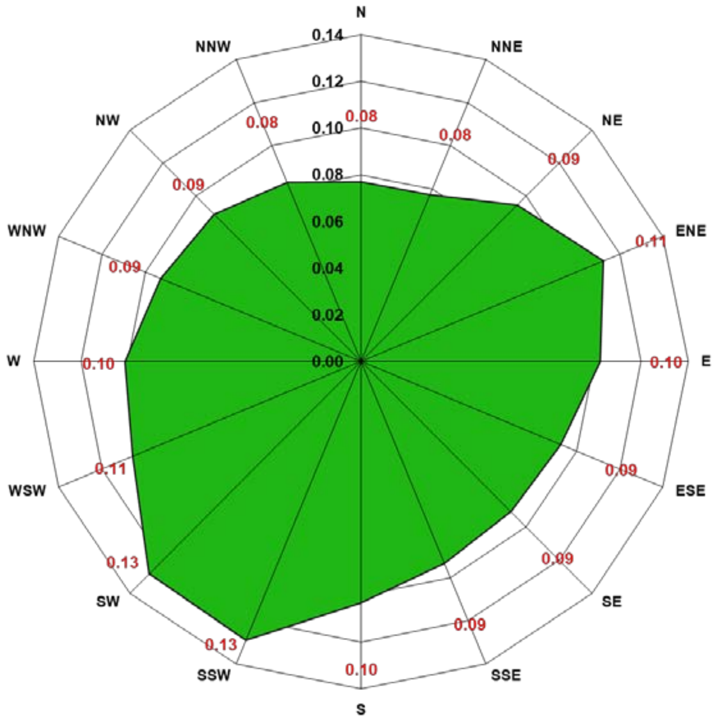

Figure 3.29 Average current speed rose at Camp Island (AMB 4) for the monitoring period from November 2017 to July 2018. The average current speed is rose is coloured in green, while the red values indicate the average current value at each specific direction

AMB 3: Elliot River

The current at Elliot River ranges from SSE to WNW with peaks at SSE and SW and average velocities are between 0.1 m/s and 0.3 m/s (as shown in Figures 3.30 and 3.31). This shows that the current is flowing along the coast. Changes in current velocity are likely the result of tidal current influence

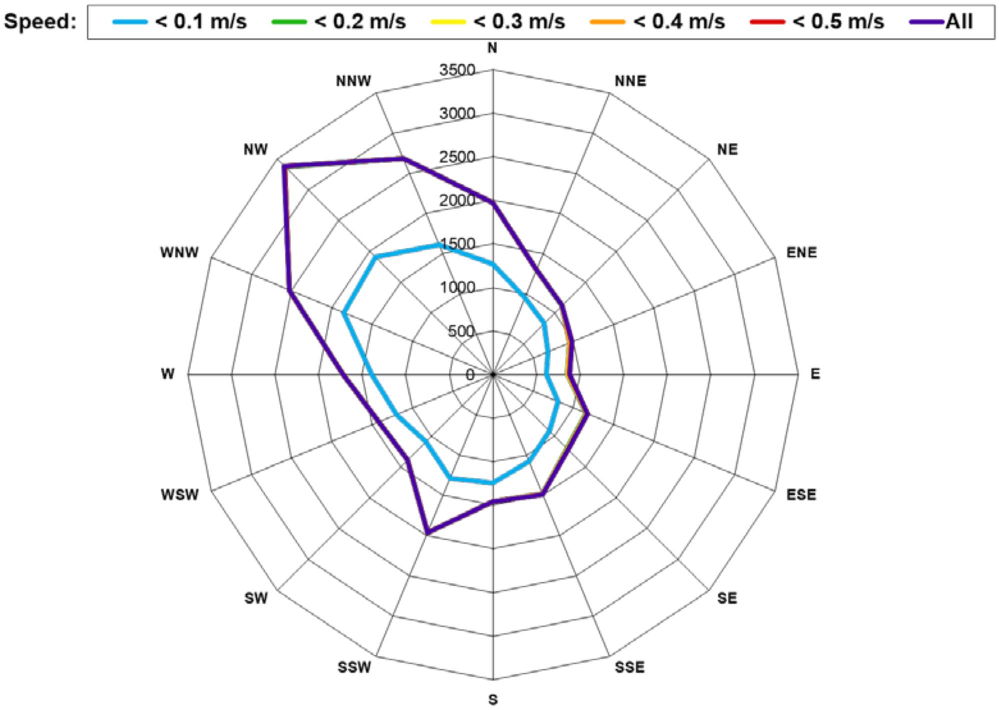

Figure 3.30 Current rose at Camp Island (AMB 4) for the monitoring period from November 2017 to July 2018. The current rose plots the number of currents recorded in each direction within the ranges of different current speeds (*cs*) indicated in the legend

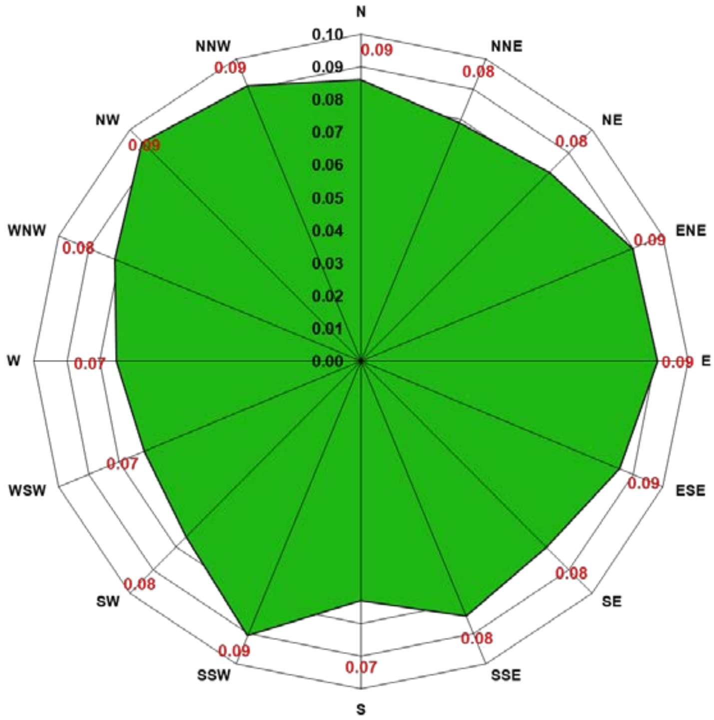

Figure 3.31 Average current speed rose at Camp Island (AMB 4) for the monitoring period from November 2017 to July 2018. The average current speed is rose is coloured in green, while the red values indicate the average current value at each specific direction

AMB 4: Camp Island

The current at Camp Island predominately flowed to the NW with peaks of 0.13-0.14 m/s average current velocities from the WSW to the NW regions (as shown in Figures 3.32 and 3.33). This shows that the current is flowing along the coast. Changes in current velocity are likely the result of tidal current influence.

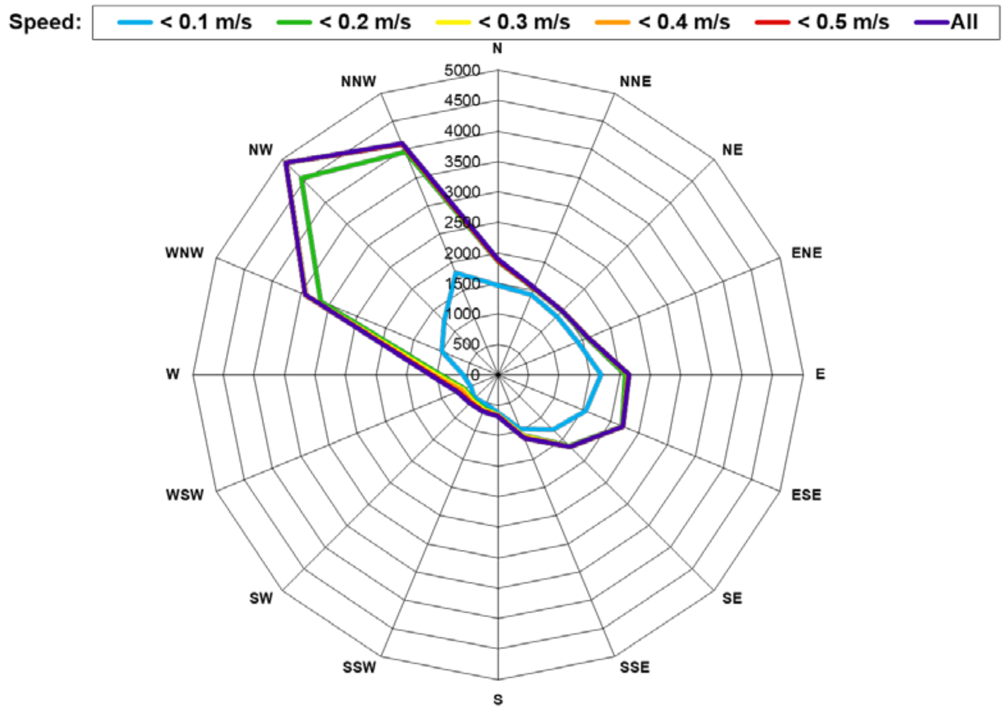

Figure 3.32 Current rose at Camp Island (AMB 4) for the monitoring period from November 2017 to July 2018. The current rose plots the number of currents recorded in each direction within the ranges of different current speeds (*cs*) indicated in the legend

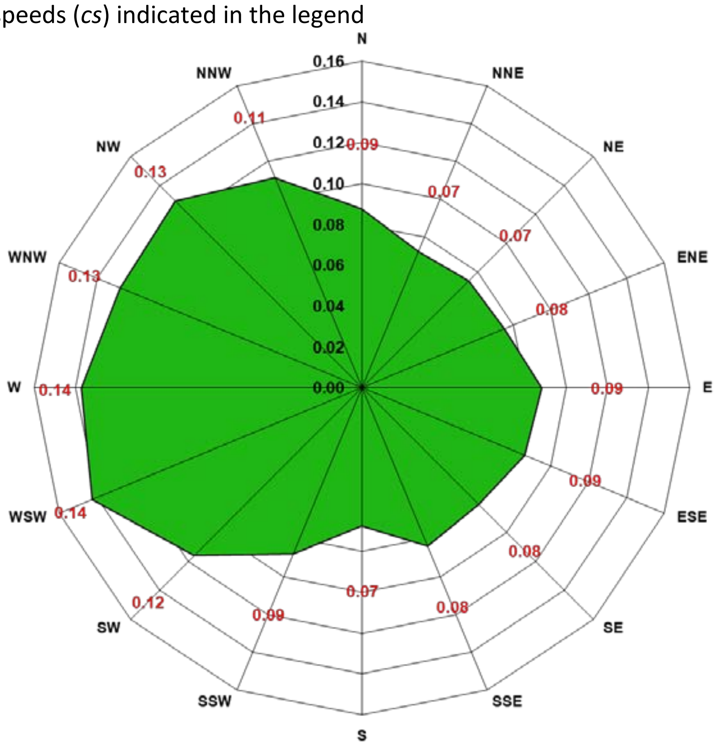

Figure 3.33 Average current speed rose at Camp Island (AMB 4) for the monitoring period from November 2017 to July 2018. The average current speed is rose is coloured in green, while the red values indicate the average current value at each specific direction

AMB 5: Holbourne

The current at Holbourne ranges from SSE to WNW with peaks at SSE and SW and average velocities are between 0.1 m/s and 0.3 m/s (as shown in Figures 3.34 and 3.35). This is due the fact that the site is sheltered on the eastern side. Changes in current velocity are likely the result of tidal current influence.

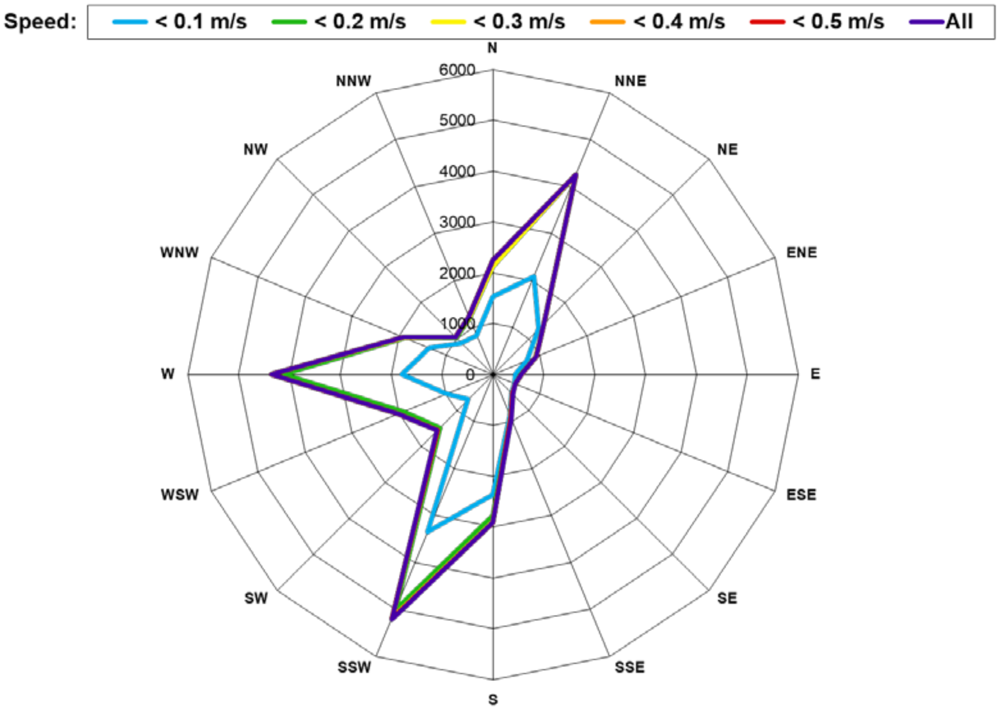

Figure 3.34 Current rose at Camp Island (AMB 4) for the monitoring period from November 2017 to July 2018. The current rose plots the number of currents recorded in each direction within the ranges of different current speeds (*cs*) indicated in the legend

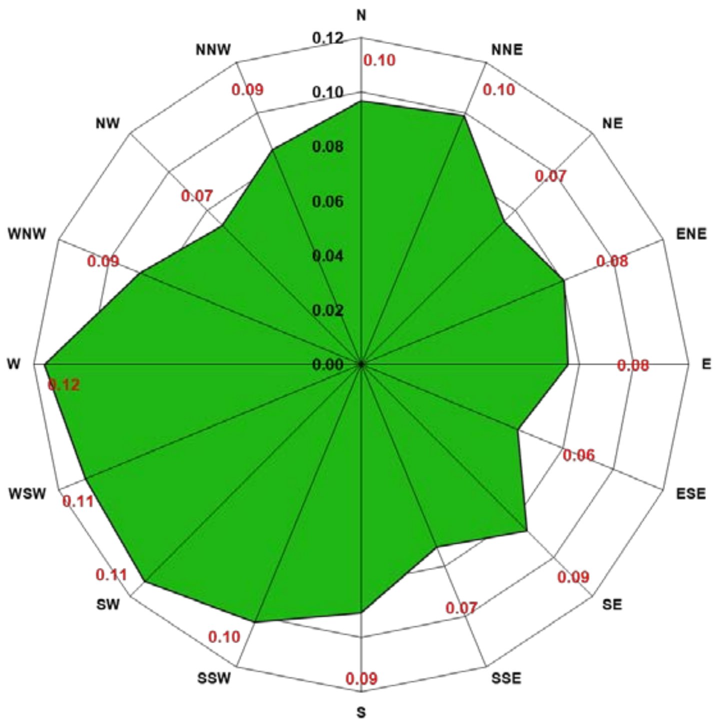

Figure 3.35 Average current speed rose at Camp Island (AMB 4) for the monitoring period from November 2017 to July 2018. The average current speed is rose is coloured in green, while the red values indicate the average current value at each specific direction

3.5 River Plumes

3.5.1 Site specific outputs

AMB1 (Euri Creek)

A stepwise regression analysis was run against the AMB1 data (Euri Creek) to identify the appropriate variable selection, excluding autocorrelation and outliers, for the multiple regression analysis. RMS of water depth, the NESW wind component, and tide amplitude explained 35% of the SSC variability (Table 3.8). The relative importance analysis suggested that RMS of water depth is the most influential parameter on SSC (93% of overall R^2) followed by the NESW wind component (7% to the overall R^2) (Figure 3.36). The relationship between the RMS water depth and SSC followed the expected trend, with SSC increasing with RMS water depth (Figure 3.37). The NESW wind component showed a relatively weak negative relationship with SSC, as indicated by the wide confidence interval in the partial effects plot (Figure 3.37).

Table 3.8 Statistical summary of the stepwise regression analysis to AMB1 data

	AMB1		
Predictors	*Estimates*	*CI*	*p*
(Intercept)	4.62	3.71 – 5.54	**<0.001**
log(RMS)	1.08	0.85 – 1.31	**<0.001**
wind NESW	-0.04	-0.07 – -0.01	**0.008**
Observations	169		
R^2 / adjusted R^2	0.352 / 0.344		

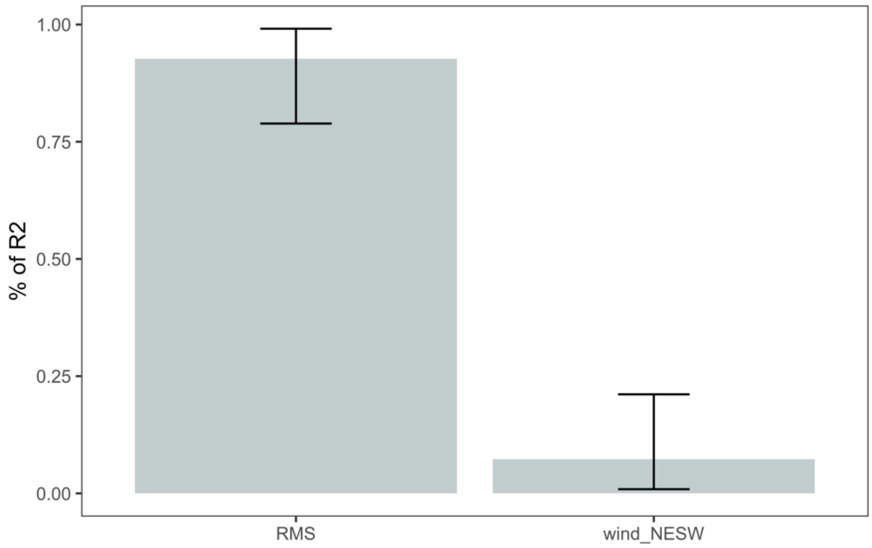

Figure 3.36 Bootstrapping relative importance analysis following a stepwise multiple regression analysis. Bars represent 95% bootstrap confidence intervals, and % of r squared values are normalized to sum 100%. Overall R^2 = 0.35

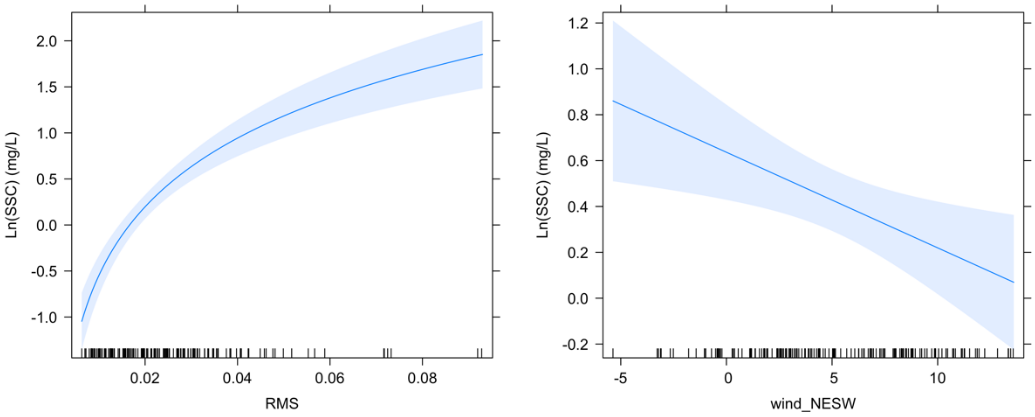

Figure 3.37 Partial effect plots for AMB1 parameters affecting the concentration of suspended solids in the water column. Grey area indicates 95% CI and rug on x-axis stand for data density

AMB2 (Bowen Spoil Grounds)

A stepwise regression analysis was run against the AMB2 data to identify the appropriate variable selection, excluding autocorrelation and outliers, for the multiple regression analysis. Euri River discharge was the only environmental parameter significantly related to SSC, but explained only 18% of the SSC variability (Table 3.9). The partial effects plot shows that SSC decreased with increasing discharge from Euri River (Figure 3.38). The weak relationship may be due to data gaps associated with logger fouling during periods of significant water discharge (there was 78% data recovery for SSC at this site across the entire monitoring period, with data losses occurring in wet season months, primarily February 2018). Therefore analysis of a dataset collected over a longer period of time at this site may yield different results.

Table 3.9 Statistical summary of the stepwise regression analysis to AMB2 data

	AMB2		
Predictors	*Estimates*	*CI*	*p*
(Intercept)	1.08	0.88 – 1.29	**<0.001**
log(Euri+1)	-4.44	-5.98 – -2.89	**<0.001**
Observations	145		
R^2 / adjusted R^2	0.182 / 0.176		

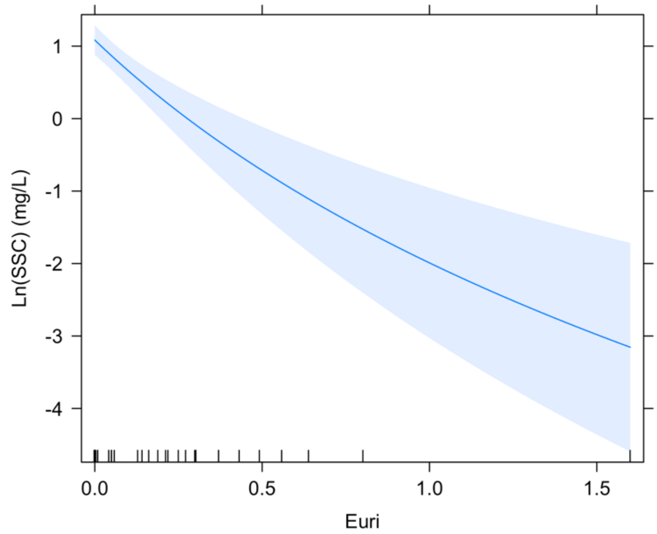

Figure 3.38 Partial effect plots for AMB2 parameters affecting the concentration of suspended solids in the water column. Grey area indicates 95% CI and rug on x-axis stand for data density

AMB3 (Elliot River)

A stepwise regression analysis was run against the AMB3 data to identify the appropriate variable selection, excluding autocorrelation and outliers, for the multiple regression analysis. RMS of water depth, the Don River discharge, and the NESW wind component explained 63% of the SSC variability (Table 3.10). The relative importance analysis suggested that RMS of water depth is the most influential parameter on SSC (79% of overall R^2), followed by Don River discharge (19% of overall R^2) and the NESW wind component (2% of overall R^2; Figure 3.39). Partial effects plots (Figure 3.40) show that SSC increases with RMS of water depth and Don River discharge, but decreases in relation to the NESW wind component.

Table 3.10 Statistical summary of the stepwise regression analysis to AMB3 data

		AMB3	
Predictors	*Estimates*	*CI*	*p*
(Intercept)	3.85	2.85 – 4.84	**<0.001**
log(RMS)	0.87	0.62 – 1.13	**<0.001**
log(Don+1)	0.51	0.45 – 0.57	**<0.001**
wind NESW	-0.05	-0.09 – -0.02	**0.001**
Observations	222		
R^2 / adjusted R^2	0.631 / 0.626		

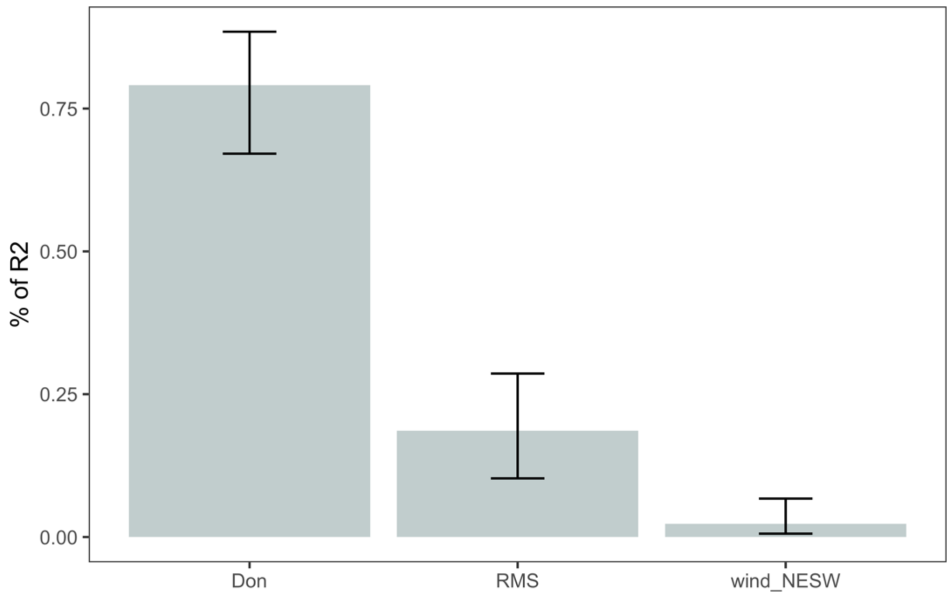

Figure 3.39 Bootstrapping relative importance analysis following a stepwise multiple regression analysis. Bars represent 95% bootstrap confidence intervals, and % of r squared values are normalized to sum 100%. Overall R^2 = 0.63

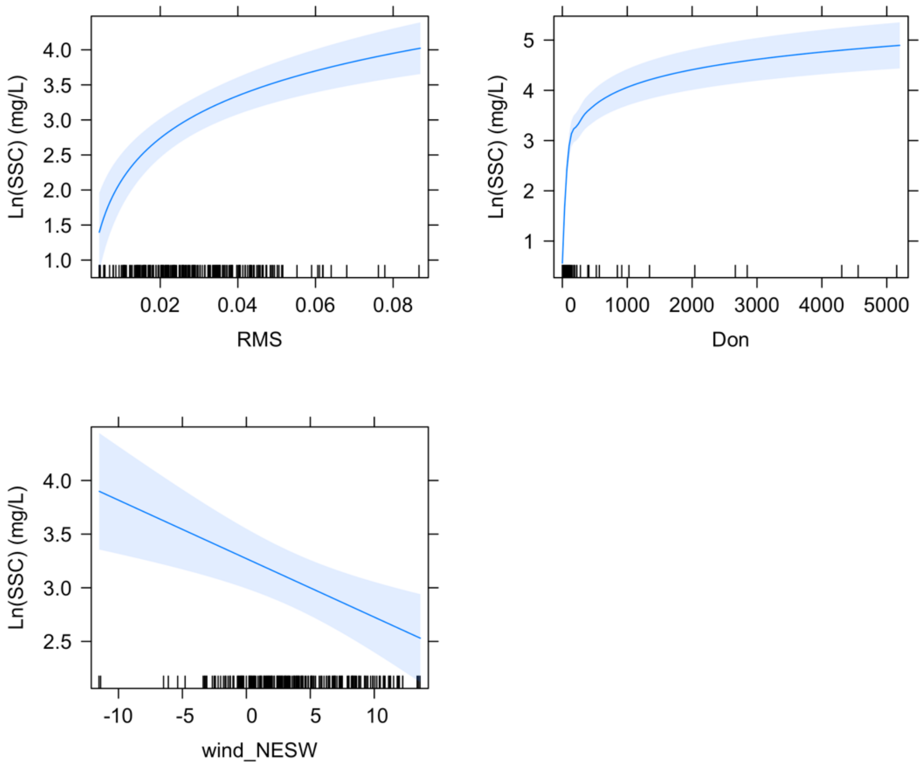

Figure 3.40 Partial effect plots for AMB3 parameters affecting the concentration of suspended solids in the water column. Grey area indicates 95% CI and rug on x-axis stand for data density

AMB4 (Camp Island)

A stepwise regression analysis was run against the AMB4 data to identify the appropriate variable selection, excluding autocorrelation and outliers, for the multiple regression analysis. RMS of water depth, the Don River discharge, and the NWSE wind component explained 41% of the SSC variability (Table 3.12). The relative importance analysis suggested that Don River discharge is the most influential parameter on SSC (65% of overall R^2), followed by RMS of water depth (19% of overall R^2)

and the NWSE wind component (16% of overall R^2; Figure 3.43). Partial effects plots (Figure 3.44) show that SSC decreases with RMS of water depth and the NWSE wind component, but increases with Don River discharge.

Table 3.12 Statistical summary of the stepwise regression analysis to AMB4 data

	AMB4		
Predictors	*Estimates*	*CI*	*p*
(Intercept)	-0.96	-1.34 – -0.58	**<0.001**
log(RMS)	-0.23	-0.32 – -0.13	**<0.001**
log(Don+1)	1.11	0.81 – 1.41	**<0.001**
wind NWSE	-0.02	-0.04 – -0.01	**<0.001**
Observations	142		
R^2 / adjusted R^2	0.407 / 0.394		

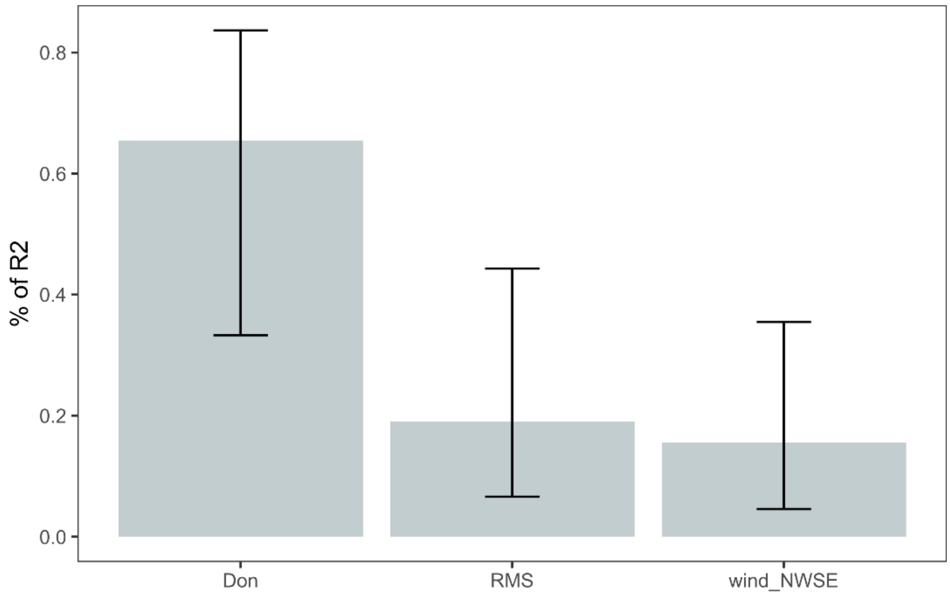

Figure 3.43 Bootstrapping relative importance analysis following a stepwise multiple regression analysis. Bars represent 95% bootstrap confidence intervals, and % of r squared values are normalized to sum 100%. Overall R^2 = 0.41

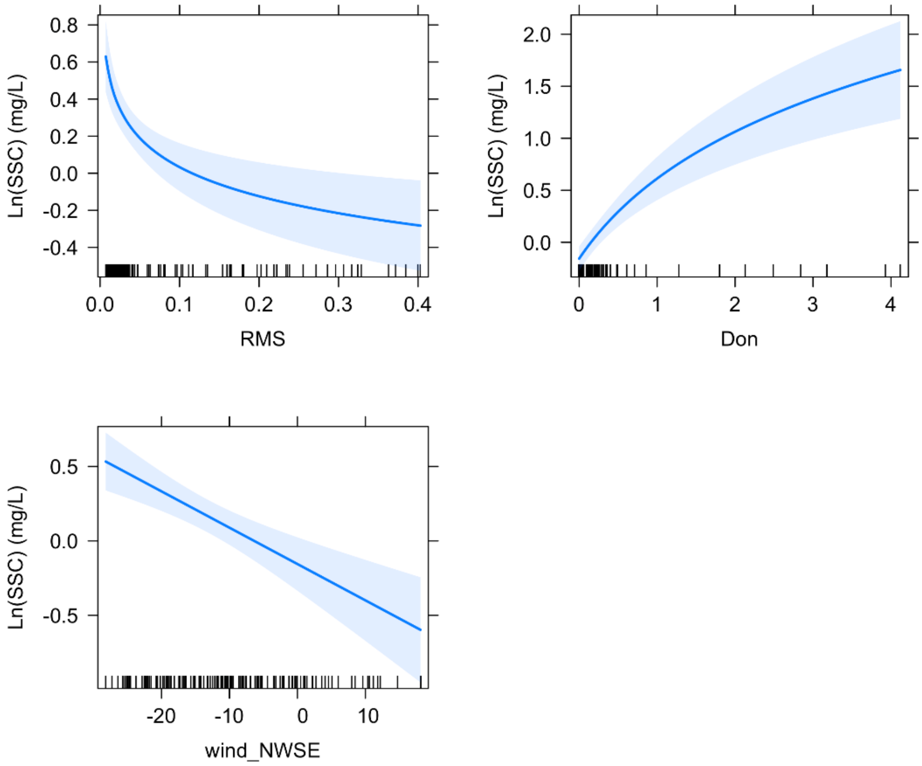

Figure 3.44 Partial effect plots for AMB4 parameters affecting the concentration of suspended solids in the water column. Grey area indicates 95% CI and rug on x-axis stand for data density

AMB5 (Holbourne Island)

A stepwise regression analysis was run against the AMB5 data to identify the appropriate variable selection, excluding autocorrelation and outliers, for the multiple regression analysis. Don River discharge and the NESW wind component explained 23% of the SSC variability (Table 3.13). The relative importance analysis suggested that Don River discharge is the most influential parameter on SSC (57% of overall R^2), followed by the NESW wind component (43% of overall R^2) (Figure 3.45). Partial effects plots show that SSC decreases with both environmental parameters, although wide confidence intervals indicate that these are weak relationships (Figure 3.46). Future analysis of data collected over a longer time period at this site may yield stronger relationships at this site. Holbourne Island is distant from sources of river discharge, and therefore it is interesting to note that river discharge was the most important factor influencing SSC at this site. It is likely that, rather than being a direct driver of SSC at Holbourne Island, river discharge is a proxy for storm events occurring in the region and directly influencing SSC.

Table 3.13 Statistical summary of the stepwise regression analysis to AMB5 data

	AMB5		
Predictors	*Estimates*	*CI*	*p*
(Intercept)	1.62	1.23 – 2.00	**<0.001**
log(Don+1)	-0.24	-0.36 – -0.11	**<0.001**
wind NESW	-0.12	-0.19 – -0.04	**0.002**
Observations	124		
R^2 / adjusted R^2	0.231 / 0.219		

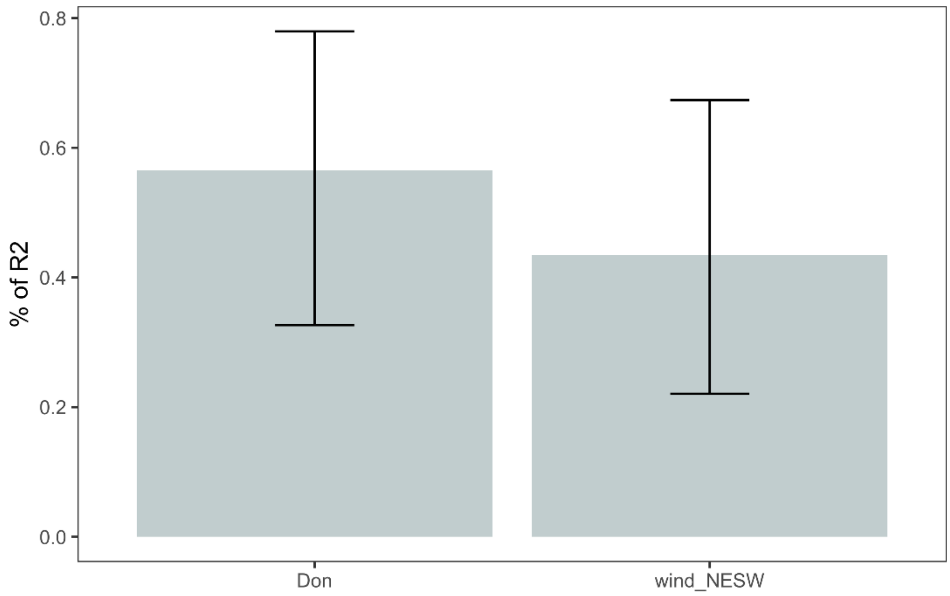

Figure 3.45 Bootstrapping relative importance analysis following a stepwise multiple regression analysis. Bars represent 95% bootstrap confidence intervals, and % of r squared values are normalized to sum 100%. Overall R^2 = 0.23

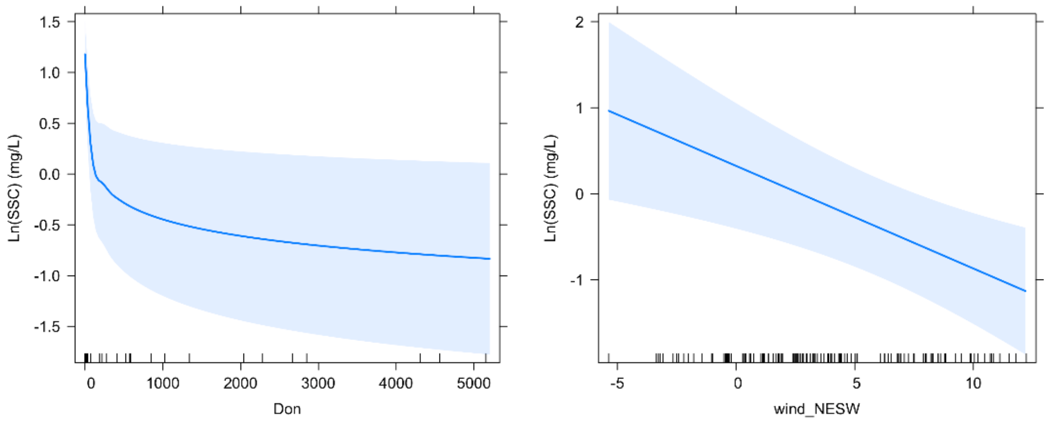

Figure 3.46 Partial effect plots for AMB5 parameters affecting the concentration of suspended solids in the water column. Grey area indicates 95% CI and rug on x-axis stand for data density

4 CONCLUSIONS AND RECOMMENDATIONS

4.1 Conclusions

4.1.1 Climatic conditions

- It is important to note when interpreting the 2017-2018 data, overall rainfall was low in the Abbot Point region but in February 2018 there was a particularly high river discharge event associated with a tropical low.
- Comparison of these data with future years will be important to characterise ambient water quality conditions, particularly after the region experiences above average rainfall in the future.
- The wind speed and direction recorded at Abbot Point has been a useful inclusion in this assessment. The daily average wind speed and direction recorded for the reporting period was predominantly from the south east, with 30% of days having wind speeds greater than 24km/hr.

4.1.2 Ambient water quality

- There is a strong seasonal pattern for water temperature, with highest temperatures experienced during summer months, while winter months experience much cooler conditions.
- The water column profile for dissolved oxygen, temperature, electrical conductivity, pH and turbidity are well mixed, though turbidity was generally highest in the bottom horizon. This becomes an important consideration when examining receptor habitats, such as corals and seagrass that are sensitive to water clarity changes. Measuring bottom horizon turbidity is a very relevant component of this program; surface measurements for turbidity, or indeed suspended solid concentrations, might not be an entirely relevant measure when the objective is to protect and enhance benthic habitats.
- Particulate nitrogen, particulate phosphorus, and chlorophyll-*a* were elevated above local relevant guidelines at some sites and during certain months. The contributing factors to these data results might include some localised signal associated with runoff from land use activities such as farming and urban runoff.
- Phytoplankton and zooplankton communities were most similar in their species composition during (November and December 2017) and were distinct during February 2018.
- Trace heavy metals, herbicides, and pesticides were non-detectable in April 2018, even at sites in close proximity to a high river discharge event in February 2018.

4.1.3 Sediment deposition and turbidity

- Continuous sediment deposition and turbidity logging data supports the pattern found more broadly in North Queensland coastal marine environments, that during dry periods with minimal rainfall, elevated turbidity along the coastline is driven by the re-suspension of sediment (Orpin and Ridd 2012), and this has been most notable here given the links drawn between RMS water depth and NTUe/SSC. Large peaks in NTUe/SSC and RMS water depth were recorded over periods longer than a week.
- For most of the sites, SSC was relatively low. However this was interspersed with periods of high SSC due to wind-driven resuspension. Sites near the reef such as Holbourne Island generally showed low SSC for most of the deployment time.
- Deposition was relatively low for most sites, particularly those sites near reefs (AMB 3, 4 and 5). Spoil Grounds had the highest deposition, with a median of 13 mg/cm^2/d. It is unclear what parameters contribute to this, however it may be attributed to relatively low RMS wave

height, indicating that benthic stresses are comparatively lower, thus possibly limiting wave oscillations at that level of the water column.

4.1.4 Photosynthetically active radiation (PAR)

- Fine-scale patterns of PAR are primarily driven by tidal cycles with fortnightly increases in PAR coinciding with neap tides and lower tidal flows. Larger episodic events which lead to extended periods of low light conditions are driven by a combination of strong winds leading to increases in wave height and resuspension of particles (Orpin and Ridd 2012), and rainfall events resulting from storms leading to increased catchment flows and an input of suspended solids (Fabricius et al., 2013).
- Patterns of light were similar among all the coastal sites. Light penetration in water is affected in an exponential relationship with depth as photons are absorbed and scattered by particulate matter (Kirk 1985; Davis-Colley and Smith 2001). Therefore variation in depth at each location means benthic PAR is not directly comparable among sites as a measure of water quality. Generally, however, shallow inshore sites reached higher levels of benthic PAR and were more variable than deeper water coastal sites and sites of closer proximity to one another were more similar than distant sites.
- While turbidity is the main indicator of water quality used in monitoring of dredge activity and benthic light is significantly correlated with suspended solid concentrations (Erftemeijer and Lewis 2006; Erftemeijer et al., 2012), the relationship between these two parameters is not always strong (Sofonia and Unsworth 2010). At many of the sites where both turbidity and benthic light were measured, the concentration of suspended solids in the water column explained less than half of the variation in PAR. As PAR is more biologically relevant to the health of photosynthetic benthic habitats such as seagrass, algae and corals it is becoming more useful as a management response tool when used in conjunction with known thresholds for healthy growth for these habitats (e.g., Chartrand et al., 2012). For this reason, it is important to include photosynthetically active radiation (PAR) in the suite of water quality variables when capturing local baseline conditions of ambient water quality.

4.2 Recommendations

4.2.1 Consolidation of the water quality loggers

It is recommended that the ambient monitoring program remain into the 2018/19 period. It will be important to ensure that the site network is ready to capture a full wet season, in order to characterise the upper water quality conditions for the region.

4.2.2 Data base repository

An electronic version of the ambient marine water quality database has been prepared as an annexure to this report. It currently comprises MS-Excel Workbooks containing raw data files including results for water chemistry (*in-situ* field measurements, nutrients, filterable metals, pesticides/herbicides) collected as during the quarterly sampling, and all the continuous high frequency logger data files for sediment deposition, PAR, turbidity, water temperature, and RMS recorded during the period January and July 2018. This data base continues to be maintained by TropWATER personal, with back up copy archived on the James Cook University network with restricted access.

5 LITERATURE SOURCED

Álvarez-Romero, J. G., Devlin, M., Teixeira da Silva, E., Petus, C., Ban, N. C., Pressey, R. L., Kool, J., Roberts, J., Cerdeira, S., Wenger, A., Brodie, J. (2013) A novel approach to model exposure of coastal-marine ecosystems to riverine flood plumes based on remote sensing techniques. Journal of Environmental Management 119, 194-207.

ANZECC and ARMCANZ (2000) Australian Water Quality Guidelines for Fresh and Marine Waters. Australia and New Zealand Environment Conservation Council and Agriculture and Resource Management Council of Australia and New Zealand, Canberra.

ANZECC and ARMCANZ (2000b) Australian Guidelines for Water Quality Monitoring and Reporting. Australia and New Zealand Environment Conservation Council and Agriculture and Resource Management Council of Australia and New Zealand, Canberra. ISBN 09578245 1 3. ISSN 1038 7072.

APHA (1998) Standard Methods for the Examination of Water and Wastewater. 20th Edition. American Public Health Association, American Water Works Association and Water Environment Foundation. Washington, U.S.A.

Bainbridge, Z. T., Lewis, S. E., Smithers, S. G., Kuhnert, P. M., Henderson, B. L., Brodie, J. E. (2014) Fine-suspended sediment and water budgets for a large, seasonally dry tropical catchment: Burdekin River catchment, Queensland, Australia. Water Resources Research, 50, 9067-9087.

Bainbridge, Z. T., Wolanski, E., Álvarez-Romero, J. G., Lewis, S. E., Brodie, J. E. (2012) Fine sediment and nutrient dynamics related to particle size and floc formation in a Burdekin River flood plume, Australia. Marine Pollution Bulletin, 65, 236-248.

Bell, A. M., Duke, N. C. (2005) Effects of Photosystem II inhibiting herbicides on mangroves—preliminary toxicology trials. Marine Pollution Bulletin, 51, 297-307.

BMA Billiton Mitsubishi Alliance (2011) Dredging and blasting environmental management plan – Hay Point Coal Terminal Expansion Phase 3 (HPX3). BM Alliance Coal Operations Pty Ltd. pp 50.

BMA Billiton Mitsubishi Alliance (2012) Environmental Management Plan (Marine Ecology) for dredging and dredged material disposal – Hay Point Coal Terminal Expansion Phase 3 (HPX3). BM Alliance Coal Operations Pty Ltd. pp 105.

Brodie, J. E., Kroon, F. J., Schaffelke, B., Wolanski, E. C., Lewis, S. E., Devlin, M. J., Bohnet, I. C, Bainbridge, Z. T., Waterhouse, J., Davis, A. M. (2012) Terrestrial pollutant runoff to the Great Barrier Reef: an update of issues, priorities and management responses. Marine Pollution Bulletin, 65, 81-100.

Bunt, J., Larcombe, P., Jago, C. F. (1999) Quantifiying the response of optical backscatter devices and transmissiometers to variations in suspended particulate matter (SPM). Continental Shelf Research 19: 1199-1220

Capone, D. G., Zehr, J. P., Paerl, H. W., Bergman, B., Carpenter, E. J. (1997). Trichodesmium, a globally significant marine cyanobacterium. Science, 276, 1221-1229.

Chartrand, K. M., Ralph, P. J., Petrou, K., Rasheed, M. A. (2012) Development of a light-based seagrass management approach for the Gladstone Western Basin dredging program. DEEDI Publication, Fisheries Queensland, Cairns.

Chartrand, K.M., Rasheed, M. A., Sankey, T.L. (2008). Deepwater seagrass dynamics in Hay Point – Measuring variability and monitoring impacts of capital dredging. Final Report to the Ports Corporation of Queensland. DPIandF Publication PR08-4082 (DPIandF, Cairns), 43 pp.

Coles, R. G., Rasheed, M. A., McKenzie, L. J., Grech, A., York, P. H., Sheaves, M., McKenna, S., Bryant, C. (2015) The Great Barrier Reef World Heritage Area seagrasses: managing this iconic Australian ecosystem resource for the future. Estuarine, Coastal and Shelf Science, 153, A1-A12.

Collier, C. J., Lavery, P. S., Ralph, P. J., Masini, R. J. (2009) Shade-induced response and recovery of the seagrass *Posidonia sinuosa*. Journal of Experimental Marine Biology and Ecology 370, 89-103

Conner, C. S., De Visser, A. M. (1992) A laboratory investigation of particle size effects on an optical backscatterance sensor. Marine Geology 108:151-159

Cook, R. D., Weisberg, S. (1982) Residuals and Influence in Regression. Chapman and Hall.

Crawley, M.J. (2007) The R Book. John Wiley and Sons, Ltd.

Davies-Colley, R. J., Smith, D. G. (2001) Turbidity, suspended sediment, and water clarity: A review. Journal of the American Water Resources Association 37:1085-1101.

De'ath, G., Fabricius, K. (2010) Water quality as a regional driver of coral biodiversity and macroalgae on the Great Barrier Reef. Ecological Applications, 20, 840-850.

DEHP (2010) Monitoring and sampling manual 2009. Environmental Protection (Water) Policy 2009. Version 2 September 2010. Queensland, Department of Environment and Heritage Protection.

Devlin, M. J., da Silva, E., Petus, C., Wenger, A., Zeh, D., Tracey, D., Brodie, J. (2013) Combining in-situ water quality and remotely sensed data across spatial and temporal scales to measure variability in wet season chlorophyll-a: Great Barrier Reef lagoon (Queensland, Australia). Ecological Processes, 2, 31. doi: 10.1186/2192-1709-2-31

Devlin, M. J., McKinna, L. W., Alvarez-Romero, J. G., Petus, C., Abott, B., Harkness, P., Brodie, J. (2012) Mapping the pollutants in surface riverine flood plume waters in the Great Barrier Reef, Australia. Marine Pollution Bulletin, 65, 224-235. doi: 10.1016/j.marpolbul.2012.03.001

Devlin, M., Petus, C., Collier, C., Zeh, D., McKenzie, L. (2013). Chapter 6: Seagrass and water quality impacts including a case study linking annual measurements of seagrass change against satellite water clarity data (Cleveland Bay) Assessment of the relative risk of water quality to ecosystems of the Great Barrier Reef: Supporting Studies. A report to the Department of the Environment and Heritage Protection, Queensland Government, Brisbane. (Vol. Report 13/30,). Townsville, Australia: TropWATER

Devlin, M., Petus, C., da Silva, E., Tracey, D., Wolff, N.H., Waterhouse, J., Brodie, J. (2015) Water Quality and River Plume Monitoring in the Great Barrier Reef: An Overview of Methods Based on Ocean Colour Satellite Data. Remote Sens. 2015, 7, 12909-12941; doi:10.3390/rs71012909

Doxaran, D., Froidefond, J. M., Castaing, P., Babin, M. (2009) Dynamics of the turbidity maximum zone in a macrotidal estuary (the Gironde, France): Observations from field and MODIS satellite data. Estuarine, Coastal and Shelf Science, 81, 321-332.

Drewry, J., Mitchell, C., Higham, W. (2008) Water quality improvement plan: final report for Mackay Whitsunday region. Mackay Whitsunday Natural Resource Management Group.

Dunn, R. J. K., Teasdale, P. R., Warnken, J., Jordan, M. A., Arthur, J. M. (2007) Evaluation of the in situ, time-integrated DGT technique by monitoring changes in heavy metal concentrations in estuarine waters. Environmental Pollution, 148, 213-220.

Erftemeijer, P. L. A., B. Riegl, B. W. Hoeksema, Todd, P. A. (2012) Environmental impacts of dredging and other sediment disturbances on corals: A review. Marine Pollution Bulletin 64, 1737-1765.

Erftemeijer, P. L. A., Lewis, R. R. R. (2006) Environmental impacts of dredging on seagrasses: a review. Marine Pollution Bulletin 52, 1553-1572.

Fabricius, K. E., G. De'ath, C. Humphrey, I. Zagorskis, Schaffelke, B. (2013) Intra-annual variation in turbidity in response to terrestrial runoff on near-shore coral reefs of the Great Barrier Reef. Estuarine, Coastal and Shelf Science 116, 57-65.

Fabricius, K. E., Logan, M., Weeks, S., Brodie, J. (2014) The effects of river run-off on water clarity across the central Great Barrier Reef. Marine Pollution Bulletin, 84, 191-200.

Folkers, A., Rohde, K., Delaney, K., Flett, I. (2014) Mackay Whitsunday water quality improvement plan 2014-2021. Draft report. Reef Catchments. Mackay. 174pp.

Fox, J., Monette, G. (1992) Generalized collinearity diagnostics. JASA, 87, 178–183.

GBRMPA (2010) Water quality guidelines for the Great Barrier Reef Marine Park 2010 current edition. Great Barrier Reef Marine Park Authority.

GBRMPA (2013) Great Barrier Reef Region Strategic Assessment Report. Australian Government, Great Barrier Reef Marine Park Authority. pp. 636.

Grömping, G. (2006) Relative Importance for Linear Regression in R: The Package relaimpo. Journal of Statistical Software, 17, 1-27.

Johansen, J. L., Pratchett, M. S., Messmer, V., Coker, D. J., Tobin, A. J., Hoey, A. S. (2015) Large predatory coral trout species unlikely to meet increasing energetic demands in a warming ocean. Scientific Reports, 5.

Jones, G. B., Mercurio, P., Olivier, F. (2000) Zinc in fish, crabs, oysters, and mangrove flora and fauna from Cleveland Bay. Marine Pollution Bulletin, 41, 345-352.

Kirk, J. T. O. (1985) Effects of suspendiods (turbidity) on penetration of solar rediation in aquatic ecosystems. Hydrobiologia, 125, 195-208.

Kroon, F. J., Kuhnert, P. M., Henderson, B. L., Wilkinson, S. N., Kinsey-Henderson, A., Abbott, B., Brodie. J. E., Turner, R. D. (2012) River loads of suspended solids, nitrogen, phosphorus and herbicides delivered to the Great Barrier Reef lagoon. Marine Pollution Bulletin, 65, 167-181.

Lahet, F., Stramski, D. (2010). MODIS imagery of turbid plumes in San Diego coastal waters during rainstorm events. Remote Sensing of Environment, 114, 332-344.

Larcombe P, Ridd PV, Prytz A, Wilson, B. (1995) Factors controlling suspended sediment ion inner-shelf coral reefs, Townsville, Australia. Coral Reefs 14:163-171

Lewis, S. E., Brodie, J. E., Bainbridge, Z. T., Rohde, K. W., Davis, A. M., Masters, B. L., Maughan, M., Devlin, M. J., Mueller, J. F., Schaffelke, B. (2009) Herbicides: A new threat to the Great Barrier Reef. Environmental Pollution, 157, 2470-2484.

Logan, M., Fabricius, K., Weeks, S., Rodriguez, A., Lewis, S., Brodie, J. (2014) Tracking GBR water clarity over time and demonstrating the effects of river discharge events. Progress Report: Southern and Northern NRM Regions. Report to the National Environmental Research Program. Reef and Rainforest Research Centre Limited, Cairns (53pp.).

Ludwig, K. A., Hanes, D. M. (1990) A laboratory explanation of optical backscatterance suspended solids sensors exposed to sand-mud mixtures. Mar Geol 94:173-179

Macdonald, R.K., (2015). Turbidity and Light Attenuation in Coastal Waters of the Great Barrier Reef (Doctoral dissertation). Retrieved from https://researchonline.jcu.edu.au/46029/

Macdonald, R.K., Ridd, P.V., Whinney, J.C., Larcombe, P., & Neil, D.T. (2013). Towards environmental management of water turbidity within open coastal waters of the Great Barrier Reef. Marine Pollution Bulletin, 74(1), 82-94.

McKenna, S. A., Rasheed, M. A. (2015) Port of Hay Point and Keswick Island Seagrass and Benthic Habitat: baseline survey – 2014', JCU Publication, Centre for Tropical Water and Aquatic Ecosystem Research Publication 46 pp.

McKenna, S., Jarvis, J., Sankey, T., Reason, C., Coles, R., Rasheed, M. (2015) Declines of seagrasses in a tropical harbour, North Queensland, Australia, are not the result of a single event. Journal of Biosciences, 40, 389-398.

Mitchell, C., Brodie, J., White, I. (2005) Sediments, nutrients and pesticide residues in event flow conditions in streams of the Mackay Whitsunday Region, Australia. Marine Pollution Bulletin, 51, 23-36.

North Queensland Bulk Ports Corporation (2009) Environmental Management Plan – Port of Hay Point. North Queensland Bulk Ports Corporation Ltd, pp47.

North Queensland Bulk Ports Corporation (2011) Long term dredge management plan Mackay Port 2012-2022. Document number E11/62581. North Queensland Bulk Ports Corporation Ltd, pp124.

Ondrusek, M., Stengel, E., Kinkade, C. S., Vogel, R. L., Keegstra, P., Hunter, C., Kim, C. (2012) The development of a new optical total suspended matter algorithm for the Chesapeake Bay. Remote Sensing of Environment, 119, 243-254.

Orpin, A. R., Ridd, P. V. (2012) Exposure of inshore corals to suspended sediments due to wave-resuspension and river plumes in the central Great Barrier Reef: A reappraisal. Continental Shelf Research 47, 55-67.

Petus, C., Chust, G., Gohin, F., Doxaran, D., Froidefond, J.M., Sagarminaga, Y. (2010) Estimating turbidity and total suspended matter in the Adour River plume (South Bay of Biscay) using MODIS 250-m imagery. Continental Shelf Research 30, 379-392.

Petus, C., Marieu, V., Novoa, S., Chust, G., Bruneau, G., Froidefond, J.M. (2013) Monitoring spatio-temporal variability of the Adour River turbid plume (Bay of Biscay, France) with MODIS 250-m imagery. Continental Shelf Research (Uncorrected proofs available online the 18th of November 2013: http://dx.doi.org/10.1016/j.csr.2013.11.011).

Petus, C., Teixera da Silva, E., Devlin, M., Álvarez-Romero, A., Wenger, A. (2014) Using MODIS data for mapping of water types within flood plumes in the Great Barrier Reef, Australia: towards the production of river plume risk maps for reef and seagrass ecosystems. Journal of Environmental Management, 137, 163-177.

R Core Team (2015) R: A language and environment for statistical computing. R Foundation for Statistical Computing, Vienna, Austria. URL http://www.R-project.org/.

Rasheed, M.A., Roder, C.A., Thomas, R. (2001) Port of Mackay Seagrass, Macro-Algae and Macro-Invertebrate Communities. February 2001. CRC Reef Research Centre, Technical Report No. 43, CRC Reef Research Centre, Townsville, 38 pp.

Rasheed, M.A., Thomas, R., McKenna, S. A. (2004) Port of Hay Point seagrass, algae and benthic macro-invertebrate community survey July 2004. DPIandF Information Series QI04084 (DPIandF, Cairns), 27 pp.

Ridd, P.V., Day, G., Thomas, S., Harradence, J., Renagi, O., Fox, D., Bunt, J., Renagi, O., Jago, C. (2001) Measurement of sediment deposition rates using an Optical Backscatter Sensor. Estuarine Coastal and Shelf Science, 52, 155-163.

Schaffelke, B., Carleton, J., Skuza, M., Zagorskis, I., Furnas, M. J. (2012) Water quality in the inshore Great Barrier Reef lagoon: Implications for long-term monitoring and management. Marine Pollution Bulletin, 65(4), 249-260.

Schroeder, T., Devlin, M. J., Brando, V. E., Dekker, A. G., Brodie, J. E., Clementson, L. A., McKinna, L. (2012) Inter-annual variability of wet season freshwater plume extent into the Great Barrier Reef lagoon based on satellite coastal ocean colour observations. Marine Pollution Bulletin, 65, 210-223. doi: 10.1016/j.marpolbul.2012.02.022.

Sofonia, J. J., Unsworth, R. K. F. (2010) Development of water quality thresholds during dredging for the protection of benthic primary producer habitats. Journal of Environmental Monitoring 12:159-163.

Standards Australia (1998) Water Quality – Sampling. Part 1: Guidance on the design of sampling programs, sampling techniques and the preservation and handling of samples. AS/NZS 5667.1:1998. Standards Australia, Homebush.

Thomas, R, Leith, M., Rasheed, M. A. (2012) Port of Hay Point Seagrass Survey - November 2011. DAFF Publication, Fisheries Queensland, Cairns, 19 pp.

Thomas, R., Rasheed, M. A. (2011) Port of Hay Point Seagrass, Algae and Benthic Macro-invertebrate Survey - October 2010. (DEEDI, Cairns).

Thomas, S., Ridd, P. V., Renagi, O. (2003) Laboratory investigation on the effect of particle size, water flow and bottom surface roughness upon the response of an upward-pointing optical backscatter sensor to sediment accumulation. Continental Shelf Research. 23, 1545-1557.

TropWATER (2015) Assessment of the contamination risk posed by sampling consumables to the detection and monitoring of filterable metals in water samples. Internal report. Centre for Tropical Water and Aquatic Ecosystem Research, James Cook University.

Waltham, N. J., Teasdale, P. R., Connolly, R. M. (2011) Contaminants in water, sediment and fish biomonitor species from natural and artificial estuarine habitats along the urbanized Gold Coast, Queensland. Journal of Environmental Monitoring, 13(12), 3409-3419.

Waltham, N., McKenna, S., York, P., Devlin, M., Campbell, S., Rasheed, M., Ridd, P. (2015) 'Port of Mackay and Hay Point Ambient Marine Water Quality Monitoring Program (July 2014 to July 2015), Centre for Tropical Water & Aquatic Ecosystem Research (TropWATER) Publication 15/16, James Cook University, Townsville, 98 pp.

Warnken, J., Dunn, R. J., Teasdale, P. R. (2004) Investigation of recreational boats as a source of copper at anchorage sites using time-integrated diffusive gradients in thin film and sediment measurements. Marine Pollution Bulletin, 49, 833-843.

Waterhouse, J., Brodie, J., Lewis, S., Mitchell, A. (2012) Quantifying the sources of pollutants in the Great Barrier Reef catchments and the relative risk to reef ecosystems. Marine pollution bulletin, 65(4), 394-406.

Wolanski, E., Delesalle, B., Gibbs, R. (1994) Carbonate mud in Mataiva Atoll, French Polynesia: Suspension and export. Marine Pollution Bulletin 29:36-41.

Wood, S. (2014) Package 'mgcv', version 1.8-3.

York, P. H., Carter, A. B., Chartrand, K., Sankey, T., Wells, L., Rasheed, M. A. (2015) Dynamics of a deep-water seagrass population on the Great Barrier Reef: annual occurrence and response to a major dredging program. Scientific Reports, 5.

Zuur, A. F. (2012) A Beginner's Guide to Generalised Additive Models with R. Highland Statistics Ltd, Newburgh UK.

6. APPENDIX

A.1 Calibration procedures

Turbidity/Deposition Calibration

The turbidity and deposition sensors on each instrument are calibrated to a set of plastic optical standards that give consistent NTU return values. This enables the calculation of raw data values into NTU values. The NTU values can then be converted into SSC and ASSD values through the SSC calibration process. Deposition sensors are calibrated to give measurements in units of mg/cm^2 using the methodology outlined in Ridd *et al* (2000) and Thomas *et al* (2003). Instruments are calibrated every six months or after every deployment. Sediment samples are taken at each deployment site and used to determine sediment calibration coefficients used to account for variations in grain size and shape that can alter the implied SSC value.

SSC Calibration

An instrument is placed in a large container (50 l) with black sides and the output is read on a computer attached to the logger. Saltwater is used to fill the container. Sediment from the study site is added to a small container of salt water and agitated. The water-sediment slurry is then added to the large container which is stirred with a small submerged pump. A water sample is taken and analysed for total suspended sediment (TSS) using standard laboratory techniques in the ACTFR laboratory at JCU which is accredited for these measurements. Approximately 6 different concentrations of sediment are used for each site. TSS is then plotted against the NTU reading from the logger for each of the different sediment concentrations. A linear correlation between NTU and SSC is then calculated. The correlations typically have an r^2 value equal to or greater than 0.9.

Light Calibration

The light sensors on each logger are calibrated every six months or after every deployment. The light sensor is calibrated against a LICOR U250A submersible sensor that was calibrated in the factory within the last 12 months. The results of the logger light sensor and LICOR U250A are compared and a calibration coefficient is used to ensure accurate reporting of PAR data. An in field comparison between the logger light sensor and LICOR U250A is made on deployment of the instruments to ensure accurate reporting of the data. In field calibration of the nephelometer light sensor against the LICOR U250A at varying depth has been carried out to account for changes in sensitivity changes at depth.

Pressure Sensor Calibration

All pressure sensors are calibrated against a pressure gauge and the pressure is converted into depth in metres.

A.2 Time series data

AMB 1: Euri Creek

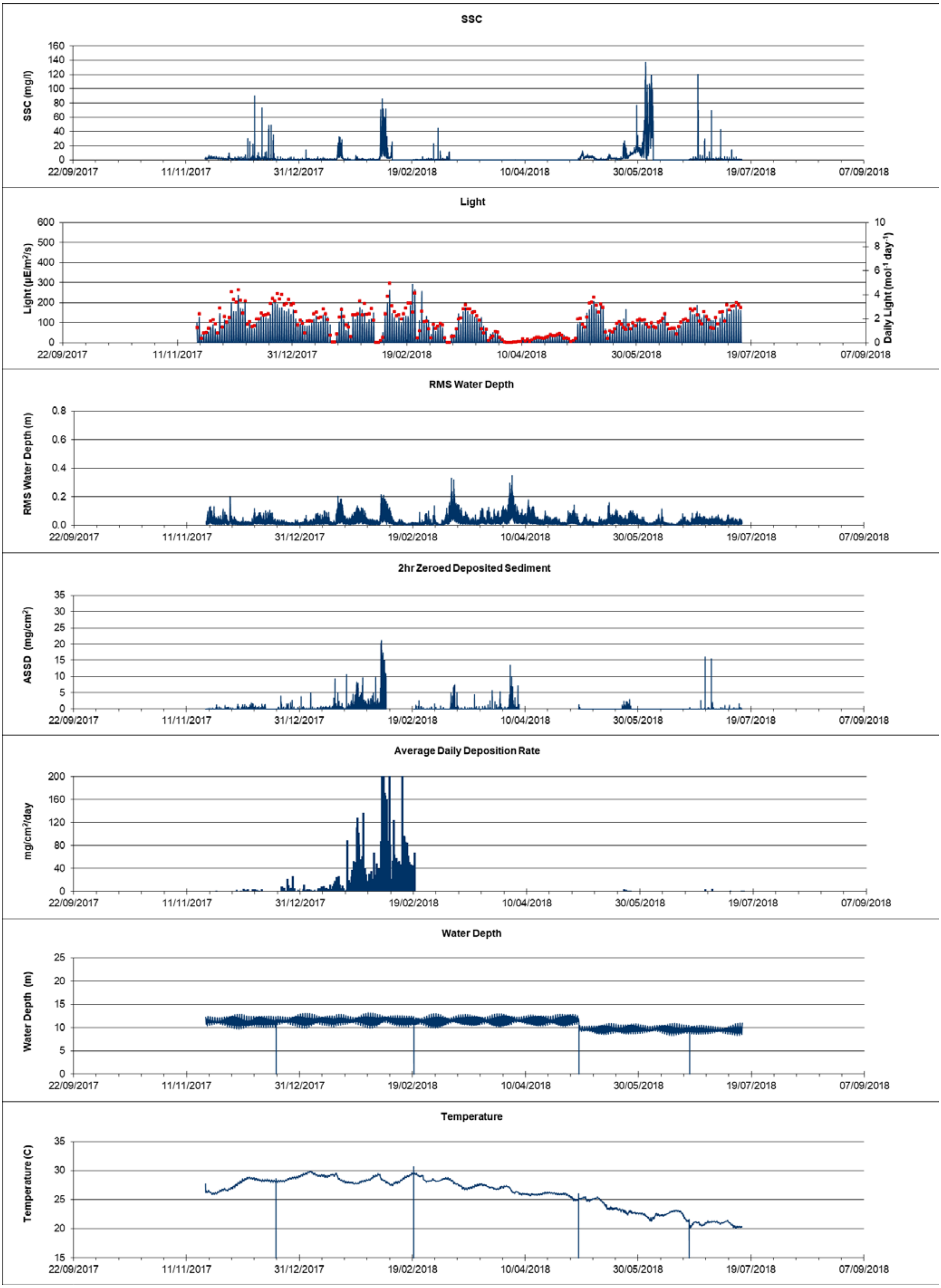

AMB 2: Spoil Grounds

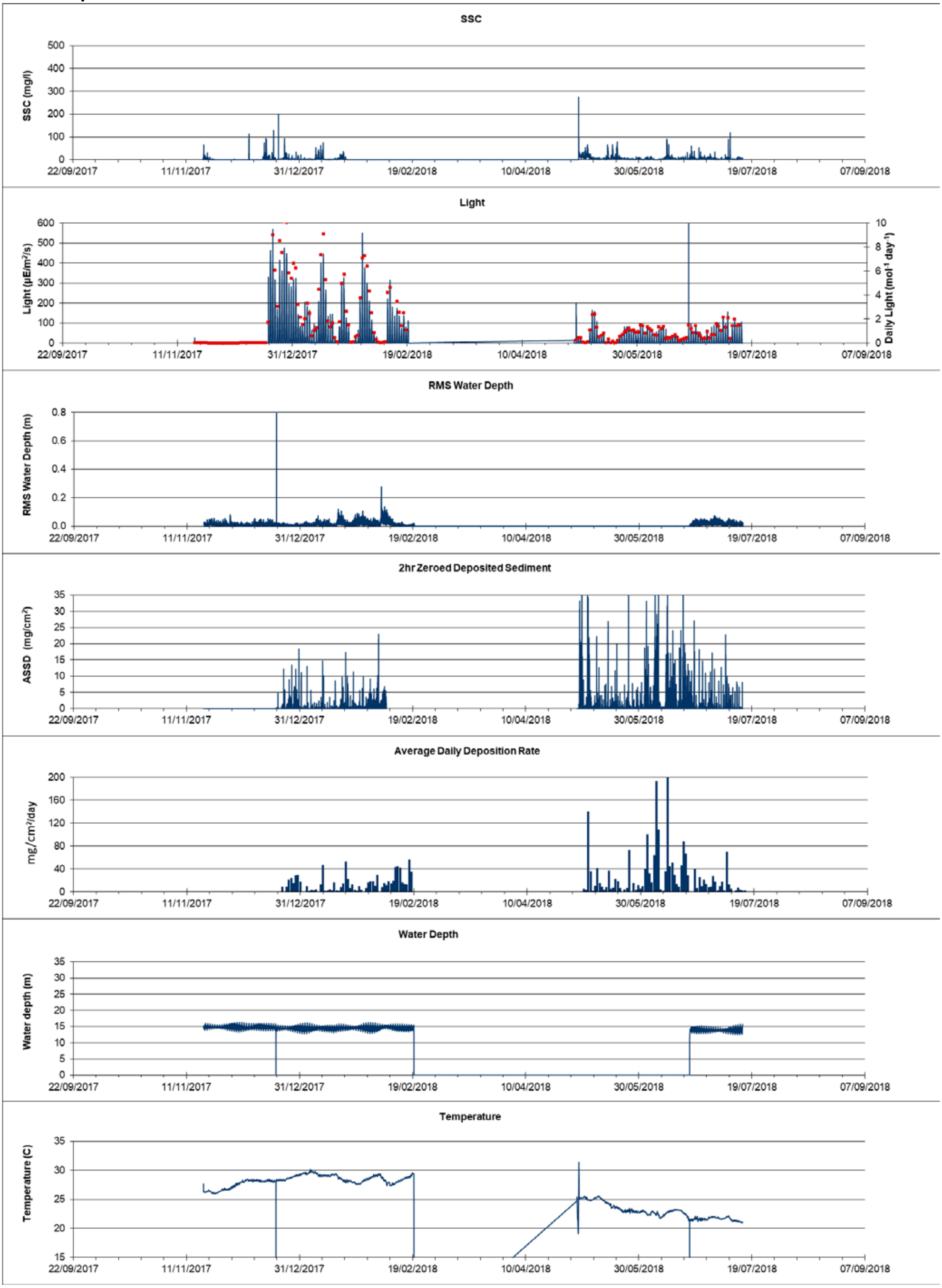

AMB 3: Elliot River

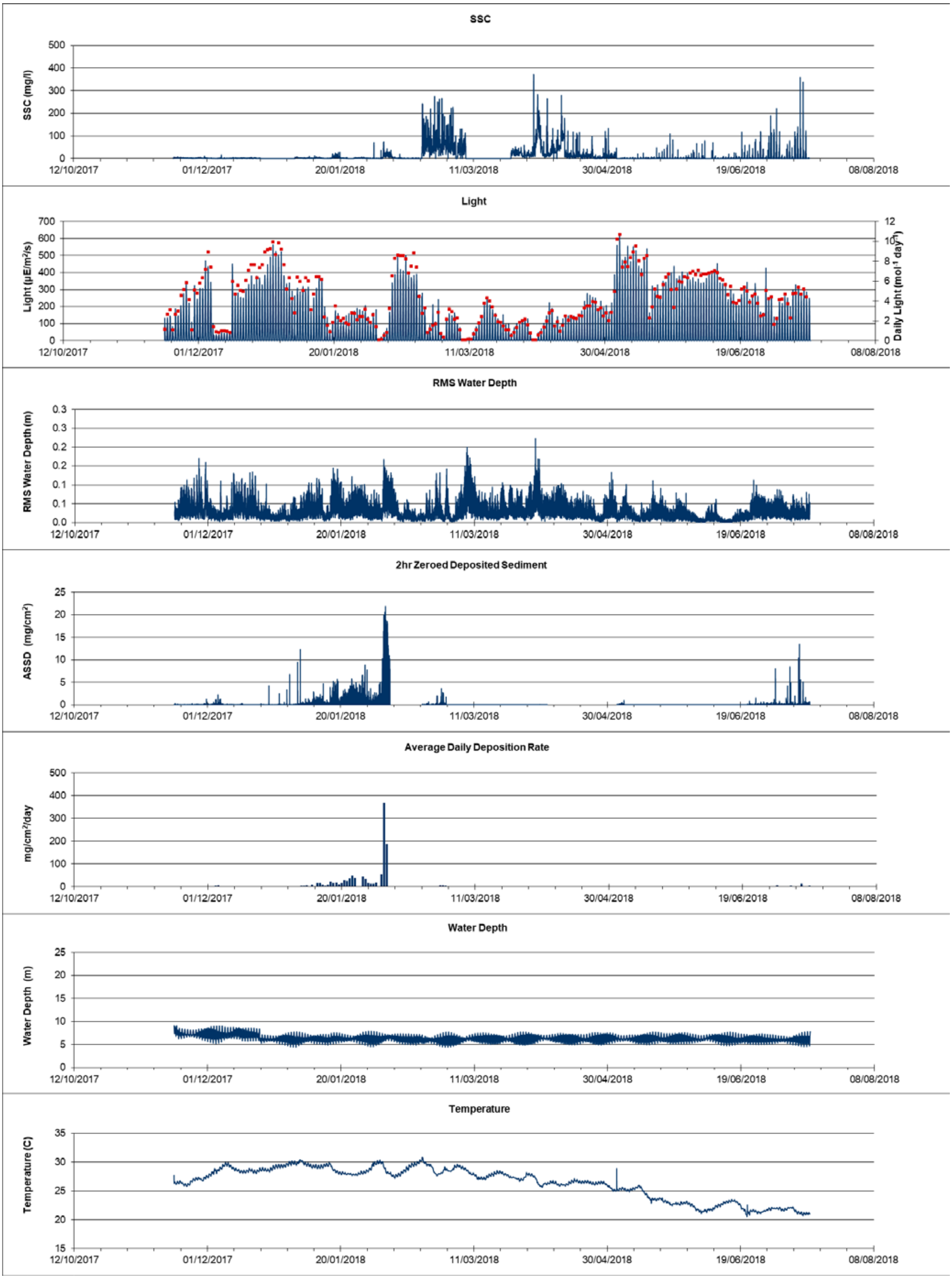

AMB 4: Camp Island

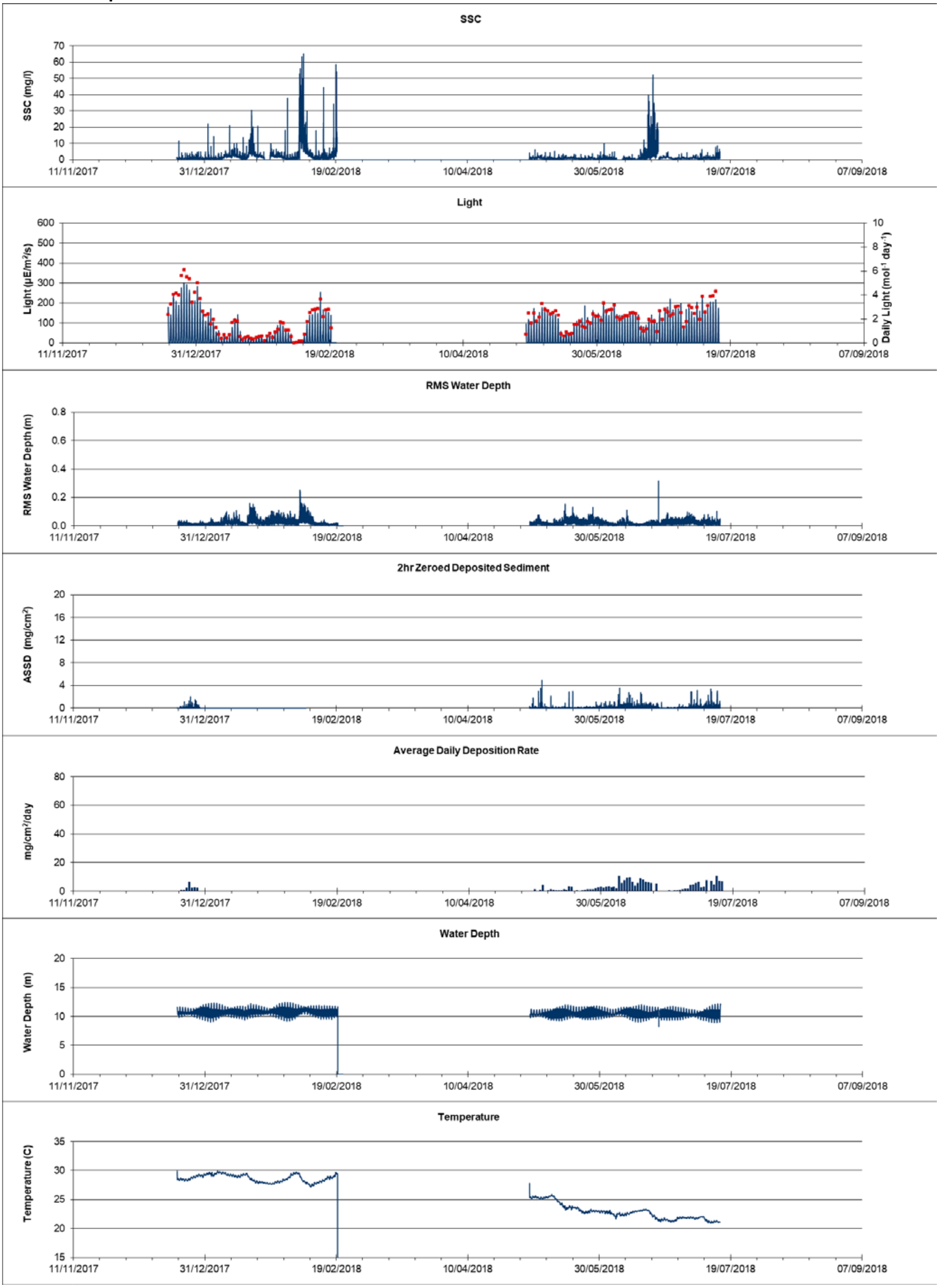

AMB 5: Holbourne

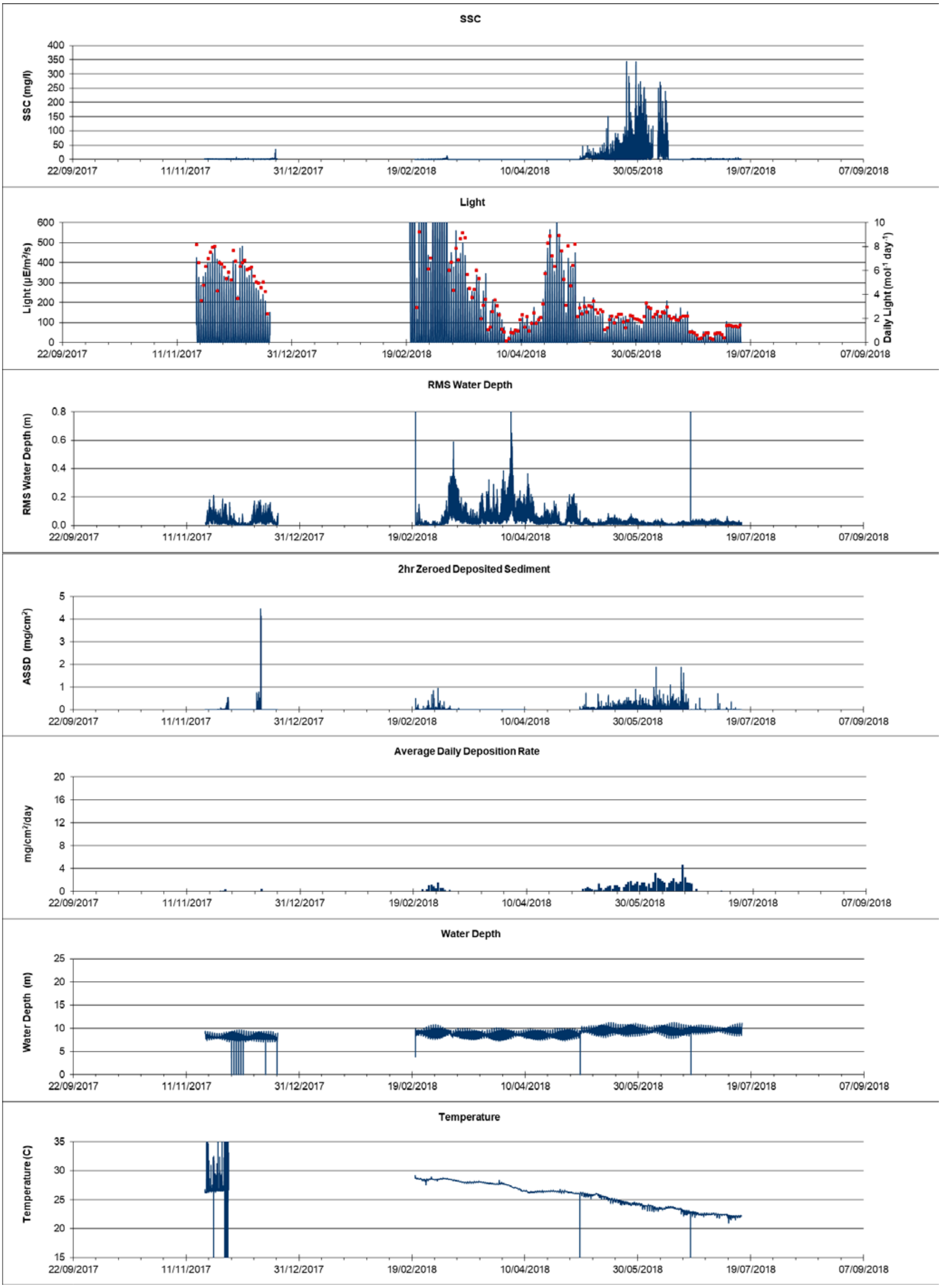

A.3 Summary of monthly statistics

AMB 1: Euri Creek

	SSC 11/2017	SSC 12/2017	SSC 01/2018	SSC 02/2018	SSC 03/2018	SSC 04/2018	SSC 05/2018	SSC 06/2018	SSC 07/2018
Mean	2.36	1.36	1.65	5.15	1.46		4.89	16.97	1.06
median	2.27	0.92	0.74	0.59	0.86		3.16	1.25	0.83
min	0.43	0.00	0.00	0.00	0.16		0.00	0.40	0.39
lower	1.80	0.47	0.52	0.33	0.60		1.64	0.86	0.69
upper	2.74	1.57	1.05	3.23	1.23		6.91	25.58	1.06
max	10.06	89.83	33.16	86.03	44.49		75.46	137.59	68.71
90th percentile	3.27	2.17	2.49	18.33	1.93		11.99	61.01	1.36
10th percentile	1.44	0.29	0.33	0.19	0.43		0.75	0.70	0.59
n	1657	4422	4142	2683	956		4069	2032	2010
St. Dev	0.93	3.17	3.35	10.88	2.89		4.85	27.46	2.32
St. Error	0.02	0.05	0.05	0.21	0.09		0.08	0.61	0.05

	ASSD 11/2017	ASSD 12/2017	ASSD 01/2018	ASSD 02/2018	ASSD 03/2018	ASSD 04/2018	ASSD 05/2018	ASSD 06/2018	ASSD 07/2018
Mean	0.02	0.08	0.41	1.16	0.07	0.36	0.21	0.02	0.04
median	0.00	0.00	0.07	0.01	0.00	0.01	0.00	0.00	0.01
min	0.00	0.00	0.00	0.00	0.00	0.00	0.00	0.00	0.00
lower	0.00	0.00	0.00	0.00	0.00	0.00	0.00	0.00	0.00
upper	0.02	0.06	0.33	0.58	0.02	0.23	0.25	0.01	0.03
max	1.20	3.93	10.45	20.65	7.44	13.49	2.96	15.98	15.47
90th percentile	0.05	0.23	1.06	3.37	0.08	0.82	0.68	0.02	0.06
10th percentile	0.00	0.00	0.00	0.00	0.00	0.00	0.00	0.00	0.00
n	1649	3557	4293	2187	4353	923	660	1336	1937
St. Dev	0.08	0.22	0.95	3.01	0.36	1.09	0.40	0.44	0.37
St. Error	0.00	0.00	0.01	0.06	0.01	0.04	0.02	0.01	0.01

	RMS 11/2017	RMS 12/2017	RMS 01/2018	RMS 02/2018	RMS 03/2018	RMS 04/2018	RMS 05/2018	RMS 06/2018	RMS 07/2018
Mean	0.03	0.02	0.03	0.02	0.04	0.04	0.03	0.02	0.02
median	0.03	0.02	0.02	0.01	0.03	0.03	0.02	0.01	0.02
min	0.00	0.00	0.00	0.00	0.00	0.00	0.00	0.00	0.00
lower	0.02	0.01	0.01	0.01	0.02	0.02	0.01	0.01	0.01
upper	0.04	0.02	0.04	0.03	0.05	0.05	0.03	0.02	0.03
max	0.20	0.12	0.20	0.22	0.33	0.34	0.16	0.11	0.07
90^{th} percentile	0.06	0.04	0.06	0.06	0.08	0.08	0.05	0.03	0.04
10^{th} percentile	0.01	0.01	0.01	0.01	0.01	0.01	0.01	0.00	0.01
n	1661	4463	4464	4030	4464	4318	4463	4319	2017
St. Dev	0.02	0.01	0.02	0.03	0.03	0.03	0.02	0.01	0.01
St. Error	0.00	0.00	0.00	0.00	0.00	0.00	0.00	0.00	0.00

	Temp 11/2017	Temp 12/2017	Temp 01/2018	Temp 02/2018	Temp 03/2018	Temp 04/2018	Temp 05/2018	Temp 06/2018	Temp 07/2018
Mean	26.44	28.32	28.72	28.57	27.53	26.08	23.97	21.87	20.85
median	26.44	28.33	28.85	28.50	27.39	26.01	23.62	22.02	20.98
min	25.89	26.85	27.64	27.39	26.67	25.22	22.37	20.13	20.04
lower	26.21	28.12	28.07	28.11	27.07	25.87	22.97	21.13	20.41
upper	26.65	28.63	29.26	29.10	28.14	26.15	25.01	22.52	21.18
max	27.72	29.29	29.93	30.60	28.82	27.41	25.97	23.18	21.40
90^{th} percentile	26.87	28.80	29.52	29.30	28.49	26.53	25.24	22.99	21.26
10^{th} percentile	26.01	27.81	27.87	27.80	26.87	25.76	22.67	20.67	20.26
n	1661	4463	4464	4030	4464	4318	4463	4319	2017
St. Dev	0.31	0.44	0.65	0.58	0.58	0.40	1.03	0.83	0.39
St. Error	0.01	0.01	0.01	0.01	0.01	0.01	0.02	0.01	0.01

	Light 11/2017	Light 12/2017	Light 01/2018	Light 02/2018	Light 03/2018	Light 04/2018	Light 05/2018	Light 06/2018	Light 07/2018
Mean	2.29	2.65	1.86	2.11	1.11	0.52	2.25	3.60	2.84
median	2.01	2.46	2.14	2.10	0.80	0.40	2.14	3.60	2.84
min	0.81	0.83	0.02	0.18	0.00	0.05	1.29	3.41	2.55
lower	1.66	1.83	1.39	1.35	0.22	0.24	1.71	3.50	2.70
upper	3.01	3.49	2.43	2.68	2.03	0.58	2.73	3.70	2.99
max	4.22	4.43	3.49	4.94	3.16	2.02	3.32	3.79	3.13
90th percentile	3.60	3.72	2.81	3.49	2.80	0.86	3.08	3.75	3.07
10th percentile	1.32	1.47	0.07	0.45	0.02	0.12	1.46	3.44	2.61
n	12	31	31	28	31	30	3	2	2
St. Dev	1.03	0.96	0.98	1.18	1.05	0.49	1.02	0.27	0.41
St. Error	0.30	0.17	0.18	0.22	0.19	0.09	0.59	0.19	0.29

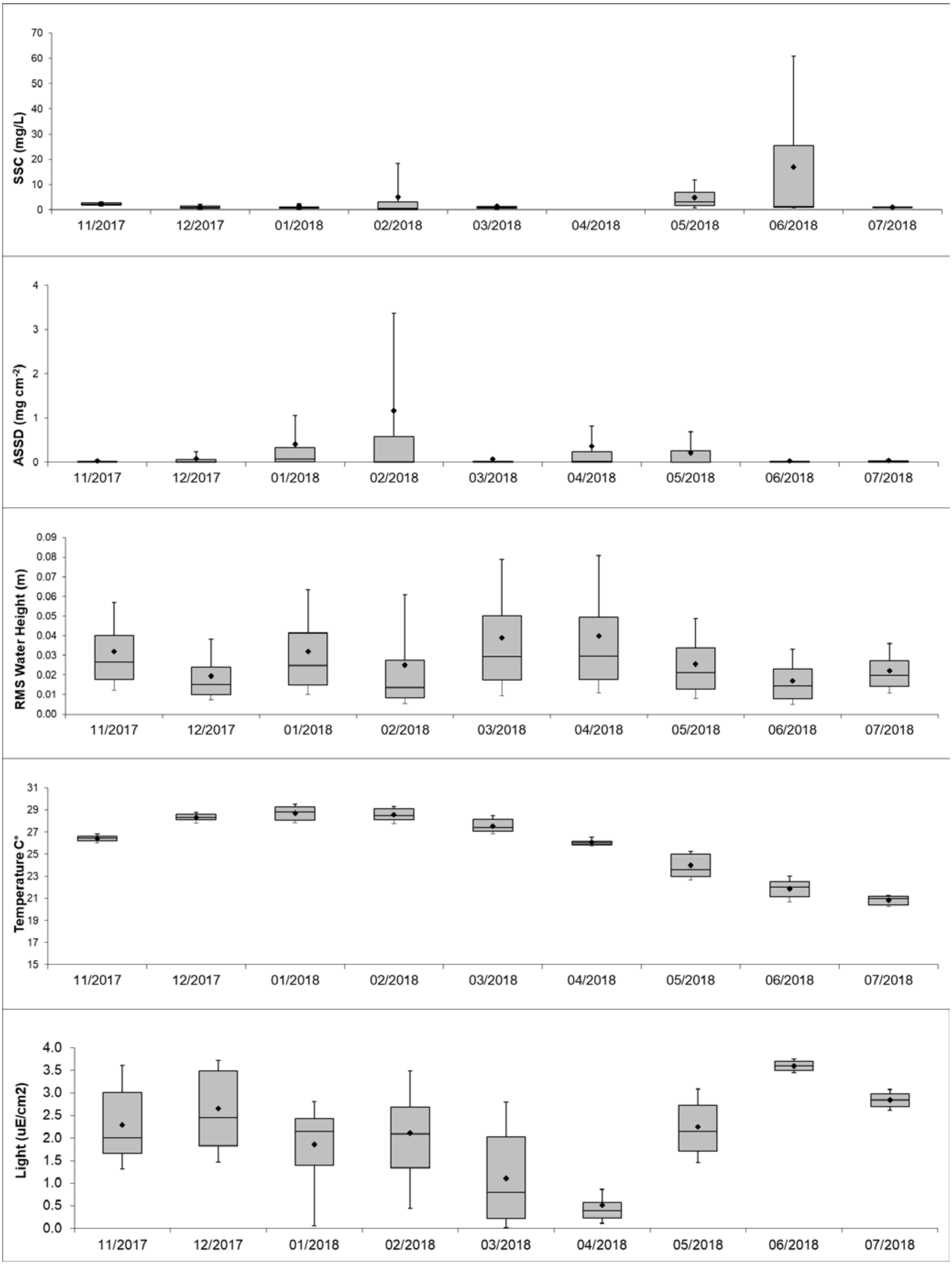
SSC (mg/L)
ASSD (mg cm⁻²)
RMS Water Height (m)
Temperature C°
Light (uE/cm2)
11/2017
12/2017
01/2018
02/2018
03/2018
04/2018
05/2018
06/2018
07/2018

AMB 2: Spoil Grounds

	SSC 11/2017	SSC 12/2017	SSC 01/2018	SSC 02/2018	SSC 03/2018	SSC 04/2018	SSC 05/2018	SSC 06/2018	SSC 07/2018
Mean	0.65	3.23	4.09				7.57	5.00	16.04
median	0.11	0.97	1.52				3.81	3.08	0.11
min	0.00	0.00	0.00				0.00	0.00	0.02
lower	0.04	0.09	0.90				2.31	2.02	0.07
upper	0.19	2.60	3.54				8.16	5.58	21.16
max	29.92	198.66	73.45				272.12	90.74	154.75
90th percentile	0.56	6.10	9.82				17.99	9.48	58.00
10th percentile	0.00	0.04	0.57				1.36	1.48	0.05
n	1627	3408	2815				4085	4000	2017
St. Dev	2.41	9.56	7.31				10.89	7.23	27.54
St. Error	0.06	0.16	0.14				0.17	0.11	0.61

	ASSD 11/2017	ASSD 12/2017	ASSD 01/2018	ASSD 02/2018	ASSD 03/2018	ASSD 04/2018	ASSD 05/2018	ASSD 06/2018	ASSD 07/2018
Mean		0.47	0.30	0.77			0.91	1.50	0.55
median		0.00	0.00	0.04			0.01	0.06	0.01
min		0.00	0.00	0.00			0.00	0.00	0.00
lower		0.00	0.00	0.00			0.00	0.00	0.00
upper		0.10	0.17	0.58			0.18	0.71	0.11
max		18.33	17.08	22.68			49.57	41.64	22.37
90th percentile		1.07	0.59	2.30			1.46	4.31	0.80
10th percentile		0.00	0.00	0.00			0.00	0.00	0.00
n		1621	4260	896			4016	4265	1937
St. Dev		1.62	1.04	2.12			3.59	4.11	1.98
St. Error		0.04	0.02	0.07			0.06	0.06	0.05

	RMS 11/2017	RMS 12/2017	RMS 01/2018	RMS 02/2018	RMS 03/2018	RMS 04/2018	RMS 05/2018	RMS 06/2018	RMS 07/2018
Mean	0.02	0.01	0.02	0.02				0.02	0.02
median	0.01	0.01	0.02	0.01				0.02	0.02
min	0.00	0.00	0.00	0.00				0.00	0.00
lower	0.01	0.01	0.01	0.01				0.01	0.01
upper	0.02	0.01	0.03	0.03				0.03	0.03
max	0.08	1.83	0.12	0.27				0.06	0.08
90th percentile	0.03	0.02	0.04	0.05				0.03	0.03
10th percentile	0.01	0.01	0.01	0.00				0.01	0.01
n	1661	4463	4464	2676				1365	2017
St. Dev	0.01	0.03	0.01	0.02				0.01	0.01
St. Error	0.00	0.00	0.00	0.00				0.00	0.00

	Temp 11/2017	Temp 12/2017	Temp 01/2018	Temp 02/2018	Temp 03/2018	Temp 04/2018	Temp 05/2018	Temp 06/2018	Temp 07/2018
Mean	26.43	28.27	28.77	28.47			24.03	22.28	21.60
median	26.41	28.24	28.92	28.55			23.93	22.35	21.66
min	25.92	26.89	27.58	27.30			19.05	20.41	20.95
lower	26.20	28.06	28.18	27.98			23.01	21.72	21.28
upper	26.67	28.44	29.29	28.97			25.06	22.84	21.91
max	27.10	29.46	30.17	29.60			31.37	23.29	22.16
90th percentile	26.77	28.97	29.60	29.21			25.31	23.07	21.98
10th percentile	26.08	27.71	27.85	27.65			22.81	21.46	21.13
n	1661	4463	4464	2676			4227	4319	2017
St. Dev	0.28	0.47	0.65	0.60			1.15	0.60	0.32
St. Error	0.01	0.01	0.01	0.01			0.02	0.01	0.01

	Light 11/2017	Light 12/2017	Light 01/2018	Light 02/2018	Light 03/2018	Light 04/2018	Light 05/2018	Light 06/2018	Light 07/2018
Mean	0.00	3.34	2.82	2.02		0.29	0.41	2.41	0.91
median	0.00	2.04	1.76	2.00		0.34	0.13	2.41	0.91
min	0.00	0.00	0.07	0.03		0.07	0.01	2.38	0.52
lower	0.00	0.03	0.62	0.38		0.22	0.07	2.39	0.71
upper	0.00	6.16	4.70	3.23		0.41	0.60	2.42	1.10
max	0.00	10.91	9.08	4.66		0.42	1.08	2.44	1.29
90th percentile	0.00	9.02	7.08	4.24		0.41	0.89	2.43	1.22
10th percentile	0.00	0.02	0.12	0.06		0.13	0.03	2.38	0.59
n	12	31	31	10		4	3	2	2
St. Dev	0.00	3.72	2.64	1.73		0.16	0.58	0.04	0.55
St. Error	0.00	0.67	0.47	0.55		0.08	0.34	0.03	0.39

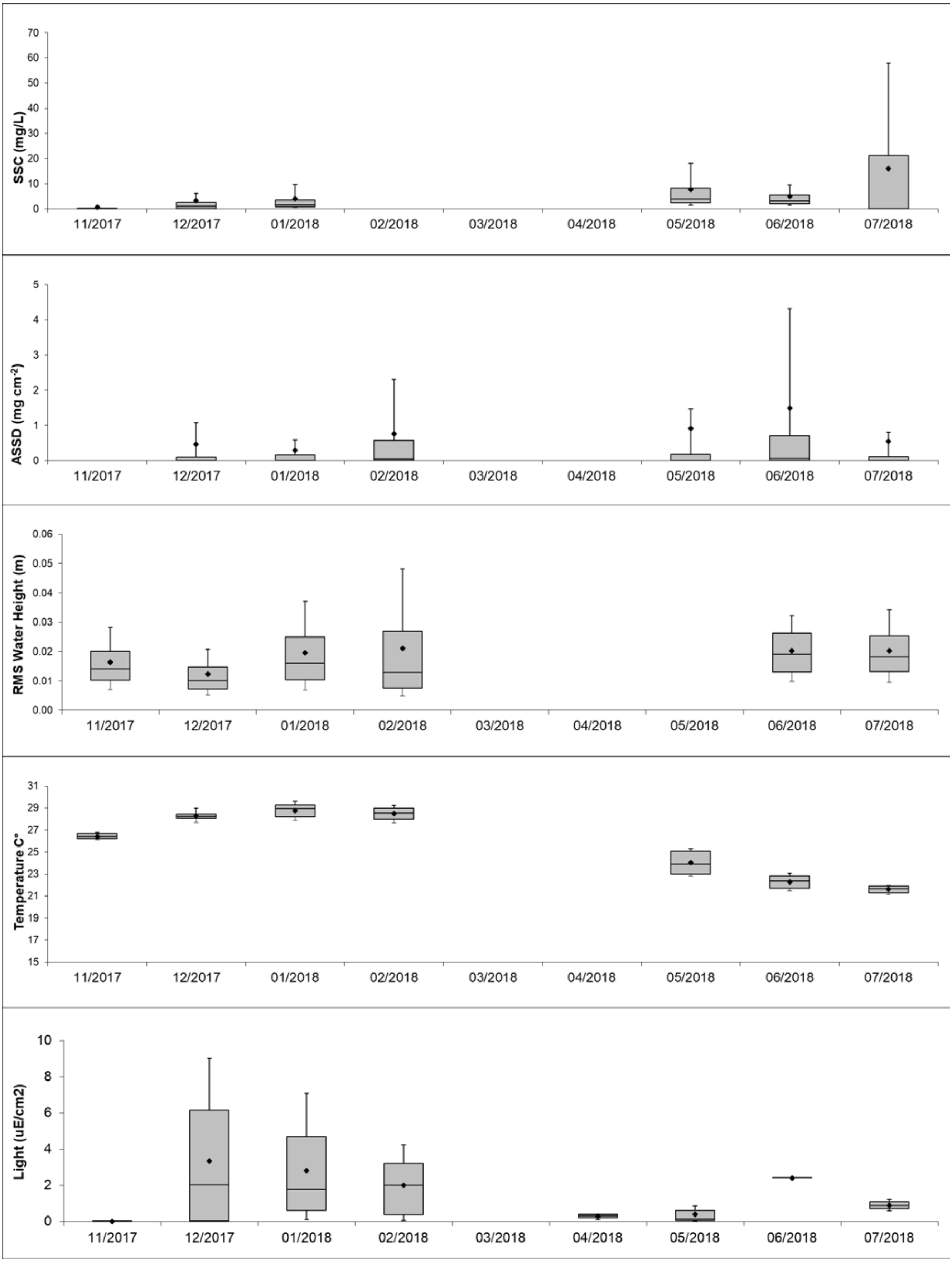
SSC (mg/L)
ASSD (mg cm-2)
RMS Water Height (m)
Temperature C°
Light (uE/cm2)
11/2017
12/2017
01/2018
02/2018
03/2018
04/2018
05/2018
06/2018
07/2018

AMB 3: Elliot River

	SSC 11/2017	SSC 12/2017	SSC 01/2018	SSC 02/2018	SSC 03/2018	SSC 04/2018	SSC 05/2018	SSC 06/2018	SSC 07/2018
Mean	2.59	1.23	2.64	30.02	41.15	33.10	1.82	61.43	0.14
median	2.40	1.08	1.95	2.50	28.79	14.34	0.60	0.14	0.01
min	0.93	0.00	0.25	0.00	2.66	0.00	0.00	0.00	0.00
lower	1.84	0.62	1.30	0.38	17.60	7.71	0.34	0.05	0.00
upper	3.15	1.60	3.02	35.90	49.43	37.19	0.88	99.86	0.06
max	10.84	16.39	28.62	274.11	227.12	372.29	108.91	453.70	13.46
90^{th} percentile	3.88	2.21	5.24	94.47	87.68	92.97	4.72	231.14	0.18
10^{th} percentile	1.45	0.34	0.70	0.19	12.24	3.38	0.18	0.00	0.00
n	1796	2871	3849	4019	1946	4275	4453	4319	1785
St. Dev	1.04	1.04	2.51	52.84	38.33	46.27	4.78	97.35	0.69
St. Error	0.02	0.02	0.04	0.83	0.87	0.71	0.07	1.48	0.02

	ASSD 11/2017	ASSD 12/2017	ASSD 01/2018	ASSD 02/2018	ASSD 03/2018	ASSD 04/2018	ASSD 05/2018	ASSD 06/2018	ASSD
Mean	0.01	0.03	0.70	1.70			0.04	0.02	0.14
median	0.00	0.00	0.30	0.06			0.01	0.00	0.01
min	0.00	0.00	0.00	0.00			0.00	0.00	0.00
lower	0.00	0.00	0.05	0.00			0.00	0.00	0.00
upper	0.02	0.02	0.94	0.70			0.04	0.01	0.06
max	1.23	6.75	12.25	21.73			0.94	1.44	13.46
90^{th} percentile	0.03	0.04	1.88	6.49			0.09	0.07	0.18
10^{th} percentile	0.00	0.00	0.00	0.00			0.00	0.00	0.00
n	1791	3337	4232	2149			427	1343	1785
St. Dev	0.04	0.20	1.01	4.09			0.09	0.08	0.69
St. Error	0.00	0.00	0.02	0.09			0.00	0.00	0.02

	RMS 11/2017	RMS 12/2017	RMS 01/2018	RMS 02/2018	RMS 03/2018	RMS 04/2018	RMS 05/2018	RMS 06/2018	RMS 07/2018
Mean	0.04	0.03	0.04	0.03	0.04	0.04	0.02	0.02	0.03
median	0.03	0.02	0.03	0.02	0.03	0.03	0.02	0.01	0.03
min	0.01	0.00	0.00	0.00	0.00	0.00	0.00	0.00	0.01
lower	0.02	0.01	0.02	0.01	0.02	0.02	0.01	0.01	0.02
upper	0.05	0.03	0.05	0.04	0.05	0.04	0.03	0.03	0.04
max	0.17	0.13	0.14	0.17	0.20	0.22	0.13	0.11	0.09
90th percentile	0.07	0.05	0.06	0.06	0.07	0.06	0.04	0.04	0.05
10th percentile	0.02	0.01	0.01	0.01	0.01	0.01	0.01	0.00	0.01
n	1803	4464	4464	4032	4464	4318	4464	4319	1873
St. Dev	0.02	0.02	0.02	0.02	0.02	0.02	0.01	0.01	0.01
St. Error	0.00	0.00	0.00	0.00	0.00	0.00	0.00	0.00	0.00

	Temp 11/2017	Temp 12/2017	Temp 01/2018	Temp 02/2018	Temp 03/2018	Temp 04/2018	Temp 05/2018	Temp 06/2018	Temp 07/2018
Mean	26.68	28.78	28.89	28.92	27.93	26.43	24.08	22.01	21.64
median	26.68	28.71	28.97	28.97	27.83	26.38	23.70	21.79	21.78
min	25.79	27.26	27.66	27.21	26.62	25.61	22.36	20.54	20.71
lower	26.29	28.44	28.11	28.09	27.35	26.13	22.96	21.48	21.24
upper	27.08	29.18	29.56	29.72	28.42	26.61	25.21	22.57	21.97
max	27.68	30.12	30.43	30.85	29.62	28.00	28.84	23.48	22.25
90th percentile	27.29	29.51	29.89	30.01	29.00	26.90	25.50	23.11	22.10
10th percentile	26.06	28.15	27.89	27.74	27.10	25.96	22.72	21.27	21.03
n	1803	4464	4464	4032	4464	4318	4464	4319	1873
St. Dev	0.47	0.54	0.78	0.89	0.69	0.44	1.13	0.69	0.40
St. Error	0.01	0.01	0.01	0.01	0.01	0.01	0.02	0.01	0.01

	Light 11/2017	Light 12/2017	Light 01/2018	Light 02/2018	Light 03/2018	Light 04/2018	Light 05/2018	Light 06/2018	Light 07/2018
Mean	5.21	5.77	3.04	4.15	1.46	3.31	6.39	4.64	4.50
median	5.16	6.30	2.42	3.03	1.10	2.67	6.64	4.56	4.73
min	1.08	0.82	0.10	0.36	0.06	0.92	2.28	1.65	2.29
lower	4.58	4.45	1.85	1.65	0.62	2.08	5.43	3.87	4.56
upper	6.34	7.68	4.07	7.42	1.96	3.45	7.25	5.45	4.99
max	8.91	9.94	6.44	8.84	4.28	10.68	9.53	7.03	5.36
90^{th} percentile	7.36	9.19	6.16	8.57	3.41	5.20	8.34	6.83	5.27
10^{th} percentile	1.95	0.96	1.43	0.80	0.07	1.53	4.37	2.57	3.56
n	13	31	31	28	31	30	31	30	7
St. Dev	2.20	2.96	1.88	3.06	1.19	2.29	1.68	1.40	1.02
St. Error	0.61	0.53	0.34	0.58	0.21	0.42	0.30	0.26	0.39

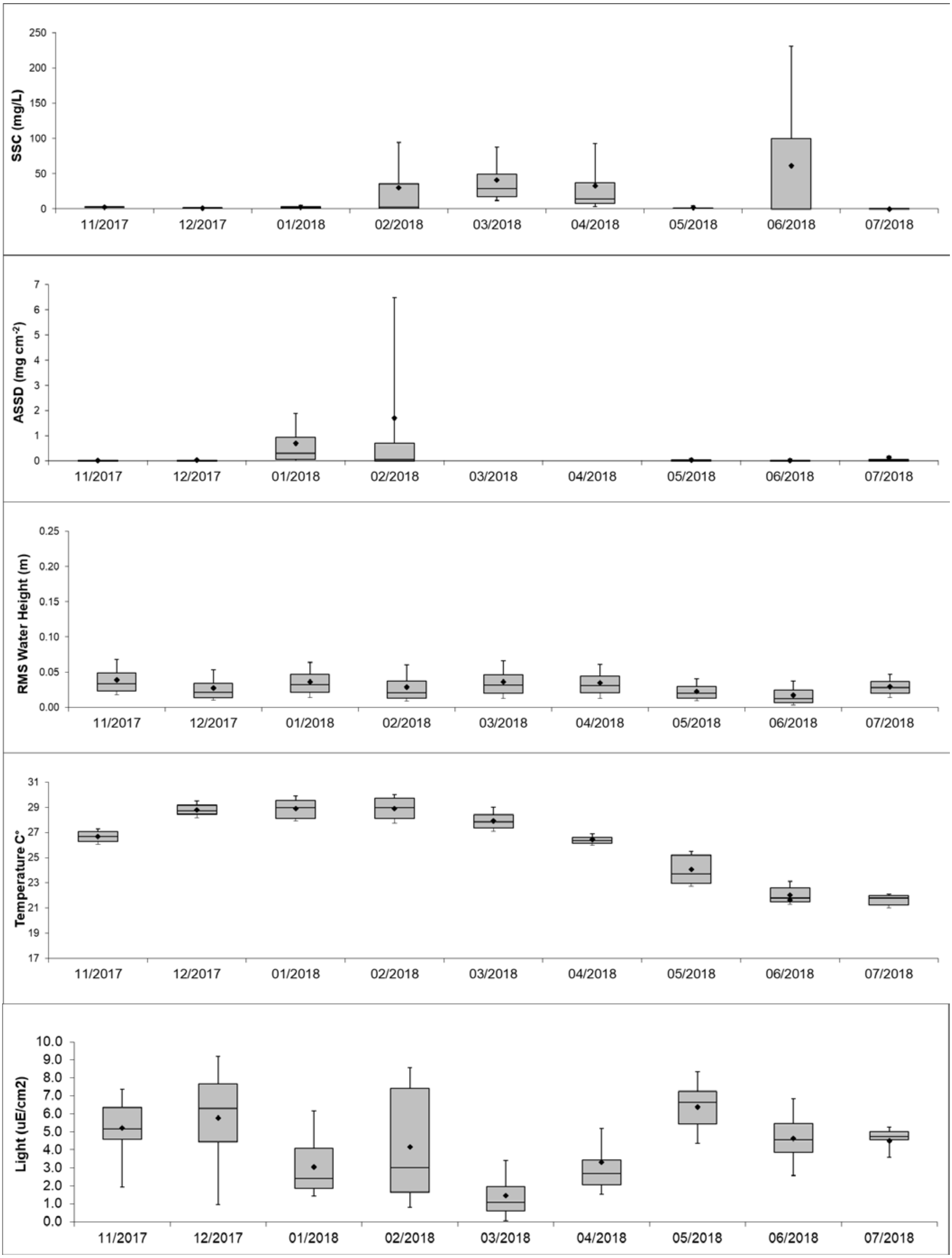
SSC (mg/L)
0
50
100
150
200
250
11/2017
12/2017
01/2018
02/2018
03/2018
04/2018
05/2018
06/2018
07/2018
ASSD (mg cm⁻²)
0
1
2
3
4
5
6
7
RMS Water Height (m)
0.00
0.05
0.10
0.15
0.20
0.25
Temperature C°
17
19
21
23
25
27
29
31
Light (uE/cm2)
0.0
1.0
2.0
3.0
4.0
5.0
6.0
7.0
8.0
9.0
10.0

AMB 4: Camp Island

	SSC 11/2017	SSC 12/2017	SSC 01/2018	SSC 02/2018	SSC 03/2018	SSC 04/2018	SSC 05/2018	SSC 06/2018	SSC 07/2018
Mean		0.73	2.24	4.57			21.78	0.16	10.42
median		0.62	1.73	1.54			0.14	0.06	10.38
min		0.00	0.14	0.00			0.03	0.00	8.94
lower		0.45	0.92	0.66			0.07	0.00	10.01
upper		0.80	2.66	4.24			28.64	0.21	10.87
max		11.37	37.89	64.13			186.32	3.58	12.17
90^{th} percentile		1.12	3.92	12.43			82.99	0.43	11.18
10^{th} percentile		0.29	0.56	0.39			0.05	0.00	9.62
n		1652	4142	2648			4098	4225	2017
St. Dev		0.62	2.42	7.78			36.86	0.25	0.64
St. Error		0.02	0.04	0.15			0.58	0.00	0.01

	ASSD 11/2017	ASSD 12/2017	ASSD 01/2018	ASSD 02/2018	ASSD 03/2018	ASSD 04/2018	ASSD 05/2018	ASSD 06/2018	ASSD 07/2018
Mean		0.08					0.05	0.16	0.19
median		0.01					0.01	0.06	0.08
min		0.00					0.00	0.00	0.00
lower		0.00					0.00	0.00	0.02
upper		0.07					0.04	0.21	0.21
max		2.04					4.81	3.58	3.38
90^{th} percentile		0.23					0.10	0.43	0.47
10^{th} percentile		0.00					0.00	0.00	0.00
n		1209					4001	4225	1932
St. Dev		0.18					0.21	0.25	0.35
St. Error		0.01					0.00	0.00	0.01

	RMS 11/2017	RMS 12/2017	RMS 01/2018	RMS 02/2018	RMS 03/2018	RMS 04/2018	RMS 05/2018	RMS 06/2018	RMS 07/2018
Mean		0.01	0.03	0.03			0.03	0.02	0.03
median		0.01	0.02	0.02			0.02	0.02	0.02
min		0.00	0.00	0.00			0.00	0.00	0.00
lower		0.01	0.02	0.01			0.02	0.01	0.02
upper		0.02	0.04	0.04			0.03	0.02	0.03
max		0.04	0.15	0.25			0.15	0.32	0.10
90th percentile		0.02	0.05	0.07			0.04	0.03	0.04
10th percentile		0.01	0.01	0.01			0.01	0.01	0.01
n		1658	4464	2663			4098	4294	2017
St. Dev		0.01	0.02	0.03			0.01	0.01	0.01
St. Error		0.00	0.00	0.00			0.00	0.00	0.00

	Temp 11/2017	Temp 12/2017	Temp 01/2018	Temp 02/2018	Temp 03/2018	Temp 04/2018	Temp 05/2018	Temp 06/2018	Temp 07/2018
Mean		28.81	28.72	28.52			24.09	22.28	21.60
median		28.75	28.85	28.55			23.69	22.41	21.77
min		28.15	27.61	27.13			22.55	21.08	20.89
lower		28.49	28.01	27.93			23.03	21.70	21.21
upper		29.14	29.32	29.12			25.29	22.81	21.90
max		29.89	29.90	29.76			27.80	23.33	22.09
90th percentile		29.30	29.55	29.50			25.47	23.11	21.97
10th percentile		28.37	27.82	27.65			22.84	21.38	21.08
n		1658	4464	2663			4098	4294	2017
St. Dev		0.36	0.68	0.70			1.07	0.63	0.36
St. Error		0.01	0.01	0.01			0.02	0.01	0.01

	Light 11/2017	Light 12/2017	Light 01/2018	Light 02/2018	Light 03/2018	Light 04/2018	Light 05/2018	Light 06/2018	Light 07/2018
Mean			0.77	2.03		1.84	2.41	2.74	2.48
median			0.58	2.55		2.07	2.13	2.74	2.48
min			0.01	0.13		0.73	1.82	2.68	2.42
lower			0.42	1.27		1.41	1.97	2.71	2.45
upper			1.08	2.80		2.49	2.70	2.77	2.51
max			1.86	3.64		2.50	3.28	2.80	2.55
90th percentile			1.69	2.82		2.50	3.05	2.79	2.53
10th percentile			0.27	0.27		1.00	1.88	2.69	2.43
n			31	13		4	3	2	2
St. Dev			0.53	1.13		0.84	0.77	0.09	0.09
St. Error			0.09	0.31		0.42	0.44	0.06	0.06

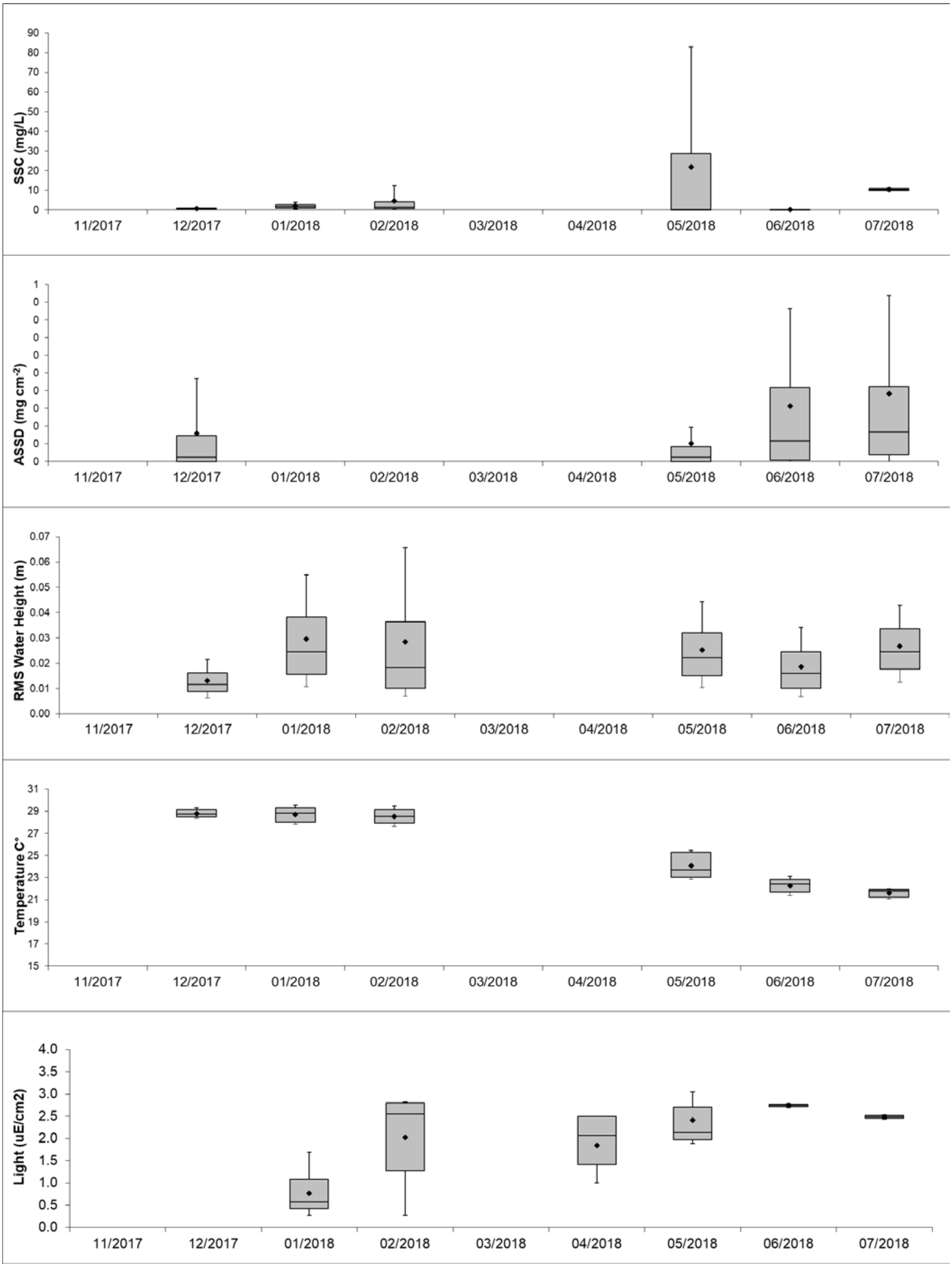
SSC (mg/L)
ASSD (mg cm⁻²)
RMS Water Height (m)
Temperature C°
Light (uE/cm2)
11/2017
12/2017
01/2018
02/2018
03/2018
04/2018
05/2018
06/2018
07/2018

AMB 5: Holbourne

	SSC 11/2017	SSC 12/2017	SSC 01/2018	SSC 02/2018	SSC 03/2018	SSC 04/2018	SSC 05/2018	SSC 06/2018	SSC 07/2018
Mean	1.38	1.39		0.22	1.58		22.16	27.41	0.58
median	1.34	1.18		0.17	0.75		8.75	4.31	0.45
min	0.89	0.80		0.00	0.07		0.00	0.00	0.06
lower	1.23	1.04		0.09	0.42		3.72	0.58	0.33
upper	1.51	1.40		0.26	1.96		25.01	40.39	0.65
max	2.76	35.68		1.59	12.71		344.04	268.44	7.16
90^{th} percentile	1.67	1.81		0.43	4.32		57.54	85.98	1.00
10^{th} percentile	1.14	0.95		0.05	0.27		0.07	0.38	0.25
n	1655	2824		1229	862		3966	2549	2010
St. Dev	0.23	1.22		0.19	1.96		36.18	42.02	0.53
St. Error	0.01	0.02		0.01	0.07		0.57	0.83	0.01

	ASSD 11/2017	ASSD 12/2017	ASSD 01/2018	ASSD 02/2018	ASSD 03/2018	ASSD 04/2018	ASSD 05/2018	ASSD 06/2018	ASSD 07/2018
Mean	0.03	0.25		0.02	0.01		0.05	0.07	0.00
median	0.00	0.04		0.00	0.00		0.02	0.02	0.00
min	0.00	0.00		0.00	0.00		0.00	0.00	0.00
lower	0.00	0.00		0.00	0.00		0.00	0.00	0.00
upper	0.01	0.15		0.01	0.01		0.06	0.09	0.00
max	0.54	4.46		0.86	0.95		0.88	1.88	0.72
90^{th} percentile	0.06	0.38		0.04	0.03		0.15	0.19	0.00
10^{th} percentile	0.00	0.00		0.00	0.00		0.00	0.00	0.00
n	691	247		1233	1512		3969	4165	1929
St. Dev	0.07	0.78		0.08	0.04		0.08	0.14	0.02
St. Error	0.00	0.05		0.00	0.00		0.00	0.00	0.00

	RMS 11/2017	RMS 12/2017	RMS 01/2018	RMS 02/2018	RMS 03/2018	RMS 04/2018	RMS 05/2018	RMS 06/2018	RMS 07/2018
Mean	0.05	0.03		0.02	0.07	0.07	0.02	0.01	0.02
median	0.04	0.02		0.01	0.05	0.06	0.02	0.01	0.01
min	0.00	0.00		0.00	0.00	0.00	0.00	0.00	0.00
lower	0.02	0.01		0.01	0.03	0.03	0.01	0.01	0.01
upper	0.06	0.05		0.02	0.10	0.09	0.03	0.02	0.02
max	0.21	0.18		0.87	0.59	0.81	0.22	0.80	0.06
90th percentile	0.09	0.07		0.03	0.15	0.15	0.04	0.02	0.02
10th percentile	0.02	0.01		0.00	0.01	0.01	0.01	0.01	0.01
n	1661	2857		1233	4464	4318	4459	4317	2017
St. Dev	0.03	0.03		0.03	0.06	0.07	0.02	0.01	0.01
St. Error	0.00	0.00		0.00	0.00	0.00	0.00	0.00	0.00

	Temp 11/2017	Temp 12/2017	Temp 01/2018	Temp 02/2018	Temp 03/2018	Temp 04/2018	Temp 05/2018	Temp 06/2018	Temp 07/2018
Mean	34.12			28.52	28.11	26.60	25.23	23.23	22.31
median	26.70			28.51	28.03	26.44	25.29	23.39	22.33
min	26.21			27.56	27.61	26.10	23.90	21.69	20.97
lower	26.56			28.45	27.88	26.35	24.53	22.75	22.16
upper	27.03			28.59	28.40	26.64	25.89	23.63	22.50
max	783.00			29.22	28.81	27.73	26.26	24.19	22.70
90th percentile	28.97			28.72	28.57	27.33	26.11	23.93	22.55
10th percentile	26.42			28.35	27.74	26.28	24.27	22.48	22.07
n	1366			1233	4464	4318	4459	4317	2017
St. Dev	52.31			0.17	0.30	0.39	0.71	0.52	0.24
St. Error	1.42			0.00	0.00	0.01	0.01	0.01	0.01

	Light 11/2017	Light 12/2017	Light 01/2018	Light 02/2018	Light 03/2018	Light 04/2018	Light 05/2018	Light 06/2018	Light 07/2018
Mean	6.51	5.27		16.77	4.83	4.36	2.86	3.21	2.60
median	6.62	5.30		19.12	3.76	2.98	3.03	3.21	2.60
min	4.30	2.37		2.93	0.10	0.96	2.51	2.97	2.48
lower	5.71	4.67		10.98	1.65	1.95	2.77	3.09	2.54
upper	7.56	6.25		22.01	6.38	7.02	3.03	3.34	2.67
max	8.01	6.81		24.98	21.22	11.09	3.04	3.46	2.73
90^{th} percentile	7.93	6.55		23.95	8.73	8.33	3.03	3.41	2.70
10^{th} percentile	5.22	3.83		6.39	0.82	1.26	2.62	3.02	2.50
n	12	14		14	31	30	3	2	2
St. Dev	1.18	1.26		7.35	4.41	3.01	0.30	0.34	0.18
St. Error	0.34	0.34		1.96	0.79	0.55	0.17	0.24	0.13

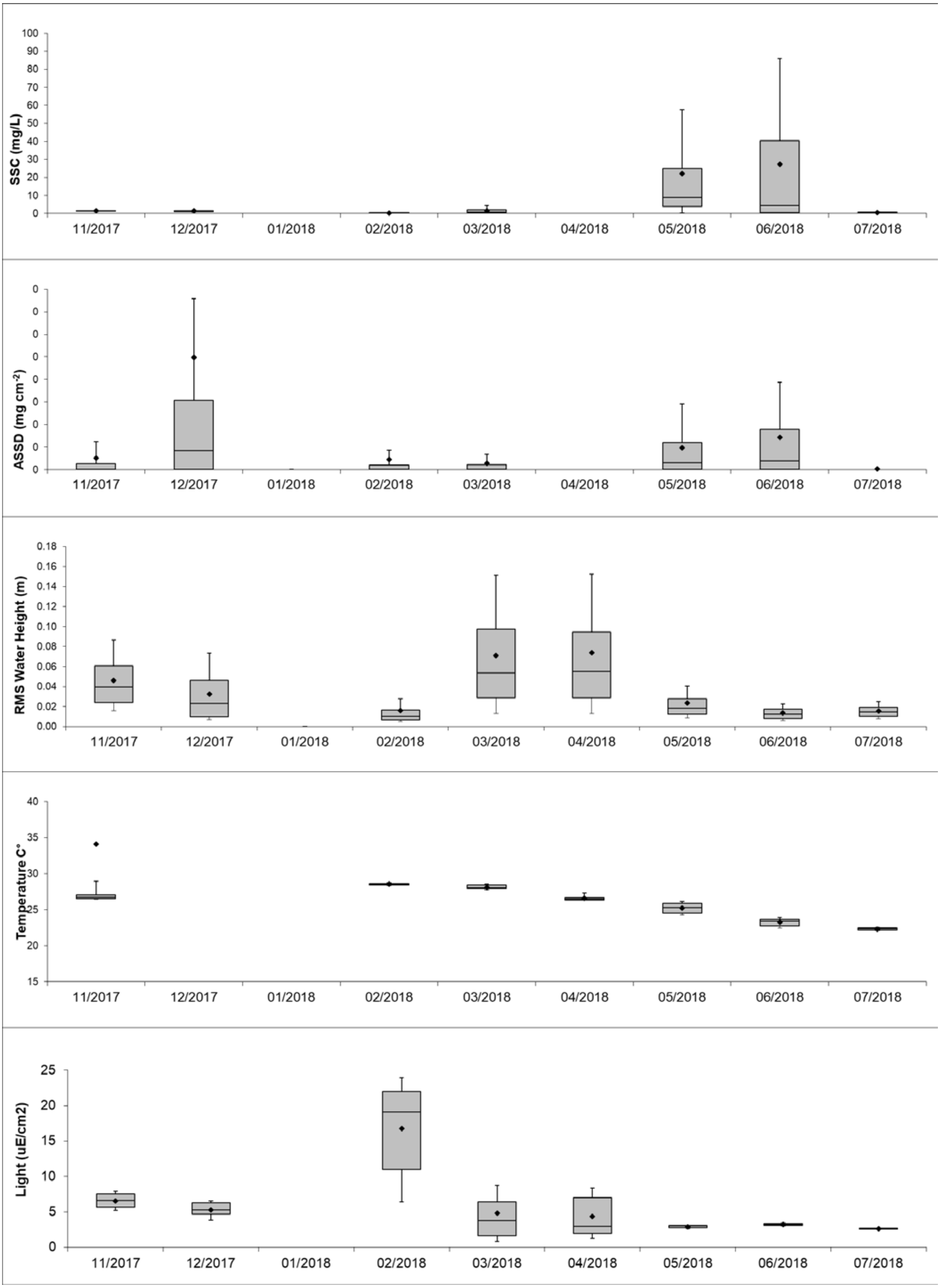
SSC (mg/L)
0
10
20
30
40
50
60
70
80
90
100
11/2017
12/2017
01/2018
02/2018
03/2018
04/2018
05/2018
06/2018
07/2018
ASSD (mg cm⁻²)
RMS Water Height (m)
0.00
0.02
0.04
0.06
0.08
0.10
0.12
0.14
0.16
0.18
Temperature C°
15
20
25
30
35
40
Light (uE/cm2)
0
5
10
15
20
25

Centre for Tropical Water and Aquatic Ecosystem Research (TropWATER)

ATSIP Building
James Cook University
Townsville Qld 4811

Phone: 07 4781 4262
Fax: 07 4781 5589
Email: TropWATER@jcu.edu.au
Web: www.jcu.edu.au/tropwater/